International Journal of Life Sciences and Biotechnology

e-ISSN:2651-4621

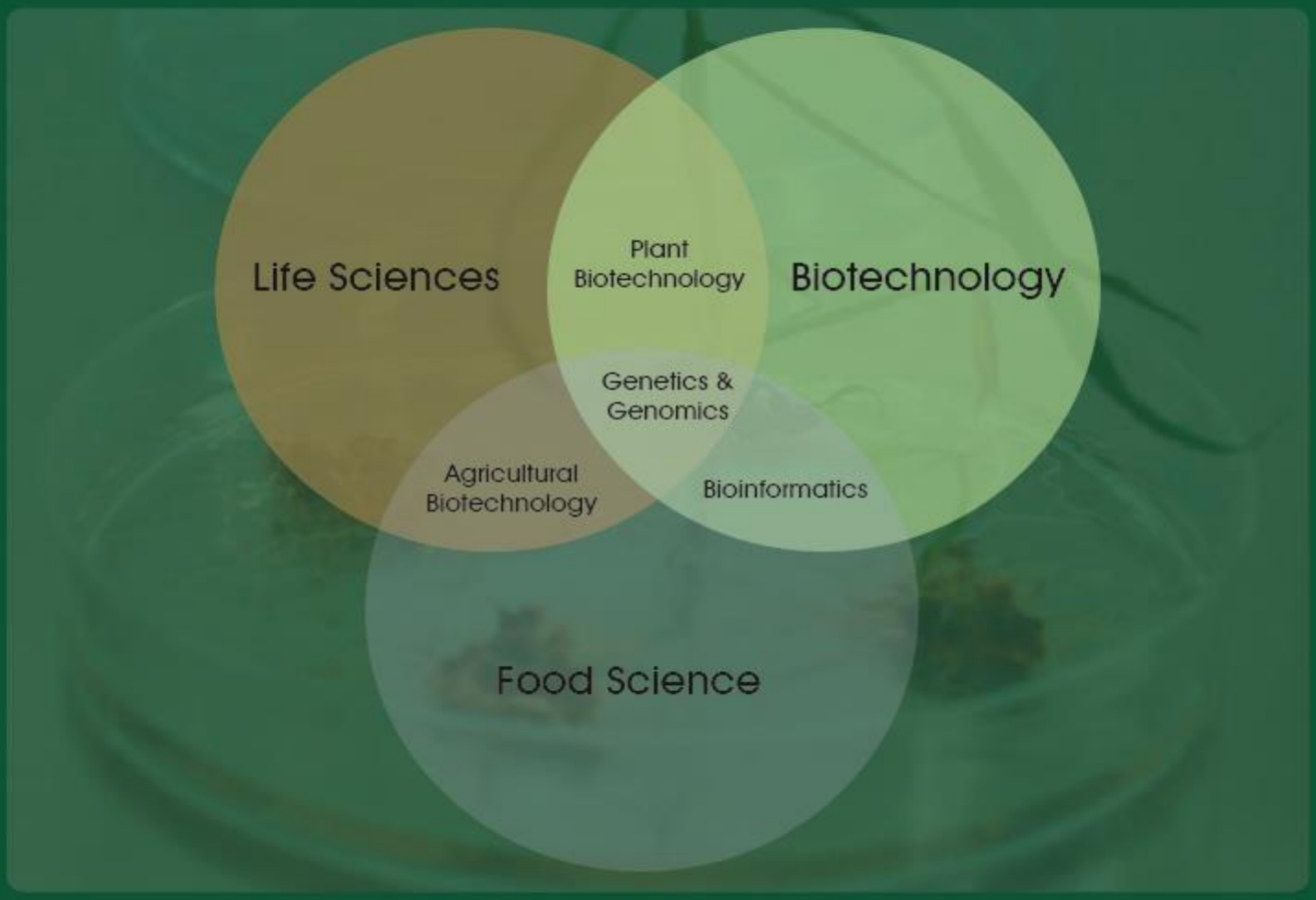

Volume/Cilt:7 **2024** **Issue / Sayı:1**

Management Office / Yönetim Ofisi

Yildiz Technical University, Faculty of Chemical and Metallurgical Engineering.
ESENLER/ISTANBUL

From The Editor;

Dear Readers and Authors,

As “International Journal of Life Sciences and Biotechnology”, we are pleased and honored to present the 18th issue of the journal. "International Journal of Life Sciences and Biotechnology" is an international double peer-reviewed open access academic journal published on the basis of research- development and code of practice.

The aims of this journal are to contribute in theoretical and practical applications in relevant researchers of Life Sciences, Biology, Biotechnology, Bioengineering, Agricultural Sciences, Food Biotechnology and Genetics institutions and organizations in Turkey, and to publish solution based papers depending on the principle of impartiality and scientific ethics principles, focusing on innovative and added value work, discussing the current and future.

With these thoughts, We are especially thankful to academicians honoring with the articles, valuable scientists involved in editorial boards and reviewers for their contributions to the evaluation processes with through their opinions/ideas/contributions/criticisms in the first issue of 2024 "International Journal of Life Sciences and Biotechnology". Hope to see you in the next issue…

15. 04. 2024
Editor in Chief
Prof. Dr. Ali Aslan

Editörden;

Değerli okurlar ve yazarlar,

"International Journal of Life Sciences and Biotechnology" olarak dergimizin on sekizinci sayısını yayın hayatına sunmaktan mutluluk ve onur duyuyoruz. "International Journal of Life Sciences and Biotechnology" dergisi araştırma- geliştirme ve uygulama ilkeleri baz alınarak yayınlanan uluslararası hakemli açık erişimli akademik bir elektronik dergidir.

"International Journal of Life Sciences and Biotechnology" dergisi Yaşam Bilimleri, Biyoloji, Biyoteknoloji, Biyomühendislik, Ziraat Bilimleri, Gıda Biyoteknolojisi ve Genetik alanlarındaki ilgili araştırmacılara, kurum ve kuruluşlara teorik ve pratik uygulamalarda katkı sağlamayı, tarafsızlık ve bilim etiği ilkelerine bağlı kalarak çözüm temelli, yenilikçi ve katma değeri olan çalışmalara odaklanan, günceli ve geleceği tartışan çalışmaların yayınlanmasını hedeflemektedir.

Bu düşüncelerle 2024 yılı birinci sayısını yayınladığımız "International Journal of Life Sciences and Biotechnology" dergisini, makaleleri ile onurlandıran akademisyenlere, Fikir / Görüş / Öneri / Katkı ve Eleştirileri ile değerlendirme süreçlerine katkılarından dolayı hakem ve yayın kurullarında yer alan kıymetli bilim insanlarına yürekten teşekkür ediyoruz. Bir sonraki sayıda görüşmek ümidiyle…

15.04. 2024
Editör
Prof. Dr. Ali Aslan

Reviewers of the Issue / Sayının Hakemleri*

* The ranking is arranged alphabetically within the academic title. * sıralama akademik unvan içinde alfabetik sıralamaya göredir.

Dr. Adil Uztemur, PhD, Ministry Of Agriculture And Forestry

Dr. Ahmad Sh. A. Lafi, PhD, University of Anbar

Dr. Ali Aslan, PhD, Van Yuzuncu Yil University

Dr. Bahadır Altun, PhD, Kirsehir Ahi Evran University

Dr. Bugrahan Emsen, PhD, Karamanoglu Mehmetbey University

Dr. Erol Aydin, PhD, Black Sea Agricultural Research Institute

Dr. Ferah Cömert Önder, PhD, Canakkale Onsekiz Mart University

Dr. Fulya Uzunoglu, PhD, Hatay Mustafa Kemal University

Dr. Hasan Akan, PhD, Harran University

Dr. Hossein Zeinalzadeh Tabrizi, PhD, Kyrgyz- Turkish Manas University

Dr. Kubilay Inci, PhD, Pamukkale University

Dr. Mehmet Ozcan, PhD, Zonguldak Bulent Ecevit University

Dr. Nevzat Batan, PhD, Karadeniz Technical University

Dr. Nurbek Aldayarov, PhD, Kyrgyz- Turkish Manas University

Dr. Ömer Sarı, PhD, Samsun Black Sea Agricultural Research Institute Directorate

Dr. Ruslan Adil Akai Tegin, PhD, Kyrgyz-Turkish Manas University

Contents/ İçindekiler

Research Articles/ Araştırma Makaleleri

Edwarsiella ictaluri: Pathogenicity and LD50 in Pangasius nasutus
Mohd Syafiq Syauqi Mohd Salim Nur Nazifah Mansor Muhamad Zudaidy Jaapar Muhamad Faizal Mohd **1-11**

Recombinant Production of Hydrophobin DewA in Pichia pastoris and Determination of Its Functions
Alpgiray Turgut Ayşenur Yazıcı Mesut Taşkın Serkan Örtücü **12-20**

Comparative Analysis of CDK4/6 Inhibitors (Ribociclib and Palbociclib) combined with Enzalutamide in Triple-negative breast cancer cells
Murat Keser Harika Atmaca Şaziye Burçak Karaca **21-27**

Morphological characterization of some local watermelon (Citrullus lanatus L.) genotypes of Turkey
Nihan Şahin **28-36**

Prevalence of Edwardsiella ictaluri in cage cultured Pangasius spp in Pahang River and their risk factors
Amira Syahidah Nordın Nur Nazifah Mansor Rimatulhana Ramly Asnor Sabuti Mohamad Shafiq Mohd Ibrahim **37-45**

Effects of Different Growing Medium on Obtaining Bulblets from Bulb Scales in Oriental Lilium 'Siberia' Cultivar
Ömer Sarı **46-51**

Exploring anti-cancer constituents and cytotoxic effects of Feijoa sellowiana fruit extract on breast cancer
Çisil Çamlı Pulat, Süleyman İlhan **52-59**

Smartphone-Based Point-of-Care Urinalysis Vivoo App: A Validation Study
Balım Bengisu Caf Gizem Çebi Haluk Çelik Aliasghar Noroozi Ali Atasever Miray Tayfun **60-73**

International Journal of Life Sciences and Biotechnology
Syafiq-Syauqi S. et al., *Edwardsiella ictaluri*: Pathogenicity and LD_{50} in *Pangasius nasutus*. International Journal of Life Sciences and Biotechnology, 2024 7(1): p. 1-11.
https://doi.org/10.38001/ijlsb.1398037
Araştırma makalesi/ Research article.

Edwardsiella ictaluri: Pathogenicity and LD_{50} in *Pangasius nasutus*

S.Syafiq-Syauqi [1], M.Nur-Nazifah [1]*, M.Zudaidy Jaapar [2], M.Muhammad-Faizal [1]

ABSTRACT
This study focuses on pathogenicity and LD_{50} of *Pangasius nasutus* against *Edwardsiella ictaluri*. *Pangasius nasutus* or 'patin buah' is a native freshwater species of peninsular Malaysia and can be found in Pahang River. The market price for this species is high as it tastes better compared to other catfish. *Edwardsiella ictaluri* is a pathogenic bacteria and the causative agent that cause enteric septicemia of catfish (ESC) in the Pangasius species. However, the prevention measures against *Edwardsiella ictaluri* are still unknown for *Pangasius nasutus* due to the lack of research and study. Therefore, the objective of this study is to identify *Edwardsiella ictaluri* isolated from *Pangasius nasutus* cultured in Pahang River using polymerase chain reaction (PCR) and to determine the pathogenicity and LD_{50} of *Pangasius nasutus* against *Edwardsiella ictaluri* through injection method. There are four different concentrations of *Edwardsiella ictaluri* (1×10^{20}, 1×10^{9}, 1×10^{8}, 1×10^{7}) that were injected intraperitoneally including normal saline water as control to a total of 50 *Pangasius nasutus*. Observation of clinical signs and mortality were carried out for 30 days and LD_{50} was determined. The earliest clinical sign was observed at concentration of 1×10^{10} cfu/ml at 2 hours postinfection of *Edwardsiella ictaluri* where pale liver and congested kidney can be observed after dissection. Other clinical signs observed are inflammation on tail and fin, hemorrhagic fin, hemorrhagic upper mandible, discoloration, and inflammation on the lower part of body. The first mortality of *Pangasius nasutus* was at concentration 1×10^{10} cfu/ml at 2 hours of post infection. The highest cumulative mortality was recorded at concentration 1×10^{10} cfu/ml with 100% of mortality rate. From the result, the value of LD_{50} of *Edwardsiella ictaluri* calculated was 1×10^{6} cfu/ml. From this study, it can be concluded that *Edwardsiella ictaluri* does affect the survivability *Pangasius nasutus* in Malaysia.

ARTICLE HISTORY
Received
29 November 2023
Accepted
5 January 2024

KEYWORDS
Pangasius nasutus, *Edwardsiella ictaluri*, enteric septicemia of catfish (ESC), pathogenicity, polymerase chain reaction (PCR)

Introduction

Pangasius nasutus is a shark catfish family *Pangasiidae*, commonly found in freshwater habitats, particularly in South and Southeast Asia. It is known for its distinctive appearance and is often sought after by local communities for its delicious taste and nutritional value. In Malaysia, it is locally referred as 'Patin Buah' and is highly regarded as a delicacy, especially when cooked with fermented durian called 'tempoyak' [9]. This unique combination of flavors creates a culinary experience that is cherished by both locals and tourists, making it an important part of the cultural heritage of the region.

Pangasius nasutus is a highly sought-after food fish known for its exceptional culinary qualities. It boasts a delectable flavor profile, characterized by its very white, fine-grained, and sweet flesh. However, despite its undeniable appeal, this species remains relatively elusive in the market. The limited availability of *Pangasius nasutus* is primarily attributed to its dependence on wild catches, which, unfortunately, has resulted in a significant reduction in its natural resources [3]. This scarcity further contributes to the challenges of procuring this remarkable fish.

Furthermore, *Pangasius nasutus* is characterized by its slow growth rate, which significantly impacts its market price. The cost of acquiring this fish is nearly five times higher than *Pangasianodon hypophthalmus*. In light of these factors, the procurement and accessibility of *Pangasius nasutus* pose considerable challenges for both consumers and suppliers alike. There is typically limited information available about the fish. Therefore,

[1] Department of Marine Science, Kulliyah of Science, International Islamic University Malaysia, Jalan Istana, 25200 Kuantan, Malaysia
[2] Department of Fisheries, Fisheries Research Institute (FRI), Glami Lemi, Titi, 71650 Jelebu, Negeri Sembilan, Malaysia
*Corresponding Author: Nur Nazifah Mansor, e-mail: nurnazifah@iium.edu.my

additional research is required in areas such as nutrition, brood stock management, breeding technology, and genetics to promote the growth of the species in commercial aquaculture [1].

Edwardsiella ictaluri is a Gram-negative bacterium that is pathogenic to fish, particularly channel catfish (*Ictalurus punctatus*). It is the causative agent of enteric septicemia of catfish (ESC) which were a significant disease in the catfish aquaculture industry. *Edwardsiella ictaluri* was first described in the 1970s and has since been recognized as a major pathogen affecting catfish farms in the United States and other parts of the world [13]. *Edwardsiella ictaluri* is a type of bacteria that can cause severe infections in channel catfish. This bacterium is a highly contagious and deadly disease that affects the digestive system of catfish.

ESC caused by *Edwardsiella ictaluri* poses a significant threat to the catfish aquaculture industry. Infected fish experience symptoms such as bloating, lethargy, loss of appetite, and ultimately death [4]. The economic impact of this disease is substantial, leading to financial losses for catfish farmers. The discovery of *Edwardsiella ictaluri* dates back to the 1970s, and since then, it has gained recognition as a major pathogen affecting catfish farms worldwide. Owing to its ability to rapidly spread and cause devastating outbreaks, strict biosecurity measures are necessary to control the transmission of this bacterium within aquaculture facilities.

However, there has been relatively little research conducted on the best identification method used to identify Edwardsiella ictaluri, the bacterium that can infect Pangasius nasutus in Malaysia. Furthermore, there has been a complete absence of studies exploring the LD50 (lethal dose 50%) of Edwardsiella ictaluri on Pangasius nasutus in Malaysia. This knowledge gap has raised significant concerns among researchers, prompting the urgent need for investigation in this area. Hence, the objective of this study is to identify isolate of Edwardsiella ictaluri using molecular biology approach (PCR) and to determine the pathogenicity and LD50 of Edwardsiella ictaluri in Pangasius nasutus through injection method.

Material and Methods

Selection of Pangasius nasutus for bacterial isolation

Samples of Pangasius nasutus were taken from a farm located at Kampung Lebak Seberang, Temerloh, Pahang. Random sampling was done where 10 pieces of fish with severe clinical signs such as fish gasping at water surface were taken and dissected. All procedures when handling and dissecting fish has obeyed the Animal Welfare act which was carried out solely for research purposes. Organs such as brain, kidney, liver and spleen in every fish sample were streaked onto TSA agar (Oxoid, England) to acquire bacterial isolates. All bacterial isolates were incubated at 28°C for 48 hours in the incubator.

Identification of bacteria *Edwardsiella ictaluri*

Isolation of *Edwardsiella ictaluri*

The isolate of *Edwardsiella ictaluri* was isolated from *Pangasius nasutus* cultured in a cage system. Then, sample of bacteria was cultured again on TSA agar (Oxoid, England) in order to obtain single and pure colony. The optimum condition for *Edwardsiella ictaluri* to grow was 28°C at 48 hours of incubation period.

DNA Extraction (G-Spin™ Total DNA Extraction Kit, Protocol F)

DNA extraction was carried out by using G-Spin™ Total DNA Extraction Kit according to protocol F for bacteria. Single colony from TSA agar were pick up and inoculated into 5 ml of Brain Heart Infusion (BHI) broth (Oxoid, England). Then, the BHI broth was incubated for 48 hours at 28°C, 100 rpm. After that, bacteria were pelleted by centrifugation for 1 min at 13,000 rpm, and supernatant was discarded. The cell pellet was resuspended completely with remnant supernatant by vigorously vortex.

To prepare the sample, 200 µl of Buffer CL, 20 µl of Proteinase K, and 5 µl of RNase A Solution was added to the sample tube. The mixture was vortexed vigorously to ensure thorough mixing. The lysate was incubated at 56°C using a preheated heat block for 6 minutes. During the incubation, the sample tube was inverted gently every 2 minutes to aid in sample lysis. Once the lysis is complete, 200 µl of Buffer BL was added to the upper sample tube and mixed it thoroughly. Then, the mixture was incubated at 70°C for 2 minutes.

The sample tube was centrifuged at 13,000 rpm for 5 min to remove un-lysed tissue particles. Then, 350 - 400 µl of the supernatant was transferred into a new 1.5 ml tube. 200 µl of absolute ethanol was added into the lysate, and mixed well by pulse vortex. After mixing, the 1.5 ml tube was briefly centrifuged to remove drops from inside of the lid.

After that, the mixture was carefully applied to the Spin Column. Then without wetting the rim, close the cap, and centrifuged at 13,000 rpm for 1 min. The filtrate was discarded and the Spin Column was placed in a new 2 ml Collection Tube.

Next, 700 µl of Buffer WA was added to the Spin Column without wetting the rim, and centrifuged for 1 min at 13,000 rpm. The flow-through was discarded and the Collection Tube was reused. Then, 700 µl of Buffer WB was added to the Spin Column without wetting the rim, and centrifuged for 1 min at 13,000 rpm. The

flow-through was discarded and placed the Column into a new 2.0 ml Collection Tube. Then, centrifuged again for additional 1 min to dry the membrane. The flow-through and Collection Tube were discarded altogether. The Spin Column was placed into a new 1.5 ml tube. Then, 50 µl of Buffer CE was added directly onto the membrane. After that, the tube was incubated for 1 min at room temperature and then centrifuged for 1 min at 13,000 rpm to elute and DNA was obtained until further used.

Polymerase Chain Reaction (PCR) and Gel Electrophoresis

The conventional Polymerase Chain Reaction (PCR) method was carried out on DNA of *E. ictaluri* extracted earlier. The species-specific primers of *Edwardsiella ictaluri* (Table 1) were employed for sequence amplification [7] and to distinguish *Edwardsiella ictaluri* from *Edwardsiella tarda*. The composition of master mix for PCR by using (Thermo Scientific™, America) was shown in (Table 2) and the final volume PCR was 50 µL.

Table 1 Specific primers used for sequence amplification

Primer	Genetic Code
IVS	5'-TTA AAG TCG AGT TGG CTT AGG G-3'
IRS	5'-TAC GCT TTC CTC AGT GAG TGT C-3'

Table 2 The composition of PCR master mix

PCR Component	Volume
Pure distilled water	43 µL
Buffer	2 µL
Mg2+	2 µL
IVS	0.5 µL
IRS	0.5 µL
Deoxynucleotide triphosphates (dNTPs)	0.5 µL
DNA polymerase	0.5 µL
Template DNA	1 µL

Edwardsiella ictaluri ATCC was used as positive control while distilled water was used as negative control. The total time taken to process PCR products was 2 hours 29 minutes. PCR condition for both of primers pairs (IVS and IRS) was shown in Table 3.

Table 3 PCR Amplification Parameter

Process	Duration	Temperature
initialization	4 minutes	94°C
denaturation	1 minute	94°C
annealing	1 minute	50°C
extension	1 minute	72°C
final elongation	10 minutes	72°C

After that, 2 µL of PCR product and 2 ul of 6× loading dye (First Base, Singapore) were mixed and electrophoresed through a 1% of agarose (First Base, Singapore) gel containing Gel Red (First Base, Singapore) and observed under Gel Doc XR+ Gel Documentation System (BioRad, California). The band sizes which can be visible for *Edwardsiella ictaluri* were 2000-bp and 1kb DNA Ladder (Thermo Scientific™ GeneRuler, America) was used.

Pathogenicity and LD_{50}

Bacteria Revirulent

The single colony of *Edwardsiella ictaluri* were cultured in 250 ml of Brain Heart Infusion (BHI) broth (Oxoid., England) and incubated at 28°C for 48 hours with 100 rpm shaking movement. Then, 1 ml of the inoculum was injected to the experimental fish via intraperitoneal and left for a period of 12 hours. After 12 hours of post-injection, the symptomatic injected fish was dissected. Bacterial samples from organs (spleen, liver, kidney, brain) were isolated and streaked onto TSA (Oxoid., England) agar plates. All agar plates were sealed with parafilm and incubated at temperature of 28°C for 48 hours in the incubator. After 48 hours, the re-virulent bacteria were obtained.

Serial Dilution and Colony Forming Unit (CFU)

A total of 10 colonies of virulent bacteria were inoculated into 250 ml of Brain Heart Infusion (BHI) broth (Oxoid., England) and then incubated at 28ºC for 48 hours with 100 rpm in the incubator shaker. Next, tenfold serial dilution was done where the ratio must be 1:10 according to Robert Koch method [17]. Next, spread plate method was done to determine the concentration of inoculum. The number of colonies in each plate was counted after 48 hours of incubation at 28ºC. The concentrations of bacteria suspension were determined by using the colony-forming unit (CFU) formula (Table 4) [18]. There were 4 different concentrations of bacteria used in this experiment which were (1×10^{10}, 1×10^{9}, 1×10^{8}, 1×10^{7}) (cfu/ml) and one control treatment.

Table 4 CFU Formula

Formula
CFU/ml = (Number of colonies × dilution factor) / volume of culture plate

Experimental Designs

In this experiment, a total of 100 fish of *Pangasius nasutus* were used with the average weight of 40 g ± 5g. These fish were acclimatized in 1-ton tank for a week to enable them to be accustomed in new environmental conditions. A total of 4 different concentrations of *Edwardsiella ictaluri* which consist of (1×10^{10} cfu/ml, 1×10^{9} cfu/ml, 1×10^{8} cfu/ml, 1×10^{7} cfu/ml), and one control treatment (saline water) was used in this experiment. Tank for each concentration of *Edwardsiella ictaluri* and control treatment was duplicated. The size of the tank used is 50 L and were set up with aeration system. The stocking density was 10 fish per tank.

All fish were injected via intraperitoneal according to concentration of *Edwardsiella ictaluri* and saline water (control). All activities when conducting this experiment has obeyed the Animal Welfare act including handling, feeding, and dissecting that was carried out solely for research purposes. Observations of fish in every tank was carried out for a period of 30 days and any clinical signs and mortality was observed and recorded daily. The experimental design conducted was shown as below (Fig 1).

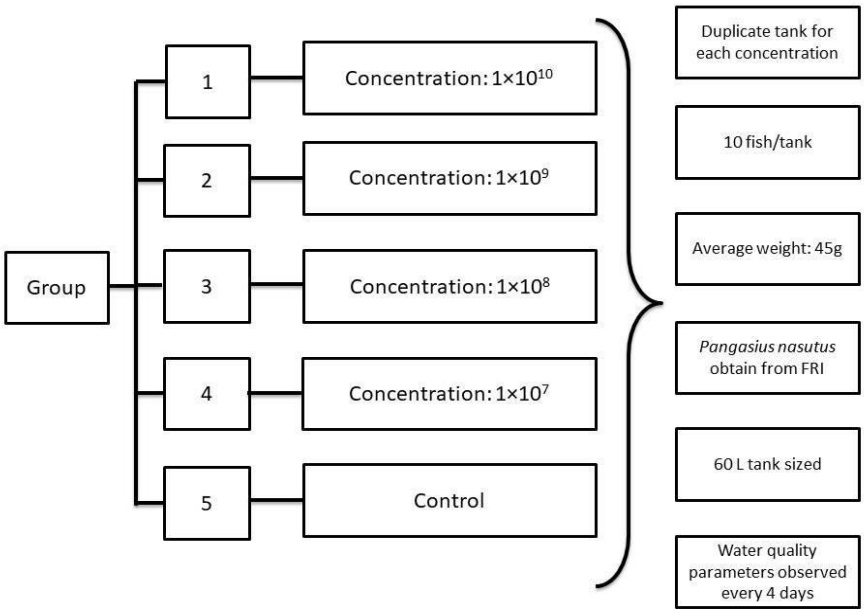

Fig 1 Experimental design

Data Analysis

Data obtained from the experiment was analyzed through statistical analysis using Paired Samples T-Test. This type of statistical analysis was used to differentiate the mean of mortality percentage and concentration of the *Edwardsiella ictaluri*. The data were analyzed by using IBM SPSS Statistic Version 20 with 95 % confidence interval. Meanwhile, LD_{50} for this experiment was measured using Curve Expert Professional Software (Version 2.7.4).

Results

Identification of *Edwardsiella ictaluri* using PCR

In this study, the species-specific primers IVS and IRS was used to identify *Edwardsiella ictaluri*. *Edwardsiella ictaluri* ATCC was used as positive control and distilled water was used as negative control. From PCR product, it showed the bacterial samples is positive *Edwardsiella ictaluri*. Positive PCR *Edwardsiella ictaluri* amplified at 2000bp. The image of PCR product on gel electrophoresis was shown in (Fig 2).

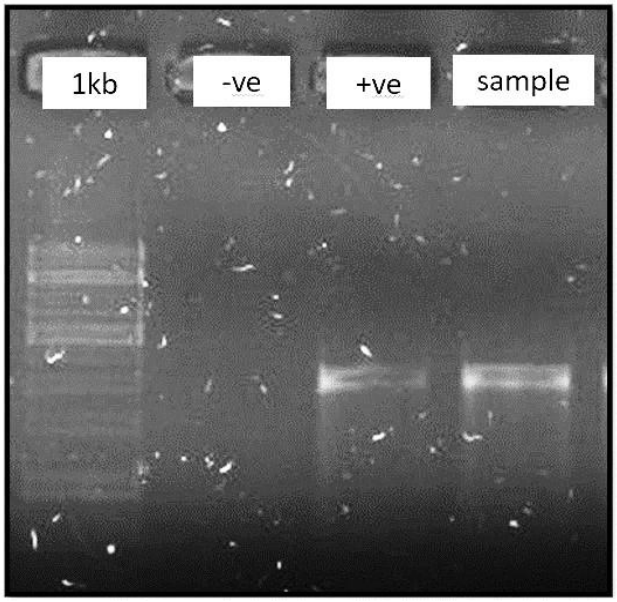

Fig 2 The image of PCR products on gel electrophoresis

Pathogenicity and Clinical Sign

The data analysis of cumulative and percentage mortality rates of *Pangasius nasutus* in 4 different concentrations of *Edwardsiella ictaluri* were obtained and calculated after 30 days of observation with results tabulated in (Table 5). The highest mortality percentage was recorded in tank with concentration of 1×10^{10} cfu/ml where mortality rate was 100%. Meanwhile, the second highest percentage of mortality was recorded in tank with concentration of 1×10^{8} cfu/ml with 80% mortality rate. The third highest mortality percentage was recorded in tank with concentration of 1×10^{7} and 1×10^{9} cfu/ml where the mortality percentage was 60%. The lowest percentage of mortality was recorded in control tank with with 0% mortality rate.

Table 5 The cumulative and percentage of mortality of *Pangasius nasutus* after been infected with *Edwardsiella ictaluri* in 4 different concentrations

Concentration	Number of experimental fish	Cumulative mortality	Percentage of mortality (%)
1×10^{10}	10	10	100
1×10^{9}	10	6	60
1×10^{8}	10	8	80
1×10^{7}	10	6	60
Control	10	0	0

The first mortality of *Pangasius nasutus* was observed in the tank with concentration of 1×10^{10} cfu/ml where fish died 2 hours post infection of *Edwardsiella ictaluri* (Fig 3). Half mortality of *Pangasius nasutus* from the whole population has been observed in the tank with concentration of 1×10^{10} cfu/ml on 19th days after post-injection. The last mortality of *Pangasius nasutus* recorded in this experiment was on 26th day after post-injection in tank with concentration of 1×10^{9} cfu/ml.

Fig 3 First mortality of *Pangasius nasutus* 2 hours post-injection

For tank infected with *Edwardsiella ictaluri* concentration of 1×10^{10} cfu/ml, the percentage of mortality was 100% where 10 fish died out of 10. Meanwhile, for tank infected with *Edwardsiella ictaluri* concentration of 1×10^{7} and 1×10^{9} cfu/ml, the percentage mortality was 60% where 6 fish died out of 10 fish. For tank infected with *Edwardsiella ictaluri* concentration of 1×10^{8} cfu/ml, the percentage mortality was 80% where 8 fish died out of 10 fish. For control tank with no infection of *Edwardsiella ictaluri*, the percentage mortality was 0% as there was no mortality recorded.

After 30 days of experiment, there were several clinical signs which has been observed including fish behaviour, external and internal organs. For fish behaviour, it has been observed that infected fish in tank infected with *Edwardsiella ictaluri* concentration of 1×10^{8} cfu/ml demonstrates erratic swimming and tend to swim vertically before dying (Fig 4).

As for external organ, it has been observed that infected fish in tanks infected with *Edwardsiella ictaluri* concentration of 1×10^{10}, 1×10^{9}, 1×10^{8}, and 1×10^{7} cfu/ml have inflammation on its tail and fin (Fig 5), hemorrhagic fin, hemorrhagic upper mandible, discoloration, and inflammation on the lower part of the body.

Fig 4 Vertical swimming of fish

Fig 5 Inflammation of tail and fin

As for internal organs, it has been observed that fish infected with all 4 concentrations of *Edwardsiella ictaluri* shown pale liver (Fig 6), congested kidney (Fig 7), and patchy liver (Fig 8). Meanwhile, infected fish in tank infected with *Edwardsiella ictaluri* concentration of 1×10^{7} cfu/ml shown white nodular on liver (Fig 9). On the other hand, dark liver (Fig 10) has been spotted in infected fish infected with *Edwardsiella ictaluri* concentration of 1×10^{8} cfu/ml. However, there were no clinical signs observed on fish in the control tank.

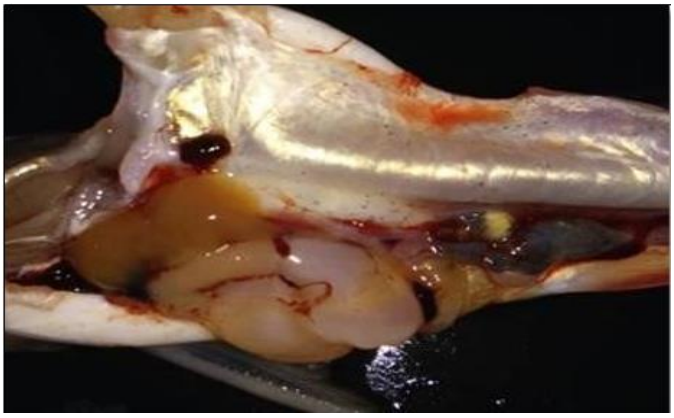

Fig 6 Pale liver

Fig 7 Congested kidney

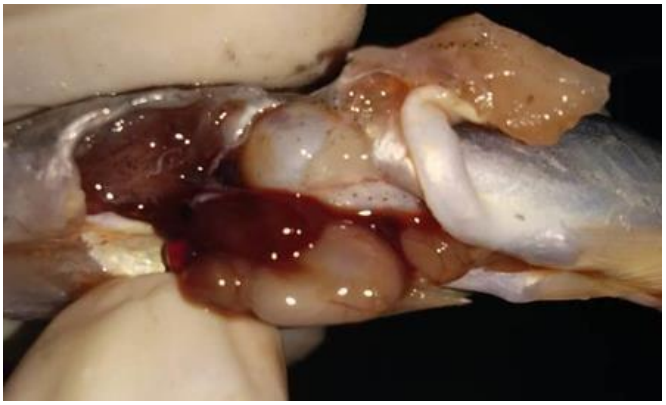

Fig 8 Patchy liver

Fig 9 White nodules on liver

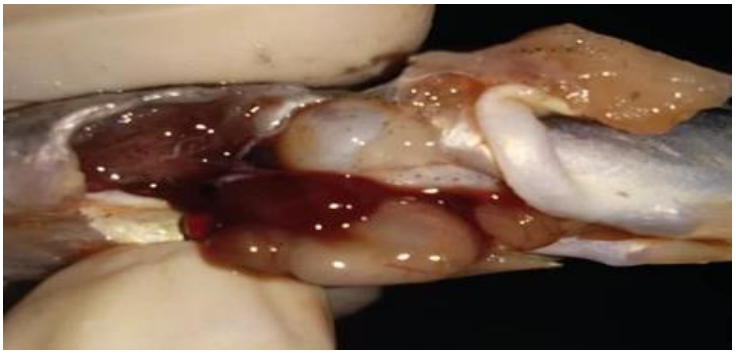

Fig 10 Dark liver

Lethal Dose 50 of *Pangasius nasutus*

The lethal dose 50 (LD_{50}) of *Edwardsiella ictaluri* was determined by plotting the graph of mortality percentage of *Pangasius nasutus* against different concentrations of *Edwardsiella ictaluri* as variables by using the Curve Expert software. Based on (Fig 11), the graph has been plotted and the linear line could be drawn which was satisfyingly validated to represent a trend line and almost pass all the plotted point in the graph. The calculation of LD_{50} has been computed by using the graph analysis and the value of LD 50 calculated in the graph was 1×10^6 cfu/ml (Fig 12).

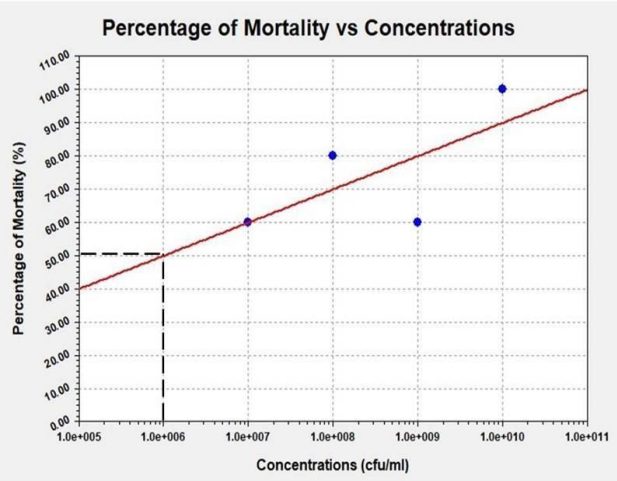

Fig 11 Graph of mortality percentage of *Pangasius nasutus* against concentration of *Edwardsiella ictaluri*

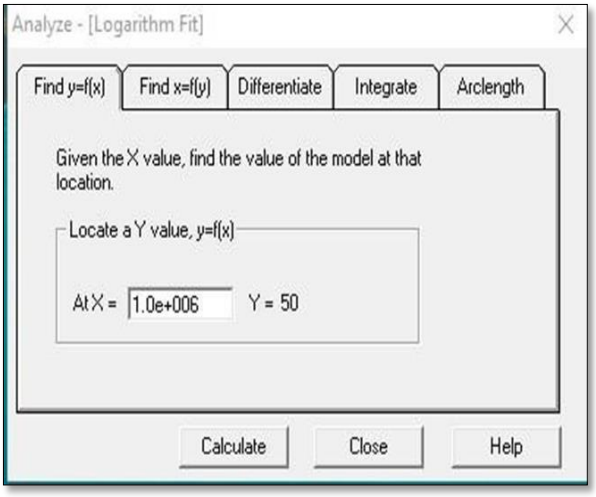

Fig 12 LD_{50} of *Edwardsiella ictaluri* on *Pangasius nasutus*

Statistical Analysis

It has been analysed that there was no significant difference between percentage mortality of *Pangasius nasutus* and concentration of *Edwardsiella ictaluri* as P or significant value is more than 0.05 ($p > 0.05$). Therefore, the null hypothesis is not rejected.

Discussion Lethal Dose 50 (LD_{50})

Table 6 Size of experimental fish and LD_{50} based on published literature

Studies on LD_{50} and Pathogenicity of *Edwardsiella ictaluri* in Catfish	**Size of fish**	**LD_{50}**
Susanti, Indrawati & Pasaribu, 2017	6-10 g	2.8×10^4 cfu/ml
Dong et al. 2015	26.7 g ±8.7 g	2.6×10^6 cfu/ml
Koswara, 2009	5-6 g	1.3×10^4 cfu/ml
Phuoc, Richard & Crumlish, 2020	15-20 g	1.1×10^7 cfu/ml
Current study	40 g ± 5g	1×10^6 cfu/ml

Based on the results of this comprehensive study, it has been determined that the LD_{50} (lethal dose for 50% of the population) of *Edwardsiella ictaluri* on *Pangasius nasutus* is 1×10^6 cfu/ml. This finding is supported by a study conducted by [12], which found that the LD_{50} of *Edwardsiella ictaluri* causing 50% mortality in *Pangasianodon hypophthalmus* with the size of 6-10 g is 2.8×10^4 cfu/ml. Moreover, [2] reported in their study that an infection of *Edwardsiella ictaluri* with a concentration of 2.6×10^6 cfu/ml can result in 50% mortality in *Pangasianodon hypophthalmus*. Another noteworthy research study conducted by [6] reported that the LD_{50} of *Edwardsiella ictaluri* on *Clarius sp* is 1.3 x 10^4 cfu/ml. Finally, according to [10], LD_{50} of *Edwardsiella ictaluri* causing 50% mortality in *Pangasianodon hypophthalmus* is 1.1×10^7 cfu/ml.

Based on findings of multiple comprehensive literatures conducted in this study, it can be inferred that the LD_{50} result obtained from current study was relatively higher by using local isolates in approximately 40 g fish. One of the most significant factors identified is the notable difference in the size of the catfish used between those literatures. Theoretically, it is wellestablished that the LD_{50} value tends to be lower in smaller-sized fish when compared to their larger counterparts. This is primarily due to the relatively underdeveloped immune system of smaller fish, rendering them more susceptible to bacterial infections [15]. The less mature immune system of smaller fish creates a vulnerability that allows bacteria to easily infect the host [16]. On the

other hand, larger fish typically possess a more evolved and robust immune system, necessitating a higher concentration of bacteria to successfully infect the host [15].

Pathogenicity and Clinical Signs

Based on the results of this experiment, it has been observed that the earliest clinical sign recorded is infected fish with a concentration of 1×10^{10} cfu/ml. After a period of 2 hours postinjection, the infected fish exhibit a pale liver and congested kidney after the dissection procedure. Furthermore, one of the notable clinical signs that can be observed in a tank with a concentration of 1×10^{8} cfu/ml is the catfish displaying a tendency to swim vertically, with its head positioned on the water surface shortly before succumbing to the infection. According to [12], their study found that *Pangasianodon hypophthalmus* infected by *Edwardsiella ictaluri* with concentrations ranging from 1×10^{4} - 1×10^{10} cfu/ml results in fish swimming vertically with their head on the water surface. Additionally, [5] also noted in their research that the infection of *Edwardsiella ictaluri* in fingerling yellow catfish can lead to the fish swimming with their head hanging on the water surface just prior to death.

The main possible reason for the observed clinical sign in fish is hypoxia, a condition characterized by low oxygen levels in the body. This can occur when the defence mechanism, particularly the immune system, is compromised. In the case of fish infected with *Edwardsiella ictaluri,* it is believed that fat degeneration occurs due to the presence of a toxin that disrupts the normal pathways of fat metabolism. This disruption ultimately leads to hypoxia, resulting in reduced blood flow and oxygen supply to the fish's body. As a consequence of hypoxia, fish may exhibit abnormal swimming behaviour, such as erratic and vertical movements. It appears as if the fish are hanging their heads on the water surface, struggling to maintain their equilibrium. This behaviour can be attributed to the fish's attempt to obtain more air supply, as the reduced blood flow limits the amount of dissolved oxygen reaching their tissues [6]. Other clinical signs that can be observed in this experiment include inflammation on the lower part of the body, tail, and fin. The main cause of inflammation on the lower abdomen of catfish is the effect of *Edwardsiella ictaluri* Lipopolysaccharide (LPS). Lipopolysaccharides, which are the main component of the exterior membrane of Gram-negative bacteria, act as endotoxins. They play a crucial role in the pathogenesis of infections caused by these bacteria. The Opolysaccharide chains of LPS are involved in resistance to complement-mediated killing. Complement is a part of the immune system that helps in clearing microbes and damaged cells from the body. By interacting with antibodies and phagocytic cells, LPS enhances the ability of the immune system to identify and eliminate pathogens. However, this immune response also leads to the promotion of inflammation and the attack on the pathogen's cell membrane.

A study by [8] highlighted the role of LPS in promoting inflammation and its impact on the pathogen's cell membrane. It was found that LPS has the ability to induce an inflammatory response and cause tissue damage in catfish. According to [11], *Edwardsiella ictaluri* LPS specifically affects internal inflammation and tissue damage in catfish. In summary, the presence of *Edwardsiella ictaluri* LPS in catfish leads to inflammation in various parts of the body, including the lower abdomen, tail, and fin. This inflammation is a result of the interaction between LPS and the immune system, which aims to clear the infection. However, this immune response can also cause tissue damage.

Next, based on the findings of this study, the clinical signs that can be observed in infected catfish include the presence of patchy, lesions, and white nodules on the liver. According to the research conducted by [14], it has been described that a majority of *Edwardsiella ictaluri* strains exhibit haemolytic activity across a range of temperatures. Haemolysin, in essence, can be defined as an extracellular toxic protein that plays a crucial role in the penetration of mucosal layers. By facilitating intracellular survival, haemolysin enables the bacteria to spread more effectively within the host organism. This phenomenon elucidates the ability of *Edwardsiella ictaluri* to colonize the layer of peritoneal muscle and internal organs of catfish, as the bacteria are capable of penetrating the mucosal layer, which serves as the fish's primary defense mechanism in its immune system.

Furthermore, based on the findings of this study, the clinical signs that can be observed in infected catfish include the presence of patchy, lesions, and white nodules on the liver. The significance of these findings is highlighted by the research conducted by [14], which indicates that a majority of *Edwardsiella ictaluri* strains exhibit haemolytic activity across a range of temperatures. Haemolysin, an extracellular toxic protein, plays a crucial role in the pathogenicity of *Edwardsiella ictaluri*. It facilitates the penetration of mucosal layers, allowing the bacteria to establish an intracellular presence. This ability to survive and replicate within host cells enhances the spread of the bacteria throughout the host organism. Consequently, *Edwardsiella ictaluri* is able to colonize the peritoneal muscle layer and internal organs of catfish. This colonization is made possible by the bacteria's ability to penetrate the mucosal layer, which serves as the first line of defense in the fish immune system.

Furthermore, clinical signs that can be observed on the catfish are hemorrhagic in the upper mandible and fin. The main cause of hemorrhagic symptoms on the fish's body is due to damaged capillary endothelium, where infectious agents are circulating in the blood vessels [12]. Therefore, this indicates that *Edwardsiella ictaluri* is a destructive septicemia blood vessel, as bleeding occurs and forms an accumulation of blood fluid in the peritoneal cavity.
This is the main reason for the congested kidney that occurs internally in the catfish's body.

Conclusion

The LD_{50} of local bacterial isolate of *Edwardsiella ictaluri* on *Pangasius nasutus* was 1×10^6 cfu/ml in approximately 40 g fish. The tank infected with *Edwardsiella ictaluri* concentration of 1×10^{10} cfu/ml recorded the highest cumulative mortality rate, with 100% mortality. The earliest clinical sign was observed in the tank with concentration of 1×10^{10} cfu/ml 2 hours post infection where pale liver and congested kidney observed after dissection procedure. The finding of this research could lead to a better treatment and prevention of *Edwardsiella ictaluri* in *Pangasius nasutus.*

Abbreviations
Brain Heart Infusion (BHI); CFU: Colony Forming Unit; E. ictaluri: Edwardsiella ictaluri; PCR: Polymerase Chain Reaction: TSA; Trypticase soy agar; ESC: Enteric Septicemia of Catfish

Acknowledgements
The author would like to thank International Islamic University Malaysia (under IIUM SDG Flagship-IRF19-0010001) for enabling this work to be accomplished.

References

1. Asdari, R., M. Aliyu-Paiko, and R. Hashim, Effects of different dietary lipid sources in the diet for Pangasius nasutus (Bleeker, 1863) juveniles on growth performance, feed efficiency, body indices and muscle and liver fatty acid compositions. Aquaculture nutrition, 2011. 17(4): p. 883-891. https://doi.org/10.1111/j.1365-2095.2011.00860.x.
2. Dong, Ha Thanh, et al., Concurrent infections of Flavobacterium columnare and Edwardsiella ictaluri in striped catfish, Pangasianodon hypophthalmus in Thailand. Aquaculture, 2015. 448: p. 142-150. https://doi.org/10.1016/j.aquaculture.2015.05.046.
3. Hassan, A., Ambak, M. A., and Samad, Crossbreeding of Pangasianodon hypophthalmus (Sauvage, 1878) and Pangasius nasutus (Bleeker, 1863) and their larval development. Journal of Sustainability Science and Management, 2011. 6(1): p. 28-35.
4. Hawke, J. P., et al., ESC-Enteric Septicemia of Catfish. SRAC Publication, 1998. 477: p. 1-6
5. Kim, J. D., and Park, S. W., Edwardsiella ictaluri infection in cultured yellow catfish Pelteobagrus fulvidraco fingerlings in Korea. Korean Journal of Fisheries and Aquatic Sciences, 2015. 48(5): p. 725-730. https://doi.org/10.5657/kfas.2015.0725.
6. Koswara, A. D., Kajian Patogenesis Infeksi Buatan Bakteri Edwardsiella ictaluri Pada Ikan Lele (Clarias Sp.), 2009.
7. Mawardi, M., et al., Identification and characterization of Edwardsiella ictaluri from diseased Pangasius pangasius, cultured in Cirata Lake, Indonesia. Biodiversitas Journal of Biological Diversity, 2018. 19(3): p. 816-822. https://doi.org/10.13057/biodiv/d190309.
8. Merino, S., et al., Cloning and sequencing of the Klebsiella pneumoniae O5 wb gene cluster and its role in pathogenesis. Infection and immunity, 2000. 68(5): p. 2435-2440. https://doi.org/10.1128/iai.68.5.2435-2440.2000.
9. Mohideen, N. H. R. H., et al., The Co-Isolation of Lactic Acid Bacteria (LAB) and A Related Pathogenic Strain from Pangasius Nasutus. International Journal of Life Sciences and Biotechnology, 2023. 6(2): p. 143-154. https://doi.org/10.38001/ijlsb.1268388.
10. Phuoc, N. N., Richards, R., and Crumlish, M., Environmental conditions influence susceptibility of striped catfish Pangasianodon hypophthalmus (Sauvage) to Edwardsiella ictaluri. Aquaculture, 2020. 523: p. 735226. https://doi.org/10.1016/j.aquaculture.2020.735226.
11. Santander, J., et al., Inflammatory effects of Edwardsiella ictaluri lipopolysaccharide modifications in catfish gut. Infection and immunity, 2014. 82(8): p. 3394-3404. https://doi.org/10.1128/iai.01697-14.
12. Susanti, W., Indrawati, A., and Pasaribu, F. H., Kajian patogenisitas bakteri Edwardsiella ictaluri pada ikan patin Pangasionodon hypophthalmus. Jurnal Akuakultur Indonesia, 2016. 15(2): p. 99-107. https://doi.org/10.19027/jai.15.99-107.

13. Walakira, J. K., et al., Identification and characterization of bacteriophages specific to the catfish pathogen, Edwardsiella ictaluri. Journal of applied microbiology, 2008. 105(6): p. 2133-2142. https://doi.org/10.1111/j.1365-2672.2008.03933.x.
14. Waltman, W. D., E. B. Shotts, and T. C. Hsu, Biochemical characteristics of Edwardsiella ictaluri. Applied and environmental microbiology, 1986. 51(1): p. 101-104. https://doi.org/10.1128/aem.51.1.101-104.1986.
15. Shoemaker, C., et al., Overview of fish immune system and infectious diseases. Dietary nutrients, additives, and fish health, 2015: p. 1-24. https://doi.org/10.1002/9781119005568.ch1.
16. Magnadottir, B., Immunological control of fish diseases. Marine biotechnology, 2010. 12: p. 361-379. https://doi.org/10.1007/s10126-010-9279-x.
17. Koch, A. L., Growth measurement. Methods for general and molecular microbiology, 2007: p. 172-199. https://doi.org/10.1128/9781555817497.ch9.
18. Sieuwerts, S., et al., A simple and fast method for determining colony forming units. Letters in applied microbiology, 2008. 47(4): p. 275-278. https://doi.org/10.1111/j.1472-765x.2008.02417.x.

International Journal of Life Sciences and Biotechnology
Turgut, A., et al., Recombinant Production of Hydrophobin DewA in *Pichia pastoris* and Determination of Its Functions.International Journal of Life Sciences and Biotechnology, 2024 7(1): p. 12-20.
https://doi.org/ 10.38001/ijlsb.1355883
Araştırma Makale/ Research article

Recombinant Production of Hydrophobin DewA in *Pichia pastoris* and Determination of Its Functions

Alpgiray TURGUT[1,2*], Ayşenur YAZICI[1,2], Mesut TAŞKIN[3], Serkan ÖRTÜCÜ[1,2]

ABSTRACT
Hydrophobins, found around the aerial hyphae and reproductive structures of fungi, are small amphipathic surfactant proteins. Due to these amphipathic properties, they can change the properties of the surfaces they are on. Thanks to these properties, hydrophilic surfaces can be obtained by imparting hydrophobic properties.. However, the low production amounts in the studies conducted to date limit biotechnological studies. In the study, pPICZα-A vector was used for high protein expression, since its restriction maps, gene functions and intracellular replication mechanisms are known. P. pastoris was used for recombinant production due to its low amount of endogenous protein production, especially capable of performing posttranslational modifications. codon optimization was first performed after obtaining the gene sequence of the DewA protein from GenBank (Uniprot ID: P52750). Firstly, the secretion signal sequence region of this sequence and the stop codon of the gene were removed. Then, the cutting region of restriction enzymes (EcoRI and XbaI) that did not cut the resulting sequence was added to the sequence. After it was synthesized commercially, it was produced recombinantly by plasmid isolation, enzyme cutting reaction and ligation processes. It was then transferred to P.pastoris by electroporation method. Optimization of methanol induction was carried out at 0.5%, 1% and 1.5%. Protein isolation was performed by taking samples every 24 hours during the incubation. After protein isolation, the surface properties on teflon and glass surfaces were examined. The optimal culture condition for DewA expression was obtained at 1% methanol concentration as 77 mg/L in 96 hour. Recombinant DewA has been proven to change the surface characteristics on the teflon and glass surfaces. Conclusions: In the study, the DewA protein of A.nidulans was cloned into the pPICZα-A vector and recombinantly produced in the P.pastoris X-33 strain for the first time.

ARTICLE HISTORY
Received
7 September 2023
Accepted
10 December 2023

KEYWORDS
HFBI
Pichia pastoris
silver staining,
surface coating

Introduction

Hydrophobins are found around the aerial hyphae and reproductive structures of fungi. They are small amphipathic surfactant proteins consisting of about 100-150 amino acids [1]. They provide their stable structure by containing 4 disulfide bonds (C1-C6, C2-C5, C3-C4 and C7-C8) and characteristically eight conserved cysteine amino acids [2]. Because they have amphipathic properties, they form a monolayer layer at hydrophilic-hydrophobic interfaces.[3] For example, they self-assemble at hydrophilic-hydrophobic interfaces such as water-air, water-oil, and water-hydrophobic solids. Because of these properties, hydrophobins play an important role in many industrial applications such as surface coatings, biosensors, self-cleaning surfaces [3,4,5]. In biological processes, various organic surfaces can be covered by proteins in seconds. Thanks to these properties, hydrophobins are widely used in fields such as regenerative medicine and tissue engineering [6]. Studies on coating proteins on surfaces have shown that the adhesion of proteins to a substrate or surface can be controlled by temperature, ionic strength, and buffer compositions [7]. In addition, adhesion and surface persistence are closely related to the size, structural stability and composition of the protein. Small and rigid proteins are preferred for surface applications as they are not prone to conformational changes after surface absorption [6,7].

[1]Department of Molecular Biology and Genetics, Faculty of Science, Erzurum Technical University, Erzurum, Turkey.
[2]Erzurum Technical University, High Technology Research and Application Centre, Molecular Microbiology Laboratory, Erzurum, Turkey.
[3]Department of Molecular Biology and Genetics, Faculty of Science, Atatürk University, Erzurum, Turkey.
*Corresponding Author: Alpgiray TURGUT e-mail: agiraytrgt@gmail.com

Eukaryotic and prokaryotic organisms are used in the production of recombinant proteins[8]. However, *P.pastoris*, which belongs to the Fungi kingdom, Ascomycota phylum, Saccharomycetes class, Saccharomcetales order, is an oval-shaped and single-celled eukaryotic creature with a diameter of 1-5 μm and a length of 5-30 μm [9], ease of application, low It is widely preferred in laboratory research due to its costly production, post-translational modifications such as glycosylation, methylation, proteolytic degradation, and low amount of endogenous protein production [10]. In addition, methylotrophic yeast is frequently used in genetic engineering and is a useful system for the efficient expression of heterologous proteins from milligram to gram [10].

There are two strong promoter genes, AOX and PGAP, that regulate protein production in *P.pastoris* [11]. PGAP provides high product yields in very short processing times [12]. However, the most preferred genes for these systems are the AOX genes. Thanks to the AOX1 gene, the transcription of foreign proteins can be controlled and efficiency is quite high [10]. When selecting vectors for protein expression, pPICZ and pGAPZ vectors are suitable. However, pPICZα-A/B/C vectors are more suitable for high throughput and are designed for simple cloning and selection, high level protein expression, and rapid detection and purification of recombinant protein. In addition, the most successful systems for the efficient production of heterologous proteins in studies carried out so far are expression systems in the presence of methanol [13].

Our study aimed to clone and produce the *Dew*A protein of *Aspergillus nidulans*, which has a high contact angle on the surface coatings, into the pPICZα-A vector by *P. pastoris* X-33 strain under the control of the AOX1 promoter. It also sheds light on the biotechnological use of recombinant *Dew*A.

Material and Methods

Strain, plasmids, and reagents

To be used in the study, pPICZα A and *P.pastoris* strain X-33 were obtained from the High Technology and Research Center. Plasmid Isolation Kit, Gel Extraction Kit, Genomic DNA Isolation Kit and 2X EcoTaq Master Mix were obtained from EcoTech Biotechnology; Restriction enzymes (*Xba*I, *Eco*RI and *Sac*I) and T4 DNA ligase were obtained from Thermo Fisher Scientific.

Construction Design, Cloning and Transformation

The amino acid sequence of *Dew*A (UniProt ID: P52750) was retrieved from UniProt (https://www.uniprot.org/). First, the secretion signal sequence and the stop codon of the *Dew*A gene were removed. Then, restriction enzymes that did not cut the obtained sequence were detected using the bioinformatics program (http://www.restrictionmapper.org/), and *Eco*RI and *Xba*I cutting sites were added to the sequence. Additionally, codon optimization was performed using the GENEWIZ tool. The sequence information of *Dew*A (Genbank ID: OQ721986) is given as supplementary material. The resulting sequence was synthesized by a commercial company in the pGSI vector containing the Amp resistance gene for selection. The pGSI plasmid containing the *Dew*A gene was transferred to *E.coli* cells by heat shock method. *Dew*A and linear pPICZαA vector were ligated with T4 ligase enzyme. The obtained ligation product (*Dew*A-pPICZαA) was transferred to *E.coli* cells by heat shock method. Positive colonies were then determined by PCR with primer 3'AOX (GCAAAATGGCATTCCTGACATCC) and α-signal factor (TACTATTGCCAGCATTGCTGC). *Dew*A-pPICZαA was linearized by setting up a cutting reaction with the *Sac*I restriction endonuclease enzyme. The purification of the obtained linear recombinant plasmid was performed by phenol-chloroform-isopropyl alcohol (25:24:1) method. (Fig 1 shows the ligation product design of DewA-pPICZαA protein)

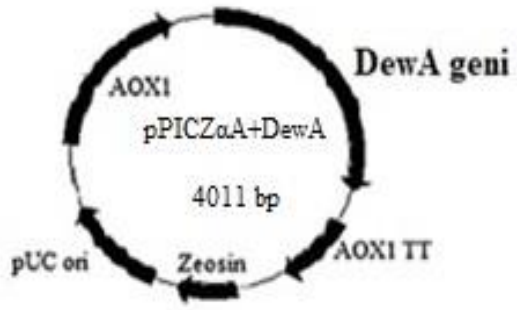

Fig 1 Design of DewA-pPICZαA

For the electroporation, 80 µl of component cells and approximately 15 µg of linear plasmid were mixed in a sterile PCR tube, then transferred to a 0.2 cm cold electroporation cuvette and incubated on ice for 5-6 minute. Electroporation was carried out by placing the cuvette in the Gene Pulser Xcell Electroporation Systems. Immediately after the electroporation process, 1 ml of 1M cold sorbitol was added to the cuvette and taken into a sterile 15 ml falcon tube. Then, incubated at 30°C for 2 hour on a shaker at 120 rpm, 50-200 µl was taken and spread on YPDS (yeast extract peptone dextrose medium containing sorbitol) agar containing 100µg/ml zeocin and incubated at 30°C for 10 days. Transformants were selected by genomic PCR using 5'AOX and 3'AOX primers. A lineralized pPICZαA vector was used as a negative control.

Recombinant production and purification of *Dew*A

Positive transformants (Fig 2) were inoculated into 25 ml of BMGY (buffered glycerol-complex medium) prepared for recombinant protein production and incubated at 150 rpm at 30°C for 24 hour. After the incubation, the cells were centrifuged at 3000 rpm for 5 minute and the supernatant was removed. The remaining pellet was dissolved in 3 ml BMYY (Buffered Glycerol-complex Medium) to remove glycerol, and then centrifuged again under the same conditions. After centrifugation, the supernatant was removed and the pellet was dissolved in 1 ml BMYY medium, then transferred to 100 ml BMMY medium prepared for protein production and incubated for 120 h at 30°C, 150 rpm. Methanol induction was optimized at 0.5%, 1% and 1.5% concentrations. During the incubation period, 2 ml of sample was taken every 24 h and centrifuged after OD_{600} measurement, and the pellet and culture filtrate was stored at -80°C until used for protein isolation.

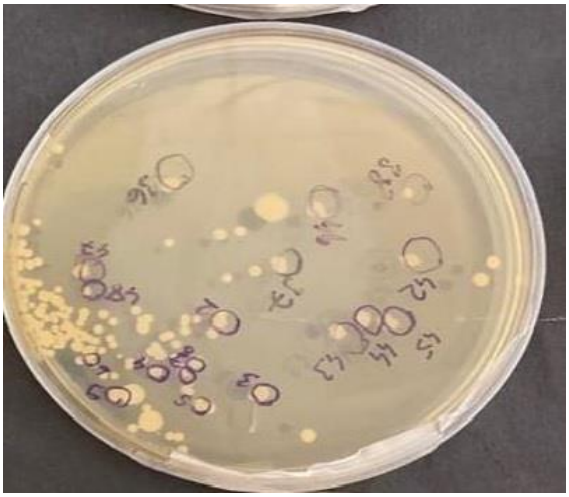

Fig 2 Positive isolates obtained after electroporation

The isolation of recombinant *Dew*A from the culture filtrate was performed according to the protocol for class 1 hydrophobins by [14]. Briefly, 20 ml of methanol, 5 ml of chloroform, and 15 ml of dH_2O were added into 50 ml of falcon tube, and 5 ml of culture filtrate was added, then mixed well and centrifuged at 10000 g for 25 minute. At the end of the period, the upper phase was removed and 5 ml of methanol was added to the remaining phase and mixed thoroughly. Then, the supernatant was removed by centrifugation at 10000g for 15 minute and the pellet was dried. The dried pellet was suspended by adding 200 µl of TFA. Then, TFA was evaporated under nitrogen gas and 100 µl of 6 M guanidine hydrochloride was added and the proteins were dissolved. Protein concentration was determined by the Bradford Assay [14].

Analyzes for recombinant proteins

SDS-PAGE and Silver Staining

Proteins were visualized on SDS-PAGE gel by silver staining technique. The resulting image was taken with a Bio-Rad gel imaging system. The silver staining technique was performed according to the protocol recommended by Lee et al [15].

According to this protocol; After the electrophoresis process, the gel was removed from the glass plates in order to visualize the proteins, and was kept in the fixation solution at +4 °C for 1 hour, and then washed in a horizontal shaker with dH_2O for approximately 1 hour. At the end of the period, dH_2O was removed and sensitizer solution was added to denature the proteins and incubated on a shaker for 1 minute. Then, after washing with dH_2O in a shaker for 10 minutes 3 times, the dH_2O was removed and placed in 0.1% silver solution. After washing in a shaker with dH_2O 3 times for 10 minutes to remove silver particles from the environment, the gel was transferred to a new tank, Developer solution was added and waited until the image

was taken. After the image was taken, the deleloper solution was removed from the tank, dH_2O was added to the gel, and washing was carried out in a shaker. Finally, the reaction was terminated by adding 0.5% acetic acid to the gel and photographed with the Bio-Rad gel imaging system.
Preparation of the solutions used;

- Gel fixation solution: 40 ml Ethanol, 10 ml Acetic Acid mixture was completed with distilled water until the total volume was 100 ml.
- Sensitizer solution: 0.04 g Sodium thiosulfate dissolved in 200 ml distilled water.
- Silver staining solution: The mixture of 0.2 g Silver nitrate and 0.02% Formaldehyde was completed with distilled water until the total volume was 200 ml.
- Developer/developer solution: The mixture of 7.5 g Sodium carbonate and 0.05% Formaldehyde was completed with distilled water until the total volume was 250 ml.

Coating of *Dew*A protein on glass and teflon surfaces

In the coating experiments, glass was preferred as the hydrophilic surface and teflon as the hydrophobic surface. Teflon and glass pieces (1x1 cm) were passed through 70% alcohol and treated with flame, then sterilized in an autoclave at 120°C and prepared for coating experiments. 100 µl of *Dew*A solution was taken and coating buffer (50 mM Tris/HCl, 1 mM $CaCl_2$, pH 8) was added so that the total volume was 1.2 ml [14]. After the glass and teflon pieces to be coated were taken into the 16-well plate, a control group was included for each sample and 250 µl of coating solution and incubated at 80°C.

Stability tests of coated surfaces

The stability of the coated surfaces was determined by hot SDS and UV application. For SDS stability, After the coated glass and teflon surfaces were exposed to 1% SDS for 60 min at 80°C, contact angles were measured and interpreted compared to the untreated control group. For UV stability, the contact angles were measured after the coated glass and teflon surfaces were exposed to UV light for 30, 60 and 90 minute and interpreted compared to the untreated control group [14].

Contact angle measurement

The contact angles of the coated glass and teflon surfaces were measured by the evaluation of the photographs taken in the system shown in Figure 5, prepared using a tilted stereo microscope suggested by [16] with Drop Snake Analysis in the ImageJ program. For this purpose, 2 µl of pure water was dropped on each of the coated surfaces with the help of a micropipette. Then, the photos of the drops were taken and transferred to the computer and the contact angles were calculated.

Results and Discussion

Construction of recombinant vector for the *P. pastoris* expression system

The pGSI-*Dew*A plasmid, which is approximately 3,268 bp long, was isolated from *E.coli* cells and restriction enzyme analysis with *Eco*RI and *Xba*I demonstrated that double digestion of plasmid an expected DNA fragment (*Dew*A gene, 411 bp) and vector backbone. The *Dew*A gene was cut from the gel and purified with the Ecotech Gel-PCR Purification Kit according to the protocol recommended by the manufacturer. The pPICZa-A plasmid was also subjected to the digestion reaction with the same enzymes. The pPICZα-A plasmid and *Dew*A gene were ligated with T4 ligase and the resulting product of approximately 4011 bp was confirmed by agarose gel (Fig 3).

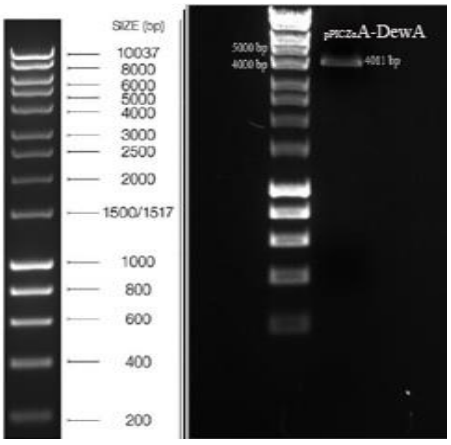

Fig 3 The pPICZa-A plasmid and the DewA gene were ligated with T4 ligase, resulting in a product of approximately 4011 bp

pPICZαA-*Dew*A plasmid was linearized with *Sac*I enzyme and was transferred to *P. pastoris* X-33 cells by electroporation. After incubation on a zeocin-containing plate for ten days, recombinant colonies were screened by PCR using AOX primers. At this stage, it is expected that the band containing the *Dew*A gene with a size of approximately 920 bp and a control band with a size of 2200 bp in which the AOX region in the genome of *P.pastoris* is amplified. Then, for sequence verification, the target band was cut from the gel and purified with the Ecotech PCR-Gel purification kit according to the protocol recommended by the manufacturer. The resulting sequence reads were combined into a single sequence and compared with the codon optimized sequence to determine whether there was a mutation.

Recombinant Production and Purification of *Dew*A

*Dew*A protein was produced by induction at 3 different methanol concentrations (0.5%, 1% and 1.5%) in studies with selected recombinant isolate in BMYY medium shaken culture. During the production, the OD_{600} value was measured by taking a sample every 24 hour until the 120th hour. For protein isolation, samples were taken every 24 hours and production amounts were determined. When Fig 4a is examined, protein production increased from the 24th hour to the 120th hour at 0.5% methanol concentration. However, the production seems to have reached its maximum at 96th hour at 1% and 1.5% methanol concentrations. In addition, protein production at 0.5% methanol concentration is approximately two times lower than at 1% and 1.5% methanol concentrations. When 1% and 1.5% methanol concentrations were evaluated among themselves, there was no statistically significant difference between protein production, especially at 96th and 120th hour ($p<0.05$). The highest production yield was reached at 1% methanol concentration at the 96th hour incubation period (77.42mg/L).

Proteins obtained at 3 different methanol concentrations at 96 hour were visualized on SDS-PAGE gel (Fig 4b) . Here, the *Dew*A protein is approximately 13 kDa, and the c-myc epitope region and His-Taq from the pPICZα-A vector were added to this protein at 2.5 kDa. Therefore, the recombinant *Dew*A protein is expected to give bands in the gel corresponding to approximately 15 kDa.

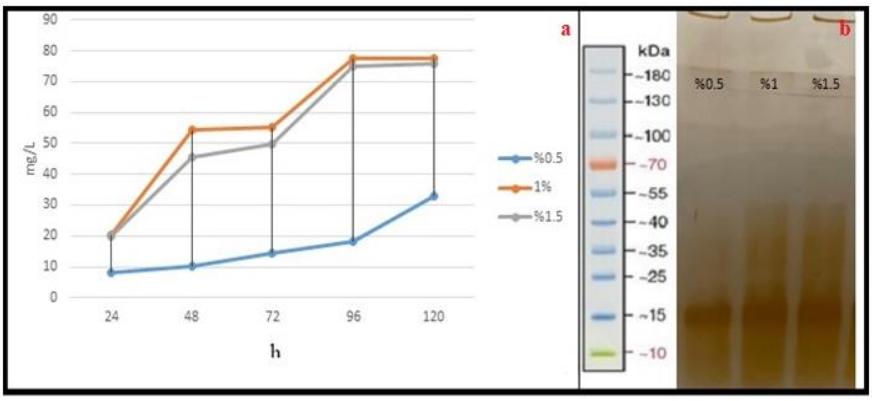

Fig 4 a: Amounts of protein produced at different methanol concentrations (mg/L) **b:** Protein bands obtained after 96 hour of incubation of three different methanol concentrations

***Dew*A protein coating on some surfaces and determination of contact angles**

In the coating experiments, glass was preferred as the hydrophilic surface and teflon as the hydrophobic surface. As a result of the measurement of contact angles, the angle determined as 6.174° on the glass surfaces (fig 5a) reached 70.125±5.18° after 100 µg *Dew*A protein coating (fig 5c). On the other hand, teflon surface angle, which was determined as 132.878° (fig 5b), decreased to 114.814±7.25° (fig 5d). As expected, the *Dew*A protein changed the characteristic of the surface.

In addition, stability tests of the coated surfaces were carried out to determine the durability of the recombinantly produced protein and its permanence on the surfaces. While the contact angle on the glass surfaces before the application was 70.125° in the experimental groups in which hot SDS was applied; after 60 minute of application, it was determined as 69.250±6.35°. On teflon surfaces, it was 114.814° before the application; it was measured as 123.388±10.72° after the application. The UV stability of the coated surfaces was measured after exposure to UV light for 30, 60 and 90 minute and interpreted compared to the untreated control group. While the contact angle before application on glass surfaces is 70.125°; as a result of 30 minute of UV application, it was determined as 7.25±1.5°. There was a statistical difference between the contact angle obtained and the contact angle of the glass surface before protein coating ($p<0.05$). On teflon surfaces, it is 114.814° before the application; After 30, 60 and 90 minute of UV application, the contact angle was measured

as 120.704±11.15°. The statistical difference between the UV applications at different times and the control contact angles was not found significant. Interestingly, according to the results obtained, the protein was not degraded by UV application on teflon surfaces and preserved its activity.

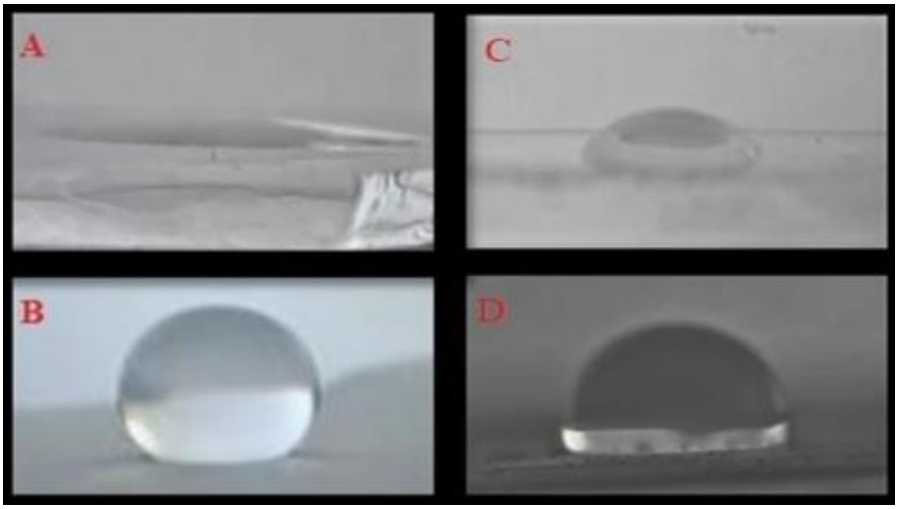

Fig 5 a: Glass surface before application, **b:** Teflon surface before application, **c:** Glass surface after application, **d:** Teflon surface after application

A. nidulans has six hydrophobins located on the conidiospore surface. Most of these hydrophobins belong to class I, potentially being used for highly stable surface functionalization. *Dew*A contributes to spore hydrophobicity and has so far been identified as the first choice hydrophobin from *A. nidulans* for biosynthetic surface modification.[17,18,19,20] *Dew*A from *A. nidulans* and other hydrophobins have been shown to be effective in increasing the hydrophobicity of glass surface coatings. In addition, *Dew*A protein layers showed high resistance to water, ethanol, detergent and temperature treatments than class I hydrophobin layers [21,22]. The angle determined as 6.174° on glass surfaces in our research findings reached 70.125±5.18° coating 100 µg *Dew*A protein. On the other hand, teflon surface angle, which was determined as 132.878°, decreased to 114.814±7.25°. While the contact angle on the glass surfaces before the application was 70.125° in the experimental groups in which hot SDS was applied; after 60 minute of application, it was determined as 69.250±6.35°. On teflon surfaces, it was 114.814° before the application; it was measured as 123.388±10.72° after the application [14]. İn their *Dew*A protein coating experiment, after 16 hour of incubation at 80 °C, the contact angle for the glass surface was 72.9±9.48° before the application of 1% SDS and the contact angle after the application was 70.3±4.03°; for teflon surface, the contact angle was 50.8±4.81° before 1% SDS application, and 79.2±13.2° after 1% SDS application. The same researchers could not explain the angle changes in these results and left them uninterpreted [14]. According to our research findings, we can explain the angle change on teflon and glass surfaces as the hydrophobic region of the *Dew*A protein with amphipathic character caused a change in the surface adhesion behavior as a result of SDS application. It is known that the adhesion and persistence of hydrophobins to surfaces will vary with protein size, structural stability, temperature, ionic strength and buffer composition [14,23]. In addition, small and hard proteins are preferred in surface applications because they are not prone to conformational changes after surface coating due to the disulfide bonds in their structures [24,25,26]. The *Dew*A protein we used in this study is one of the small and hard hydrophobins that do not allow conformational changes in parallel with the literature. The high stability of the *Dew*A protein in SDS application, especially on glass surfaces, is probably due to the disulfide bonds it contains.

In UV applications, *Dew*A protein remained intact and its activity was preserved by UV application on teflon surfaces [27,28]. In this study, *Dew*A degradation, which occurs after 30 minute, especially on glass surfaces, can be explained by the damage of the disulfide bonds that form the rigid structure of the protein under the influence of UV. In addition, it is known that UV stimulation of tryptophan and tyrosine side chains in proteins damages the structure of disulfide bridges. In our study, protein coating was successfully performed on both glass and teflon surfaces. UV treatment was applied to both surfaces. While there was no protein degradation in the coating on teflon surfaces and the activity was preserved, protein degradation occurred in the protein coating on glass surfaces after 30 minute and the activity could not be preserved. This deformation on glass surfaces can be explained by the damage of UV-induced disulfide bridges.

While no change was detected in the amount and conformation of the proteins coated on the glass surface with SDS application, the contact angle measured on the teflon surface increased. Recombinantly produced *Dew*A protein is a class I protein and is insoluble in solutions containing surfactants such as SDS. Therefore, it is not surprising that the contact angle does not change according to the results obtained from the glass surfaces. In a study with *P. pastoris*, hydrophobin was produced at a concentration of 0.5% methanol at 90 hour at 300 mg/L under the control of the AOX1 promoter in the HFBI hydrophobin pPICZα-A vector from *Trichoderma reesei*. However, this protein is included in class II hydrophobins [29]. Another class I hydrophobin protein such as *Dew*A is *Rod*A and *Rod*B; It was also produced in *P. pastoris* under the AOX promoter and ultimately produced at a concentration of 0.5% methanol at the 120th hour in amounts of 21 mg/L and 24mg/L. respectively [28]. In our study, the highest efficiency production of *Dew*A protein, which is a class 1 hydrophobin, was obtained as 77.42 mg/L at 1% methanol concentration at 96th hour. It is clear that the production of hydrophobins using recombinant methods is more effective than the production of natural strains by traditional methods. However, except for some recombinant strains, the hydrophobin production capacity of most fungi is below 150 mg/L [5,30]. Although current production methods seem sufficient for small-scale applications such as medical applications, biosensors and drug formulations [3,30], production efficiency should be increased for larger industrial applications [31]. The main strategies used to increase the production and yield of hydrophobins are to increase the expression of hydrophobins using wild strains and recombinant DNA technology [32]. In particular, the fact that some wild strains do not secrete hydrophobin into the culture medium makes large-scale production difficult [3]. The strategy to increase yield in studies with wild strains is usually the optimization of the culture. For example, using different carbon sources and nitrogen sources, hydrophobin production from *Ceratocystsis ulmi* was increased 5 times more than the control group [33]. The type of culture is also important, some researchers have emphasized that solid-state fermentation can be an effective alternative to submerged culture in the production of hydrophobin [34]. While culture optimization is required to increase yield according to previous studies, although high efficiency production was achieved without culture optimization in our research, culture optimization can be made in our future studies.

Conclusion

In this study, we aimed to produce recombinant class I hydrophobin *Dew*A *from Aspergillus nidulans*, which was determined to have a high contact angle in the literature. As a result of optimizations, the most suitable culture condition for *Dew*A expression was obtained at 77 mg/L 1% methanol concentration in 96 hours. Recombinant *Dew*A has been proven to change surface properties on teflon and glass surfaces. It showed a strong hydrophobic character, especially on the glass surface. These results demonstrated that recombinant *Dew*A may have biotechnological applications. This information will be used in future studies to investigate the detailed reasons for the different surface characteristics of the *Dew*A protein on glass and teflon surfaces, to determine whether the production process optimized by performing it on the Erlen scale can be optimized by transferring it to the fermenter scale, to evaluate the effect of different carbon and nitrogen sources in recombinant production and to determine the production efficiency and results. It sheds light on studies on cost. Additionally, in this study, the *Dew*A protein of A.nidulans was cloned into the pPICZa-A vector and produced recombinantly in *P. pastoris* X-33 strain for the first time.

Abbreviations

AOX, alcohol oxidase; SDS, sodium dodecyl sulfate; TFA, trifluoroacetic acid; YPDS, Yeast Extract Peptone Dextrose Medium containing sorbitol; BMYY, buffered complex medium containing methanol; BMGY, buffered complex medium containing glycerol.

Acknowledgments

The authors would like to thank Erzurum Technical University for their financial support for the Project.

Funding

This study was supported by Erzurum Technical University BAP coordination unıt with the project numbered 2019/11. (August 2019- August 2021).

Data Availability statement

All data generated and analyzed during this study are included in this published article.

Compliance with ethical standards

Conflict of interest / Çıkar çatışması

The author declare no conflict of interest.

Ethical standards

This article does not include any studies with human participants or animals by any of the authors.

Authors' contributions

AT and SÖ formed the outline of the study and AT played an active role in all study steps. MT played a role in the analysis of the data and AY played a role in the cloning steps. All authors read and approved the manuscript.

References

1. Sarlin, T., et al. İdentification and characterization of gushing-active hydrophobins from Fusarium graminearum and related species. J Basic Microbiol, 2012. (52)2: p.184-194. doi: https://doi.org/10.1002/jobm.201100053
2. Ren, Q., Kwan, A.K., Sunde, M. Two forms and two faces, multiple states and multiple uses: Properties and applications of the self-assembling fungal hydrophobins Biopolymers, 2013. (100)6: p. 601– 612. doi: https://doi.org/10.1002/bip.22259
3. Bayry, J., et al. Hydrophobins Unique fungal proteins. PLoS pathog, 2012. (8)5: p.1-16. doi: 10.1371/journal.ppat.1002700.
4. Wösten, H.A. and Scholtmeijer, K. Applications of hydrophobins: current state and perspectives. Appl Microbiol Biotechnol, 2015. 99: p.1587–1597. doi: https://doi.org/10.1007/s00253-014-6319-x
5. Kulkarni, S., Nene, S., Joshi, K. Production of Hydrophobins from fungi. Biocatal Agric Biotechnol, 2017. 61: p.1-11. https://doi.org/10.1016/j.procbio.2017.06.012
6. Rabe, M., Verdes, D., Seeger, S. Understanding protein adsorption phenomena at solid surfaces. Adv Colloid Interface Sci, 2011. (162) 2: p.87-106. https://doi.org/10.1016/j.cis.2010.12.007
   Linder, M.B., et al. Hydrophobins: the protein-amphiphiles of filamentous fungi, FEMS Microbiol Rev, 2005. (29)5: p.877 896. https://doi.org/10.1016/j.femsre.2005.01.004
7. Demain, A.L., Vaishnav, P. Production of recombinant proteins by microbes and higher organisms. Biotechnology Advances. 2009. (27)3: p. 297–306. doi: https://doi.org/10.1016/j.femsre.2005.01.004
8. Higgins, D.R., Cregg, J.M. (1998). Introduction to Pichia pastoris. Methods Mol Biol. 103:1-15.
9. Cereghino, G.P., et al. Production of recombinant proteins in fermenter cultures of the yeast Pichia pastoris. Curr Opin Biotechnol, 2002. (13)4: p.329–332. https://doi.org/10.1016/S0958-1669(02)00330-0
10. Rajamanickam, V., et al. A novel bi-directional promoter system allows tunable recombinant protein production in Pichia pastoris. Microb Cell Fact, 2017. (152)16: p.1-7. doi: https://doi.org/10.1186/s12934-017-0768-8
11. Cos, O., et al. Operational strategies, monitoring and control of heterologous protein production in the methylotrophic yeast Pichia pastoris under different promoters. Microb Cell Fact, 2006. 5(17): p.1-20. doi: https://doi.org/10.1186/1475-2859-5-17
12. Veenhuis, M. and Klei, I.J. Yeast and filamentous fungi as model organisms in microbody research. BBA, 2006. 1763(2): p.1364-1373. https://doi.org/10.1016/j.bbamcr.2006.09.014
13. Schmoll, M., et al. Recombinant production of an Aspergillus nidulans class I hydrophobin (DewA) in Hypocrea jecorina (Trichoderma reesei) is promoter-dependent. Appl Microbiol Biotechnol, 2010. 88: p.95-103. doi: https://doi.org/10.1007/s00253-010-2710-4
14. Lee, D., et al. Strontium influence on the oxygen electrocatalysis of La2−xSrxNiO4±δ (0.0 ≤ xSr ≤ 1.0) thin films. J Mater Chem A Mater, 2014. 18: p.6480-6487. doi: https://doi.org/10.1039/C3TA14918H
15. Chau, T.T., et al. A review of factors that affect contact angle and implications for flotation practice. Adv Colloid Interface Sci, 2009. (150)2: p.106-115. https://doi.org/10.1016/j.cis.2009.07.003
16. Fokina, O., et al. Immobilization of LccC Laccase from Aspergillus nidulans on Hard Surfaces via Fungal Hydrophobins. Appl. Environ. Microbiol, 2016. (82)21: p.6395–6402. doi: https://doi.org/10.1128/AEM.01413-16
17. Boeuf, S., et al. Engineering hydrophobin DewA to generate surfaces that enhance adhesion of human but not bacterial cells. Acta Biomater, 2012. (8)3: p.1037–1047. https://doi.org/10.1016/j.actbio.2011.11.022
18. Rieder, A., et al. The impact of recombinant fusion-hydrophobin coated surfaces on E. coli and natural mixed culture bioflm formation. Biofouling ,2011. (27)10: p.1073–1085. DOI: https://doi.org/10.1080/08927014.2011.631168
19. Weickert, U., et al. Optimizing biliary stent patency by coating with hydrophobin alone or hydrophobin and antibiotics or heparin: an in vitro proof of principle study. Adv. Med. Sci, 2011. (56)2: p.138–144. doi: https://doi.org/10.2478/v10039-011-0026-y
20. Winandy, L., et al. Comparative analysis of surface coating properties of five hydrophobins from Aspergillus nidulans and Trichoderma reseei. Sci Rep, 2018. 8: p.12033. DOI: https://doi.org/10.1038/s41598-018-29749-0
21. Grunbacher, A., et al. Six hydrophobins are involved in hydrophobin rodlet formation in Aspergillus nidulans and contribute to hydrophobicity of the spore surface. PLoS One, 2014. (9)4: p.1-10. doi: https://doi.org/10.1371/journal.pone.0094546
22. Heinonen, H., et al. Engineered Hydrophobin for Biomimetic Mineralization of Functional Calcium Carbonate Microparticles. J. Biomater. Nanobiotechnology, 2014.(5)1: p.1–7. DOI: https://doi.org/10.4236/jbnb.2014.51001
23. Banach, M., et al. Role of Disulfide Bonds in Stabilizing the Conformation of Selected Enzymes—An Approach Based on Divergence Entropy Applied to the Structure of Hydrophobic Core in Proteins. Entropy, 2016. (18)3: p. 1-21. https://doi.org/10.3390/e18030067
24. Kalinowska, B., et al. Intrinsically disordered proteins-relation to general model expressing the active role of the water environment. Adv. Protein Chem. Struct. Biol, 2014. 94: p.315–346. DOI: https://doi.org/10.1016/B978-0-12-800168-4.00008-1
25. Takahashi, T., et al. Ionic interaction of positive amino acid residues of fungal hydrophobin RolA with acidic amino acid residues of cutinase CutL1. Mol. Microbiol, 2015. (96)1: p.14–27. DOI: https://doi.org/10.1111/mmi.12915
26. Petersen, M.T.N., Gajula, G.P., Petersen, S.B. UV Light Effects on Proteins: From Photochemistry to Nanomedicine. Molecular Photochemistry, 2012. p. 125-158. Various Aspects, Dr. Satyen Saha (Ed.), ISBN: 978-953-51-0446-9, InTech open, Available from: https://www.intechopen.com/chapters/34624
27. Petersen, N., et al. Flash Photolysis of Cutinase: Identification and Decomposition Kinetics of Transient Intermediate Formed Upon UV Excitation of Aromatic Residues. Biophys J, 2009. (97)1: p.211-226. https://doi.org/10.1016/j.bpj.2009.01.065
28. Nejad, A.L., Mahani, M.T., Hosseinkhan, S. Heterologous expression of a hydrophobin HFB1 and evaluation of its contribution to producing stable foam. Protein Expr. Purif, 2016. 118: p.25-30. https://doi.org/10.1016/j.pep.2015.09.025

29. Scholtmeijer, K., Wessels, J., Wösten, H.A.B. Fungal hydrophobins in medical and technical applications. Appl Microbiol Biotechnol, 2001. 56: p.1-8. DOI: https://doi.org/10.1007/s002530100632
30. Khalesi, M., Gebruers, K., Derdelinckx, G. Recent Advances in Fungal Hydrophobin Towards Using in Industry. Protein J ,2015.34: p.243–255. DOI: https://doi.org/10.1007/s10930-015-9621-2
31. Vergara, A., Hernández, S., Revah, S. Phenomenological Model of Fungal Biofilters for the Abatement of Hydrophobic VOCs. Biotechnol Bioeng, 2006. (33)6: p.1182–1192. DOI: https://doi.org/10.1002/bit.21989
32. Takai, S. and Richards, W.C. Cerato-ulmin, a Wilting Toxin of Ceratocystis ulmi: Isolation and some Properties of Cerato-ulmin from the Culture of C. ulmi. J Phytopatho, 1978. (73)2: p.129 -146. https://doi.org/10.1111/j.1439-0434.1978.tb04205.x
33. Vigueras, G., et al. Hydrophobic response of the fungus Rhinocladiella similis in the biofiltration with volatile organic compounds with different polarity. Biotechnol Lett, 2009. (31)8: p.1203–1209. DOI: https://doi.org/10.1007/s10529-009-9987-3

International Journal of Life Sciences and Biotechnology
Keser, M., H. Atmaca, and S. B. Karaca, Comparative Analysis of CDK4/6 Inhibitors (Ribociclib and Palbociclib) combined with Enzalutamide in Triple-negative breast cancer cells. International Journal of Life Sciences and Biotechnology, 2024. 7(1): p. 21-27.
https://doi.org/10.38001/ijlsb.1427002
Araştırma Makale/ Research article

Comparative Analysis of CDK4/6 Inhibitors (Ribociclib and Palbociclib) Combined with Enzalutamide in Triple-Negative Breast Cancer Cells

Murat Keser [1]*, Harika Atmaca [2], Saziye Burcak Karaca [3]

ABSTRACT
Triple-negative breast cancer (TNBC) is recognized as a challenging subtype due to its poor prognosis. Recent molecular profiling studies have unveiled a significant subset expressing the androgen receptor (AR) subset which may respond to AR-blocking agents, offering a potentially effective treatment strategy. This study aims to investigate the potential synergistic cytotoxic and apoptotic effects of the AR antagonist enzalutamide (ENZA) in combination with CDK4/6 inhibitors palbociclib (PB) or ribociclib (RB) and compare the effectiveness of these combinations in TNBC cells. Results revealed that ENZA in combination with PB or RB induced synergistic cytotoxic cytotoxicity in all tested TNBC cell lines. While synergistic cytotoxic combinations of ENZA with PB did not induce apoptosis in any TNBC cell line, ENZA+RB combinations exhibited a synergistic apoptotic effect. This study suggests the ENZA+RB combination may be more favorable due to its apoptosis-inducing effect. However, these data need to be further supported by detailed in vivo and clinical studies.

ARTICLE HISTORY
Received
25 January 2024
Accepted
29 February 2024

KEYWORDS
Triple-negative breast cancer,
enzalutamide,
palbociclib,
ribociclib

Introduction

Breast cancer stands as the most prevalent form of cancer among women globally, with one million new cases diagnosed annually [1]. Constituting 10-20% of all breast cancers, triple-negative breast cancer (TNBC) is identified by the absence of estrogen receptor (ER), progesterone receptor (PR), and human epidermal growth factor receptor 2 (HER-2) expression TNBC, known for its aggressive clinical behavior, bleak prognosis, and lack of targeted therapy, has become a focal point for researchers [3]. Recent molecular profiling studies have exposed significant molecular diversity within TNBC, revealing a subset that expresses the androgen receptor (AR), identified in 70–90% of breast cancer cases [4]. We now understand that this receptor plays a crucial role in the pathology and development of breast cancer [5]. This finding suggests that TNBC patients with a positive AR [AR(+)] subset may respond to AR-blocking agents, offering a potentially effective treatment strategy.

Enzalutamide (ED), an approved androgen receptor antagonist for prostate cancer, has shown potent anti-cancer effects in preclinical studies on TNBC cells, supporting the idea that AR inhibition is a promising target for TNBC [6]. Currently, clinical trials are in progress to explore the efficacy of neoadjuvant enzalutamide, both in combination with and without chemotherapy, for patients with TNBC. Palbociclib (PB) and Ribociclib (RB) stand out as highly selective inhibitors of cyclin-dependent kinase 4 and 6 (CDK4/6). They function by impeding the phosphorylation of the retinoblastoma (Rb) protein, subsequently arresting the cell cycle at the G1 phase. [7]. Hence, targeting CDK4/6 emerges as a crucial therapeutic approach for breast cancer owing to its pivotal role in the cell cycle and the proven efficacy of inhibitors in BC cases [8]. Additionally, the activation of androgen receptors (AR) contributes to enhanced cell survival by regulating the cell cycle; androgen deprivation induces G1 arrest [9]. It's worth mentioning that the expression of androgen receptor-dependent genes reaches its peak during the G1 phase and gradually decreases throughout the cell. These inhibitors present an effective therapeutic approach against breast cancer, where CDK4/6 activity is often dysregulated [10]. Literature indicates that ENZA enhances the cytostatic effect induced by PB and RB in AR-

[1] University of Health Sciences Izmir Tepecik Education and Research Hospital, Department of Medical Oncology, Izmir/Türkiye
[2] Manisa Celal Bayar University, Faculty of Engineering and Natural Sciences, Department of Biology, Manisa/ Türkiye
[3] Ege University, School of Medicine, Department of Internal Medicine, Medical Oncology, Izmir/Türkiye
*Corresponding Author: Murat KESER, e-mail: drmksr35@gmail.com

positive/RB-competent TNBC cells, suggesting that the combination of enzalutamide and CDK4/6 inhibitors may be a therapeutic strategy for AR(+)/RB-competent TNBC [11], [12].
The objective of this study is to investigate the potential synergistic effects of enzalutamide in combination with PB or RB and determine which combination is more effective in TNBC cells. The synergistic cytotoxic and apoptotic effects of these combinations were compared in AR-positive (MDA-MB-453 and BT-549), and AR-negative (MDA-MB-231 and MDA-MB-468) TNBC cell lines.

Material and Methods

Cell lines and cell culture

The cell lines utilized in this study were sourced from the Ege University Tülay Aktaş Oncology Laboratory cell line stock. Breast cancer cells were cultivated in RPMI 1640 medium containing with 10% (v/v) FBS and 2 mM L-glutamine. To prevent microbial contamination, penicillin-streptomycin solution (1%) was added to the medium. Cells were cultured in a 37°C incubator with 5% CO_2. During the study, cells were cryopreserved in liquid nitrogen for further analysis.

Preparation of drugs

A concentrated solution of ENZA was formulated with a concentration of 20 mg/mL by dissolving 40 mg of ENZA in 2 mL of dimethyl sulfoxide (DMSO). PB (PD0332991) and RB (LEE011) were procured from Sigma. To prepare a 5 mM stock solution, 5 mg of PB was dissolved in 1.7 mL of DMSO. 5 mg RB was dissolved in 2 mL of DMSO to obtain a 5 mM solution.

Assessment of cell viability via MTT assay

MTT (2,5-diphenyl-2H-tetrazolium bromide) assay was employed for the analysis of cell viability. For this purpose, breast cancer cells were seeded in 96-well culture plates (10.000 cells/well) and treated with drugs alone or in combination for 24, 48, and 72 hours. After adding 10 µl of MTT solution to each well, plates were kept at 37°C in a CO_2 incubator for 4 h. After the incubation period, cells were drained and 200 µL DMSO was added and mixed. Cell viability percentages were calculated based on the optical density determined with a multimode plate reader at 490 nm wavelength.
The IC_{50} values are calculated using cell viability percentages via GraphPad software. The Combination Index (CI) is the synergistic, additive, or antagonistic effects of drug combinations in pharmacology. CI values were calculated via CalcuSyn software. The interpretation of Combination Index (CI) values is as follows: CI < 0.1: very strong synergism, 0.1-0.3: strong synergism, 0.3-0.7: synergism, 0.7-0.85: moderate synergism, CI = 1: additivity, and CI > 1: antagonism [13].

DNA fragmentation analysis

Apoptotic cells after treatment with drugs and drug combinations were determined using a cell death detection ELISA kit (Merck). 100 µl of coating solution is pipetted into each well, covered, and incubated overnight at +4°C. After thorough removal of the coating solution, 200 µl of incubation buffer is added to all samples and kept at +25°C for 30 min. The solution is then removed, and wells are rinsed three times with 300 µl washing solution per well. Then, sample solution (100 µl) is pipetted into each well, and for background determination, 100 µl of incubation buffer is added to two wells. The microplate is covered and incubated for 90 min. at RT. After removing the solution and rinsing the wells, 100 µl of Conjugate solution is added, except for the blank position. Following a 90-minute incubation and subsequent rinsing, 100 µl of substrate solution is pipetted into each well. The microplate is then incubated on a shaker for 10 min. Well contents are homogenized, and measurements are taken at 405 nm for a substrate solution blank, or at 490 nm as the reference wavelength.

Statistical analysis

Statistical analysis was conducted using GraphPad Prism software (La Jolla, CA, USA). The data were assessed using a one-way analysis of variance (ANOVA) followed by Dunnett's test for multiple comparisons. Values with $p < 0.05$ were considered statistically significant.

Results and Discussion

Cytotoxic effects of ENZA, PB, and RB on human TNBC cell lines

ENZA was administered to breast cancer cells at concentrations of 1, 5, 10, 20, 40, and 80 µM throughout 24, 48, and 72 hours. PB and RB were administered at concentrations of 10, 25, 50, 75, and 100 µM. All tested drugs showed concentration and time-dependent cytotoxic activity against all tested breast cancer cells (Figures 1, 2, and 3). IC_{25} and IC_{50} values of drugs were calculated from viability plots at 72 hours and presented in Table 1.

ENZA reached its peak effectiveness at 72 hours in all breast cancer cells (Figure 1). ENZA was most effective in the MDA-MB-231 cell line with an IC_{50} value of 69.5 ± 0.8 µM, whereas it demonstrated the least efficacy in the MDA-MB-468 cell line with an IC_{50} value of 82.0 ± 2.1 µM.

MDA-MB-231 is a TNBC cell line that is proficient in RB but lacks AR expression. The effectiveness of enzalutamide in AR-negative MDA-MB-231 cells suggests that its anti-cancer properties may involve mechanisms beyond its primary action on AR. These alternative mechanisms could include targeting other receptors or signaling pathways that are involved in cancer cell proliferation, survival, or metastasis. Additionally, ENZA might induce cellular changes or alterations in gene expression profiles that lead to the inhibition of tumor growth or the induction of cancer cell death, irrespective of AR status. Further research is needed to fully elucidate the precise molecular mechanisms underlying efficacy of ENZA in AR-negative breast cancer cells.

Table 1 Calculated IC_{25} and IC_{50} values of Enzalutamide (ENZA), Palbociclib (PB), and Ribociclib (RB) on human TNBC cell lines at 72 h

	AR(+) TNBC cell lines				**AR(-) TNBC cell lines**			
	RB-negative		**RB-proficient**		**RB-negative**		**RB-proficient**	
	BT-549		**MDA-MB-453**		**MDA-MB-468**		**MDA-MB-231**	
	IC_{25}	**IC_{50}**	**IC_{25}**	**IC_{50}**	**IC_{25}**	**IC_{50}**	**IC_{25}**	**IC_{50}**
ENZA	35.4 ± 0.4	78.2 ± 0.2	32.8 ± 1.4	72.0 ± 0.4	42.4 ± 0.5	82.0 ± 2.1	30.4 ± 1.2	69.5 ± 0.8
PB	31.5 ± 1.2	78.0 ± 0.8	38.9 ± 0.2	82.0 ± 1.4	32.4 ± 1.1	78.0 ± 1.0	28.7 ± 0.4	71.0 ± 1.4
RB	24.8 ± 0.6	58.0 ± 1.2	21.7 ± 2.4	49.0 ± 0.6	29.8 ± 3.2	72.0 ± 3.6	28.2 ± 0.8	68.0 ± 2.7

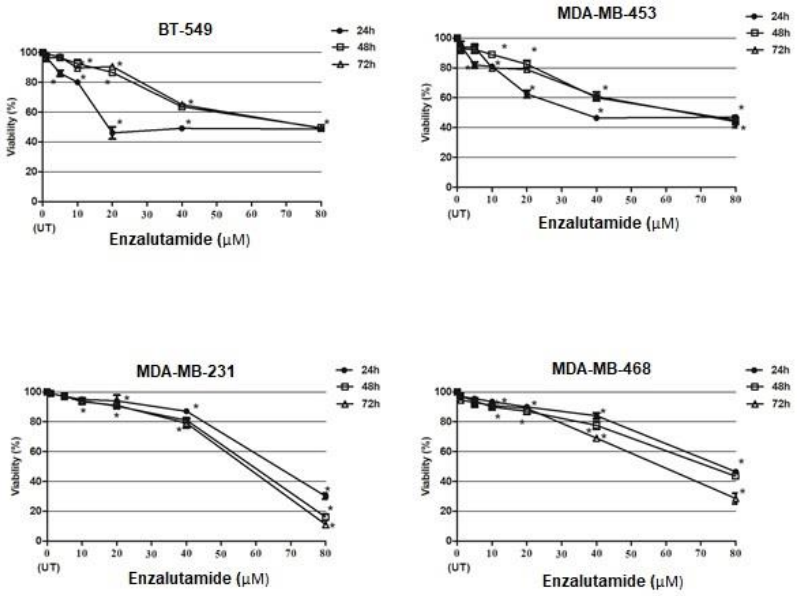

Fig 1 Effect of increasing concentrations of Enzalutamide on TNBC cells at 24, 48 and 72 h ($p<0.05$)

In the literature, the effect of ENZA was tested on TNBC cell lines and results revealed a dose- and time-dependent cytotoxicity in all breast cancer cells. IC_{50} values of ENZA were between 25 and 60 µM for tested breast cancer cells [11]. In another study, ENZA was tested on 11 different TNBC cell lines and the IC_{50} values ranged from 4 µM to >50 µM [14]. The reason for the significant variation in IC_{50} values of ENZA across different breast cancer cell lines may be because these cell lines exhibit different phenotypic characteristics from each other.

PB was also tested on both AR(+) and AR(-) TNBC cell lines and showed dose- and time-dependent cytotoxic activity against all TNBC cell lines (Figure 2). PB was most effective in the AR(-)MDA-MB-231 cell line with an IC_{50} value of 71.0 ± 1.4 µM, whereas it demonstrated the least efficacy in the AR(+)MDA-MB-453 cell line with an IC_{50} value of 82.0 ± 1.4 µM.

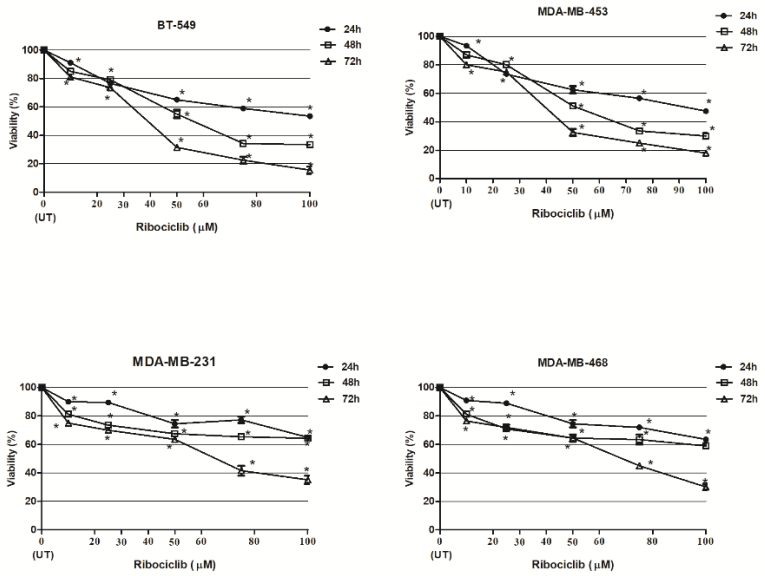

Fig 2 Effect of increasing concentrations of Palbociclib on TNBC cells at 24, 48, and 72 h ($p<0.05$)

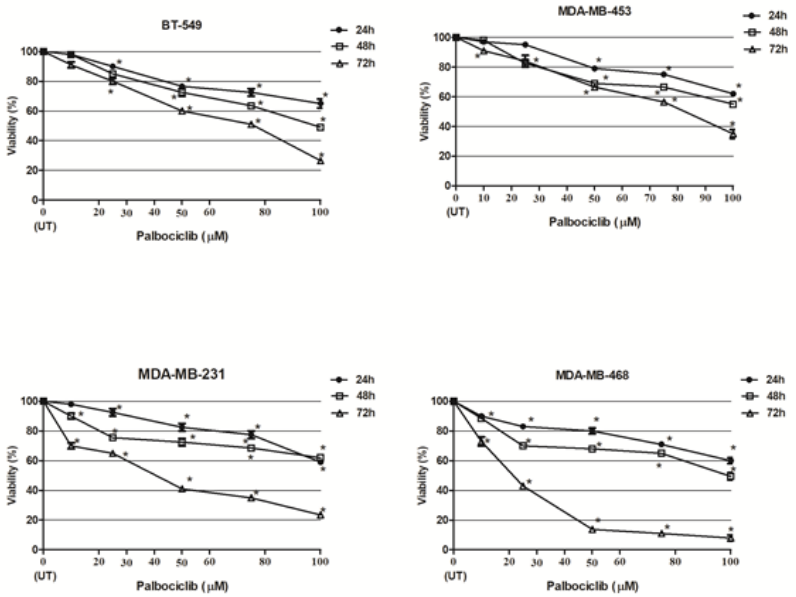

Fig 3 Effect of increasing concentrations of Palbociclib on TNBC cells at 24, 48, and 72 h ($p<0.05$)

RB reached its peak effectiveness at 72 hours in all breast cancer cells (Figure 3). RB was most effective in AR(+)MDA-MB-453 the cell line with an IC_{50} value of 49.0 ± 0.6 μM, whereas it demonstrated the least efficacy in the AR(-) MDA-MB-468 cell line with an IC_{50} value of 72.0 ± 3.6 μM. In the literature, it has been demonstrated in various studies that both PB and RB exhibit dose- and time-dependent cytotoxic effects in breast cancer cell lines [11], [12]. However, a study revealed that palbociclib markedly impeded cell growth in RB-proficient cells (MDA-MB-453 and MDA-MB-231), while exhibiting no significant impact on RB-negative cells (MDA-MB-468) [12].

Synergistic cytotoxic combinations of ENZA with PB or RB

After determining the individual cytotoxic effects of the drugs and calculating their IC_{50} values, the potential synergistic effects of ENZA in combination with PB or RB were investigated in TNBC cells. Various combinations were prepared with varying concentrations of drugs and applied to TNBC cell lines for a duration of 72 h.

CI value for the combination of 80 uM ENZA and 25 uM PB was calculated as 0.105 in BT-549 cells, indicating strong synergism and thus considered a highly synergistic cytotoxic combination (Table 2). In MDA-MB-231 cells, The CI value for the combination of 80 uM ENZA and 25 uM PB was calculated as 0.102 and considered strong synergism, whereas the CI value was 0.325 for the combination of 80 uM ENZA and

50 uM PB and considered synergistic cytotoxic (Table 2). In MDA-MB-453 cells, 80 uM ENZA and 25 uM PB resulted in synergistic cytotoxicity at 72 h (CI value: 0.310) (Table 2). In MDA-MB-468 cells, The CI value for the combination of 80 uM ENZA and 25 uM PB was calculated as 0.126 and considered strong synergism, whereas the CI value was 0.343 for the combination of 80 uM ENZA and 50 uM PB and considered synergistic cytotoxic (Table 2). In previous studies, it was shown that the combination of ENZA with PB amplifies the cytostatic effect in AR-positive/RB-proficient TNBC cells [12]. As shown in Table 2, ENZA in combination with PB induced synergistic cytotoxic effects in all tested TNBC cell lines.

The combination of 80 uM ENZA and 25 uM RB in BT-549 cells was interpreted as strong synergism with a CI value of 0.119 (Table 2). In MDA-MB-231 cells, the CI value for the combination of 80 uM ENZA and 25 uM RB was calculated as 0.100 and considered strong synergistic cytotoxic, whereas the CI value was 0.352 for the combination of 80 uM ENZA and 50 uM RB and considered synergistic cytotoxic (Table 2). In MDA-MB-453 cells, the CI value for the combination of 80 uM ENZA and 25 uM RB was calculated as 0.110 and considered strong synergism, whereas the CI value was 0.302 for the combination of 80 uM ENZA and 50 uM RB and considered synergism (Table 2). In MDA-MB-468 cells, The CI value for the combination of 80 uM ENZA and 25 uM RB was calculated as 0.143 and considered strong synergism, whereas the CI value was 0.326 for the combination of 80 uM ENZA and 50 uM RB and considered synergistic cytotoxic (Table 2). In a study by Choupani et al., the cytotoxic effect of ENZA in combination with RB was investigated in AR- and AR+ TNBC cells, and all tested combinations reduced clonogenic proliferation and cell viability in both TNBC cells [11]. Understanding of the complex interaction between AR and CDK4/6 signaling pathways may pave the way for new therapeutic approaches in the treatment of TNBC, so the underlying molecular mechanisms of these combinations should be studied in detail.

Table 2 Combination index (CI) values of ENZA in combination with RB or PB in TNBC cells. CI < 0.1 indicates very strong synergism, 0.1- 0.3 indicates strong synergism, 0.3-0.7 indicates synergism, 0.7-0.85 moderate synergism, CI = 1 indicates additivity, and CI > 1 indicates antagonism. (*values indicating synergistic cytotoxic combinations) [13].

ENZA (µM)	PB (µM)	BT-549	MDA-MB-231	MDA-MB-453	MDA-MB-468
5	25	0.105*	0.924	0.933	1.102
5	50	0.912	0.855	0.978	1.025
80	25	0.836	0.102*	0.310*	0.126*
80	50	0.887	0.325*	0.899	0.343*
ENZA (µM)	**RB (µM)**				
5	25	0.981	1.247	0.958	1.240
5	50	0.945	1.025	0.896	1.139
80	25	0.119*	0.100*	0.110*	0.143*
80	50	1.056	0.352*	0.302*	0.326*

Detection of apoptosis in synergistic cytotoxic combinations

The measurement of DNA fragmentations was performed to determine whether combinations identified as synergistically cytotoxic induce apoptotic cell death in TNBC cells. While previous studies in the literature have demonstrated that PB does not induce apoptosis in TNBC cells [12], we investigated apoptotic cell death at synergistic concentrations obtained in our study. No apoptotic cell death was induced with the application of the ENZA+PB combination in any TNBC cells tested, parallel to the findings in the literature (Figure 4). However, despite previous findings indicating the synergistic effectiveness of combinations of ENZA with RB, the synergistic apoptotic effect has not been investigated. The androgen receptor (AR) influences the transcriptional activity of genes related to evading apoptosis and promoting cellular proliferation. Therefore, AR signaling leads to tumor growth [9].

Previously it was demonstrated that RB triggers apoptosis in the TNBC cell line MDA-MB-231 [15]. Similarly, there are studies indicating that ENZA also induces apoptosis in cancer cells [16], [17]. Based on this information, here we investigated for the first time the apoptotic effects of synergistic cytotoxic combinations of ENZA with RB in TNBC cells. Results revealed that ENZA in combination with RB resulted in synergistic apoptotic effect in all tested TNBC cells at 72 h (Figure 5).

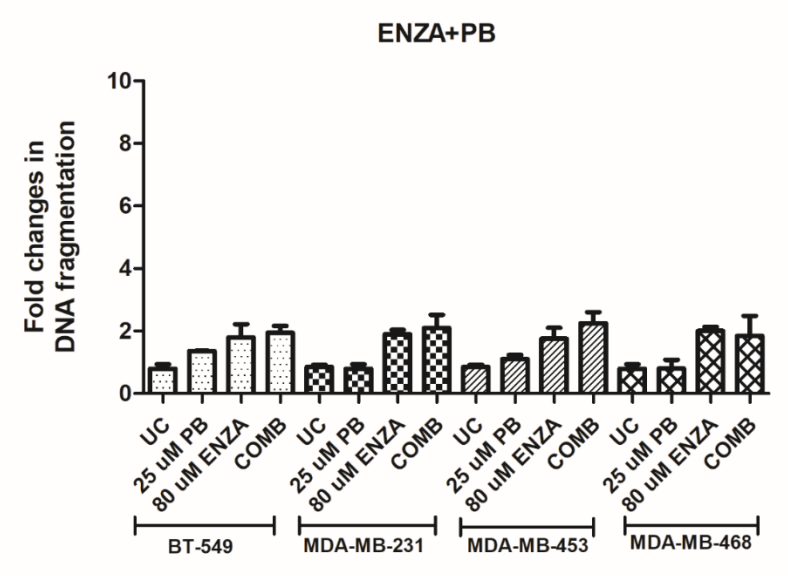

Fig 4 Evaluation of apoptosis in TNBC cell lines after treatment with 25 µM PB and 80 µM ENZA synergistic cytotoxic combination at 72 h. The combination treatment of ENZA and PB does not lead to apoptosis in TNBC cells ($p>0.05$) (UC: untreated control)

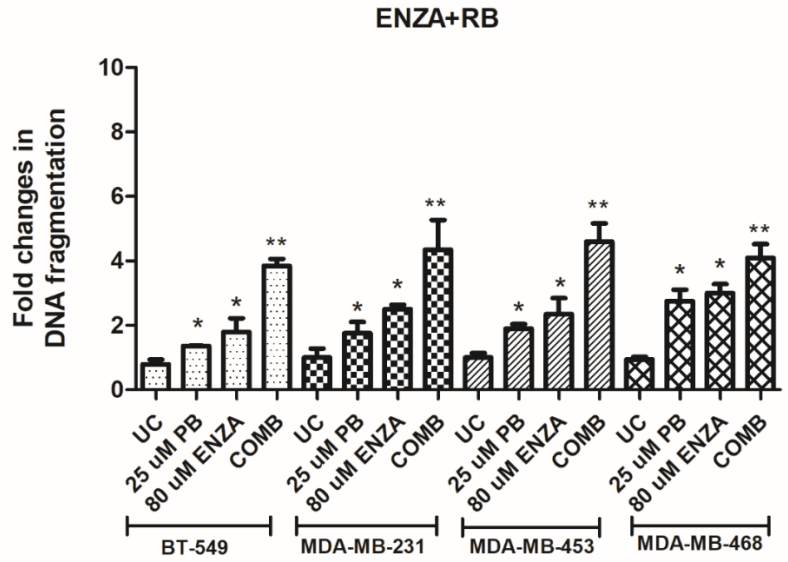

Fig 5 Evaluation of apoptosis in TNBC cell lines after treatment with 25 µM RB and 80 µM ENZA synergistic cytotoxic combination at 72 h. ENZA+RB combination treatment resulted in apoptosis in all tested TNBC cells at 72 h ($p<0.05$* as compared to untreated control (UC), $p<0.05$** as compared to single cells alone)

Conclusion

In conclusion the c,ombined application of ENZA with either PB or RB resulted in synergistic cytotoxicity across all tested TNBC cell lines. While synergistic cytotoxic combinations of ENZA with PB did not trigger apoptosis in any TNBC cell line, combinations of ENZA with RB demonstrated a synergistic apoptotic effect. This research implies that the ENZA+RB combination could be more advantageous owing to its apoptosis-inducing impact. However, these findings necessitate further support through comprehensive *in vitro* studies, including western blot analysis of target proteins. Additionally, additional *in vivo* and clinical studies are warranted to corroborate these findings. The present investigation has certain constraints; primarily, only four TNBC cell lines were employed, and there could exist additional protein profiles or mutants that play a role in the varying impacts of PB, RB, ENZA, and their combination in these particular cell lines.

Abbreviations

AR: Androgen receptor; CI: Combination index; DMSO: Dimethyl sulfoxide; ENZA: Enzalutamide; ER: Estrogen receptor; FBS: Fetal bovine serum; HER-2: Human epidermal growth factor receptor 2; IC50: Half-maximal inhibitory concentration; TNBC: Triple-negative breast cancer, PB: Palbociclib; PR: Progesterone receptor; RB: Ribociclib; Rb: Retinoblastoma;

Funding
This study received project support from the Turkish Medical Oncology Society (Proje No: P-TTOD-2021-142).

Availability of data and material
Please contact the corresponding author for any data request.

References

1. Sung H., et al., "Global Cancer Statistics 2020: GLOBOCAN Estimates of Incidence and Mortality Worldwide for 36 Cancers in 185 Countries," CA. Cancer J. Clin., vol. 71, no. 3, pp. 209–249, May 2021, doi: 10.3322/caac.21660.
2. Cleator, S., W. Heller, and R. C. Coombes, "Triple-negative breast cancer: therapeutic options," Lancet Oncology, vol. 8, no. 3. Elsevier, pp. 235–244, Mar. 2007. doi: 10.1016/S1470-2045(07)70074-8.
3. Kumar P. and R. Aggarwal, "An overview of triple-negative breast cancer," Archives of Gynecology and Obstetrics, vol. 293, no. 2. 2016. doi: 10.1007/s00404-015-3859-y.
4. Coussy F., et al., "Response to mTOR and PI3K inhibitors in enzalutamide-resistant luminal androgen receptor triple-negative breast cancer patient-derived xenografts," Theranostics, vol. 10, no. 4, 2020, doi: 10.7150/thno.36182.
5. Rampurwala, M., K. B. Wisinski, and R. O'Regan, "Role of the androgen receptor in triple-negative breast cancer," Clin. Adv. Hematol. Oncol., vol. 14, no. 3, 2016.
6. Traina T. A., et al., "Enzalutamide for the treatment of androgen receptor-expressing triple-negative breast cancer," J. Clin. Oncol., vol. 36, no. 9, 2018, doi: 10.1200/JCO.2016.71.3495.
7. Spring, L. M., "CDK 4/6 Inhibitors in Breast Cancer: Current Controversies and Future Directions," Current Oncology Reports, vol. 21, no. 3. 2019. doi: 10.1007/s11912-019-0769-3.
8. Turner N. C., et al., "Palbociclib in Hormone-Receptor–Positive Advanced Breast Cancer," N. Engl. J. Med., vol. 373, no. 3, 2015, doi: 10.1056/nejmoa1505270.
9. Jacob, A., et al., "Androgen receptor signaling in prostate cancer and therapeutic strategies," Cancers, vol. 13, no. 21. 2021. doi: 10.3390/cancers13215417.
10. G. Murphy, C. G., "The Role of CDK4/6 Inhibitors in Breast Cancer," Current Treatment Options in Oncology, vol. 20, no. 6. 2019. doi: 10.1007/s11864-019-0651-4.
11. Choupani, E., et al., "Combination of androgen receptor inhibitor enzalutamide with the CDK4/6 inhibitor ribociclib in triple negative breast cancer cells," PLoS One, vol. 17, no. 12 December, 2022, doi: 10.1371/journal.pone.0279522.
12. Liu C. Y., et al., "Combination of palbociclib with enzalutamide shows in vitro activity in RB proficient and androgen receptor positive triple negative breast cancer cells," PLoS One, vol. 12, no. 12, 2017, doi: 10.1371/journal.pone.0189007.
13. Chou, T. C., "Frequently asked questions in drug combinations and the mass-action law-based answers," Synergy, vol. 1, no. 1. 2014. doi: 10.1016/j.synres.2014.07.003.
14. Caiazza F., et al., "Preclinical evaluation of the AR inhibitor enzalutamide in triple-negative breast cancer cells," Endocr. Relat. Cancer, vol. 23, no. 4, 2016, doi: 10.1530/ERC-16-0068.
15. Li T., et al., "Ribociclib (LEE011) suppresses cell proliferation and induces apoptosis of MDA-MB-231 by inhibiting CDK4/6-cyclin D-Rb-E2F pathway," Artif. Cells, Nanomedicine Biotechnol., vol. 47, no. 1, 2019, doi: 10.1080/21691401.2019.1670670.
16. Abazid, A., et al., "The androgen receptor antagonist enzalutamide induces apoptosis, dysregulates the heat shock protein system, and diminishes the androgen receptor and estrogen receptor β1 expression in prostate cancer cells," J. Cell. Biochem., vol. 120, no. 10, 2019, doi: 10.1002/jcb.28929.
17. Chang, C. Y., J. T. Chen, T. H. Chen, and R. M. Chen, "Enzalutamide Induces Apoptotic Insults to Human Drug-Resistant and -Sensitive Glioblastoma Cells via an Intrinsic Bax-Mitochondrion-Cytochrome C Caspase Cascade Activation Pathway," Molecules, vol. 27, no. 19, 2022, doi: 10.3390/molecules27196666.

International Journal of Life Sciences and Biotechnology
Sahin, N., Morphological Characterization of Some Local Watermelon (*Citrullus lanatus* L.) Genotypes of Turkey. International Journal of Life Sciences and Biotechnology, 2024 7(1): p. 28-36.
https://doi.org/10.38001/ijlsb.1427002
Araştırma Makale/ Research article

Morphological Characterization of Some Local Watermelon (*Citrullus lanatus* L.) Genotypes of Turkey

Nihan Sahin [1]*

ABSTRACT
The scope of this study, some of the local Turkish watermelon genotypes were evaluated morphologically. A total of 20 local genotypes and three commercial varieties were assessed regarding their cotyledon, leaf, fruit, and seed phenotypes. An extensive morphological analysis was performed on a diverse set of genotypes. Traits such as cotyledon shape and color intensity, leaf size and lobing, and fruit size, shape, and color were measured and compared. Hierarchical clustering analysis, correlation matrices, and principal component analysis were employed to interpret the data. The study revealed significant morphological variability among the watermelon genotypes. Cotyledons ranged from narrow to broad, with a predominance of large sizes and dark green coloration. Leaf characteristics varied widely, with a notable distribution across different sizes and degrees of lobing. Fruit analysis showed a broad spectrum of shapes, sizes, and colors, indicating a rich genetic diversity. Two main genotype clusters were identified, suggesting a clear distinction based on morphological traits.

ARTICLE HISTORY
Received
08 January 2024
Accepted
04 March 2024

KEYWORDS
Watermelon genotypes, morphological characteristics, genetic diversity, leaf morphology, fruit variation, phenotypic variability, heirlooms

Introduction

Due to its diverse geographical layout and varying ecological conditions in different regions, Türkiye is situated at a significant intersection of global gene centres and origins [1]. The significance of 3,708 out of the total 10,754 taxon present in its flora is heightened by the fact that they are exclusive to this particular region [2]. Despite not being a genetic centre for watermelon, Türkiye has benefited from its favourable geographical location, diverse climate, and historical presence on trade routes. As a result, a wide range of watermelon genotypes have been introduced, and their diversity has further expanded due to the fact that watermelon is a non-self-fertilized plant [1].
Currently, there is a greater understanding of the inheritance of the physical characteristics of watermelon, and many of these characteristics have been identified in the genome[3-14]. This accumulation of knowledge facilitates the utilization and assessment of local watermelon varieties in the breeding research [15].
Numerous investigations have been conducted to identify local varieties[14, 16-32]. Those local varieties could play a crucial role in new cultivars' development and genetic variation [33]. This is due to their ability to adapt to the specific ecological conditions of the region and their potential to provide resistance against prevalent diseases or pests in the area [34]. The genetic base of cultivated watermelon is rather limited [35]. Hence, the identification and conservation of plant genetic resources holds a significant research topic [15].
South Africa is a significant hub for the genetic resources of *C. lanatus*, serving as a key genetic centre[17, 22, 36]. The endeavours to collect, categorize, and safeguard resources in this region have commenced belatedly in comparison to other regions worldwide, and until recently, have not been accorded the requisite significance McGregor [15]. The South African Plant Genetic Resources Centre has preserved a combined total of 179 genetic samples of watermelon from Namibia, Botswana, and South Africa. The Namibian National Institute of Botanical Research has conserved 89 genetic sources, while the National Centre for Plant Genetical Resources and the Zambian Institute of Agricultural Research have preserved 89 and 75 genotypes, respectively. However, there is a scarcity of information regarding these resources, and it remains uncertain whether any conflicts exist among the institutions concerning genetic resources [15]. In their study, Maggs-Kölling and Christiansen [36] conducted a comparison between local varieties of Namibia and commonly cultivated varieties (Congo, Sweet Princess, and Crimson Sweet) in order to assess their morphological characteristics. The researchers discovered that local varieties can serve as significant sources of plant vigour,

[1] Tekirdag Namık Kemal University , Faculty of Agriculture, Department of Horticulture
*Corresponding Author: Nihan Sahin, e-mail: nihansahin@nku.edu.tr

durability, and seed characteristics. In his 2007 study, Goda [17] analyzed the morphological traits of 30 accessions collected from various locations of Sudan, including the western, northern, and central areas. The researcher grouped the accessions under study into various morphotypes. According to Hakimi and Madidi [37] research on the physical traits of indigenous Moroccan variations, the degree of diversity among these varieties ranged from 17% to 43% across different features.

India and East Asia are recognized as secondary genetic centres for the watermelon species[18, 19, 38, 39]. Research conducted in these places, such as Anatolia, has revealed a significant level of morphological variation among the researched indigenous watermelon species [18, 19, 28, 30, 38-40].

Türkiye is located in an area abundant in genetic resources for watermelon. Previous studies in the country have conducted morphological characterizations of numerous local watermelon genotypes [1, 23, 31, 41-49]. In the scope of this study, some of the local Turkish watermelon genotypes were evaluated morphologically to understand morphological features and diversities. A total of 20 local genotypes and three commercial varieties were assessed regarding their cotyledon, leaf, and fruit phenotypes.

Material and Methods

Genetic materials, were evaluated before the aspect of their seed characteristics [50], supplied from different sources were evaluated in this study. Three commercial standard varieties are used as a control provided from the local seed market; seventeen of them were provided by YYY's personal collection, and three of them which are originally from Türkiye were supplied by United States Department of Agriculture (USDA) (Table 1).

Table 1 Origin information of genetic materials

Accession No/Cultivar	Provience/Country	Donor
Washington	-	Standard variety
Galaxy	-	Standard variety
Crimson Sweet	-	Standard variety
94004	Çanakkale/Türkiye	Affiliation of YYY/YYY
94005	Mersin/Türkiye	Affiliation of YYY/YYY
94006	Sakarya/Türkiye	Affiliation of YYY/YYY
94017	Uşak/Türkiye	Affiliation of YYY/YYY
94027	Unknown/Türkiye	Affiliation of YYY/YYY
94047	Unknown /Türkiye	Affiliation of YYY/YYY
94051	Unknown /Türkiye	Affiliation of YYY/YYY
94054	Sakarya/Türkiye	Affiliation of YYY/YYY
94058	Tekirdağ/Türkiye	Affiliation of YYY/YYY
94064	Tekirdağ/Türkiye	Affiliation of YYY/YYY
94081	Unknown /Türkiye	Affiliation of YYY/YYY
94100	Rize/Türkiye	Affiliation of YYY/YYY
94120	Unknown /Türkiye	Affiliation of YYY/YYY
94123	Unknown /Türkiye	Affiliation of YYY/YYY
94127	Unknown /Türkiye	Affiliation of YYY/YYY
94128	Unknown /Türkiye	Affiliation of YYY/YYY
94131	Unknown /Türkiye	Affiliation of YYY/YYY
PI169240 / cv. Kaymakam	Istanbul/Türkiye	USDA
PI169264 / cv. Yenidunya	Bursa/Türkiye	USDA
PI169294 / cv. Cinilikiz	Manisa/Türkiye	USDA

The experiment was designed according to a randomized plot experimental design with 20 plants on each plot. Plants were planted in a high tunnel, 1.5 x 2 m within and between rows. Cultural practices applied during the vegetation period according to [51]. Morphological observations were conducted according to the International Union for the Protection of New Varieties of Plants' (UPOV) TG/142/5 (proj.1) document [52]. For cotyledons three parameters (size, shape, and intensity of green color), for leaves six parameters (leaf length, leaf width, leaf blade size, leaf blade ratio length/width, color, degree of lobing, blistering, color of veins), for fruits eighteen parameters (fruit weight, fruit shape in longitudinal section, depression at base, shape of apical part, depression at apex, ground color of skin, conspicuousness of veining, pattern of stripes, width of stripes, main color of stripes, conspicuousness of stripes, margin of stripes, size of insertion of peduncle, size of pistil scar, grooving, waxy layer, thickness of pericarp, main color of flesh) were investigated in the study. Collected data were evaluated by R statistical environment for correlation, principal component (PCA), and hierarchical clustering analyses [53].

Results and Discussion

Cotyledons

Evaluated genotypes regarding cotyledon shapes were 21.73% narrow, 52.17% elliptical, and 26.08% broad characteristics. Cotyledon sizes of the genotypes were observed as 8.70% small, 21.73% medium, and 69.56% large. The intensity of green color on cotyledons varied among the genotypes, as 43.47% had medium intensity and 55.52% was dark.

In their studies on Distinctiveness, Uniformity, and Stability testing in watermelon, Choudhary, Pandey [38] also examined the differences in cotyledon shapes during the seedling stage. They have reported that the Sugar Baby and Charleston Grey varieties exhibit narrow elliptical cotyledons, the African-origin Arka Manik variety has medium elliptical cotyledons, and the Japanese-origin Asahi Yamato and African-origin Thar Manak varieties have broad elliptical cotyledons. Sarı, Solmaz [1], in their studies conducting the morphological characterization of Turkish-origin accessions, also examined criteria such as cotyledon shape, size, and the intensity of the green color in cotyledons. In the study, 54% of the examined accessions had elliptical cotyledons, 46% had broad cotyledons, and no narrow elliptical cotyledon structure was observed among them. Our study observed that 21.73% of the genotypes examined according to cotyledon shapes had narrow, 52.17% had elliptical, and 26.08% had broad structures. Although the studies of Solmaz [54] cover the Southeastern Anatolia, Aegean, Marmara-Thrace, Central Anatolia, and Mediterranean Regions, they predominantly contain samples from the Southeastern Anatolia and Aegean Regions. However, the differences between the two studies may also stem from being conducted in completely different ecologies.

In the studies conducted by Solmaz, Sarı [55], the cotyledon size of the examined accessions was observed as 4% small, 44% medium, and 52% large. They have reported that the intensity of the green color in the cotyledons was medium in all accessions. In our study, however, it was observed that 8.70% of the parents examined according to cotyledon size had small, 21.73% had medium, and 69.56% had large structures, and concerning the intensity of the green color in cotyledons, 43.47% of the examined parents had medium intensity, and 55.52% had dark intensity. The distributions of these two characters reviewed in our study also support the positive relationship in the factor analysis. Still, the findings of Solmaz, Sarı [55] were not the same Szamosi, Solmaz [31], in their comparative study examining Hungarian and Turkish origin accessions, reported that only 2% of the Hungarian accessions were narrow and 98% were elliptical.

Leaves

In the study, it has been observed that leaf widths range between 28.23 cm and 19.96 cm, leaf lengths between 27.13 cm and 19.7 cm, and petiole lengths between 13.53 cm and 8 cm. Alimari, Zaid and Fadda [16] examined leaf width, length, and petiole length in their study investigating the genetic diversity among Palestinian local varieties. Their results indicated leaf widths ranged from 14.8 cm to 11.3 cm, leaf lengths from 15.3 cm to 12.1 cm, and petiole lengths from 8.5 cm to 5.4 cm. Choudhary, Pandey [38] classified leaves as large if they were longer than 14 cm, wider than 12 cm, and had a petiole length over 9 cm. In their findings, the Charleston Grey variety was described as having long, broad leaves with long petioles. According to this classification, most local varieties examined in our study were classified into the large leaf category according to Choudhary, Pandey [38], but most local varieties examined in our study were classified as medium-sized.

According to leaf size, it was observed that 26.08% of the examined lines and standard varieties are small, 47.82% are medium, and 26.08% are large. When examined according to the leaf length/width ratio, 4.34% were broad, 56.52% medium, and 39.13% narrow. Regarding leaf colors, 8.69% were yellowish-green, 39.13% green, and 52.17% were grayish-green. No bluish-green leaf type was observed among the lines and standard varieties examined in the study. Based on the degree of leaf lobing, 4.34% were observed to be very weak, 17.39% weak, 8.69% between weak and medium, 65.21% medium, and 4.34% strong. No examples of very strong leaf lobing degrees were encountered in the study.

When local varieties were examined for leaf curliness, 30.43% were weak, 56.52% medium, and 13.04% strongly curled. The vein color characteristic was green in all genotypes, without variation.

Solmaz, Sarı [55] reported in their studies on Turkish-origin genotypes that 39% had a wide leaf length/width ratio, 60% medium, and 1% narrow. Regarding leaf color, no yellowish-green or bluish-green colors were encountered among the genotypes; 28% had green leaves, and 72% had grayish-green leaves. Regarding the degree of leaf lobing, 12% of the genotypes were weak, 51% medium, and 49% strong. As for leaf curliness, 42% were weak, 47% medium, and 11% strong.

Fruits

In the research by Soltani, Ebadi [30] on Iranian watermelons, the study of plant growth form, leaf, and fruit characteristics concluded that fruit morphological characters are useful indicators for determining genetic variation and selection. Additionally, Gichimu, Owuor [20 and Dida 2009] found in their study on Kenyan

genotypes and commercial varieties that commercial varieties exhibit less genetic diversity than non-commercially bred accessions and varieties. In our study, according to fruit sizes, genotypes showed a distribution of 21.73% small, 21.73% between small to medium, 39.13% medium, 13.04% between medium to large, and 4.34% large. Based on the fruit shape in the longitudinal section, 52.17% of the local genotypes and standard varieties had a circular shape, 43.47% were broad elliptical, and 4.34% were medium elliptical. When examining the characteristics of the depression at the fruit base, 47.82% had no or very superficial base depression, 26.08% had superficial base depression, and 26.08% had medium base depression.

Among the genotypes examined within the scope of our study, high variation in fruit characteristics was observed. According to the shape of the apical part of the fruit, 47.82% of the genotypes exhibited a truncate shape, 8.69% between truncate to round, and 43.47% round. In terms of the depression at the apex, 17.39% of the genotypes showed absent or very shallow, 43.47% had shallow, and 39.13% had medium depression at the apex. The ground color of the skin varied from very light green to very dark green. The genotypes were 34.78% very light green, 26.08% light green, 8.69% from light green to green, 13.04% green, 4.34% dark green, 4.34% from dark green to very dark green, and 8.69% very dark green.

Strong fruit grooving was not observed among the genotypes; 86.95% had no or indistinct grooving, 8.69% had weak grooving, and 4.34% had medium grooving. The genotypes included in the study also exhibited a wide variety in terms of stripe pattern. The genotypes were 27.8% only one color, 8.3% one colored and veins, 5.6% one color, veins and marbled, 8.3% one color and marbled, 8.3% two colors, veins and marbled, and 41.7% veins only. The conspicuousness of the veins was inconspicuous or very weakly conspicuous in 56.52% of the genotypes, weak in 8.69%, medium in 17.39%, and strong in 17.39%.

The pattern of the stripes among the genotypes was 26.08% one color, 8.69% one color with veins, 8.69% one color with veins and marbled, 8.69% one color and marbled, 8.69% two colors with veins and marbled, and 39.13% veins only. When examining the stripe width, 52.17% had very narrow, 8.69% narrow, 13.04% medium, 8.69% wide, and 17.39% very wide. The main stripe color distribution was 8.69% yellow, 13.04% very light green, 4.34% light green, 39.13% green, 26.08% dark green, and 8.69% very dark green. The conspicuousness of stripes varied among the genotypes, with 34.78% having inconspicuous or very weakly conspicuous stripes, 4.34% weak, 39.13% medium, 17.39% strong, and 4.34% very strong. In the samples examined, the margin of stripes was observed as 58.3% diffuse, 25% medium, and 16.7% sharp. Regarding the size of the insertion of the peduncle, it was found that 17.39% of the samples had a small insertion, 13.04% had a medium insertion, and 69.56% had a large insertion. The size of the pistil scar was small in 34.78% of the samples, medium in 34.78%, and large in 30.43%. A waxy layer was either not observed or was very weak in 56.52% of the samples, medium in 4.34%, and very strong in 39.13%. Regarding pericarp thickness, 13.04% of the fruit samples were thin, 4.34% were between thin and medium, 26.08% were medium, 4.34% were between medium and thick, 43.47% were thick, and 8.69% were very thick. In genotypes, the fruit flesh color was observed as 8.69% white, 17.39% yellow, 17.39% pink, 30.43% pinkish-red, 21.73% red, and 4.34% dark red.

Correlation between morphological traits

The heatmap showed on Figure 1 is a correlation matrix that illustrates the relationships between different characteristics of cotyledons, leaves, and fruits. Size, shape, and intensity of green color of the cotyledons may have correlations with each other. For instance, larger cotyledons might also tend to be a darker green, which could be indicated by a red square where CSI and CCI intersect.

Length and width of the leaves are likely correlated (larger leaves are both longer and wider), which would appear as a red square at the intersection of LL and LW. The ratio of length to width (LL/W) would have a strong positive correlation with length (LL) and a strong negative correlation with width (LW), showing as a red square with LL and a blue/purple square with LW. Leaf color (LC) and degree of lobing (LDoL) or blistering (LB) might not be directly related to the size of the leaves but may show correlation with each other if certain leaf colors are associated with specific morphologies.

Fruit weight (FW) is likely correlated with the dimensions of the fruit (such as length and width), and this would show as red squares where FW intersects with size-related variables. The shape in longitudinal section (FLS), depression at base (FDB), and shape of apical part (FAS) may show correlations with each other, indicating that certain shapes are commonly associated with specific features at the fruit's base or apex. Ground color of the skin (FGC) and main color of the flesh (FC) may or may not be correlated depending on whether there's a common pigmentation pattern in the species studied. The degree of grooving (FG), conspicuousness of veining (FVC), and pattern of stripes (FPS) might be related to one another if they are features that tend to occur together in certain varieties. The color characteristics like the main color of stripes (FMSC), conspicuousness of stripes (FSC), and margin of stripes (FMS) are likely to show correlations, as these are all coloration patterns on the fruit's skin.

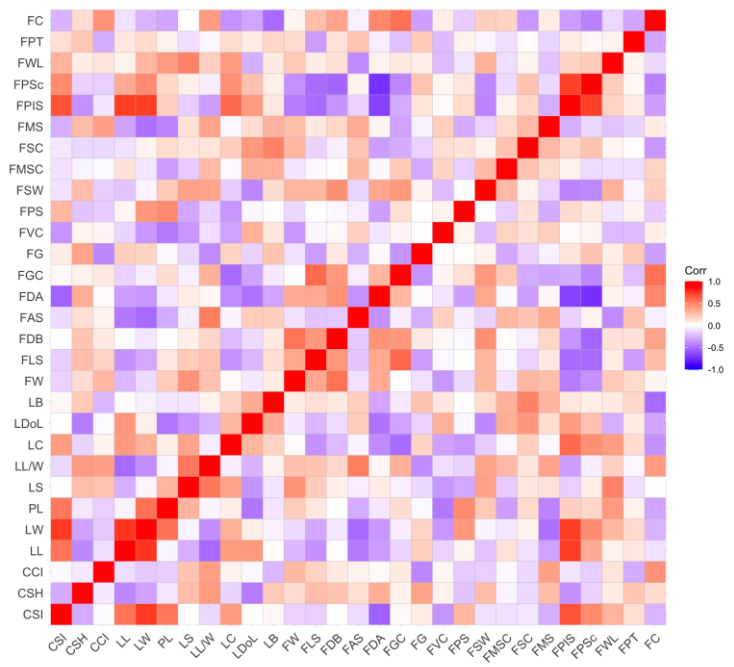

Fig 1 Correlation between the evaluated characters

CSI; Cotyledon: Size, CSH; Cotyledon: Shape, CCI; Cotyledon: Intensity of Green Color, LL; Leaf: Length, LW; Leaf: Width, PL; Leaf: Peduncule Length, LS; Leaf: Size, LL/W; Leaf: Blade Ratio Length/Width, LC; Leaf: Color, LDoL; Leaf: Degree of Lobing, LB; Leaf: Degree of Blistering, FW; Fruit: Weight, FLS; Fruit: Shape in Longitudinal Section, FDB; Fruit: Depression at Base, FAS; Fruit: Shape of Apical Part, FDA; Fruit: Depression at Apex, FGC; Fruit: Ground Color of Skin, FG; Fruit: Grooving, FVC; Fruit: Conspicuousness of Veining, FPS; Fruit: Pattern of Stripes, FSW; Fruit: Width of Stripes, FMSC; Fruit: Main Color of Stripes, FSC; Fruit: Conspicuousness of Stripes, FMS; Fruit: Margin of Stripes, FPIS; Fruit: Size of Insertion of Peduncle, FPSc; Fruit: Size of Pistil Scar, FWL; Fruit: Waxy Layer, FPT; Fruit: Thickness of Pericarp, FC; Fruit: Main Color of Flesh [14.07 cm (H) X 15.01 cm (W)]

There may also be interesting correlations between categories, such as whether certain leaf characteristics correlate with fruit characteristics. For example, the intensity of green color in cotyledons (CCI) might correlate with the main color of flesh in fruits (FC) if a deeper green in early plant development is an indicator of certain fruit pigmentation.

Principal components and hierarchical cluster analyses

There is vector map of PC analysis of variables in Figure 2. The first main component (Dim1), accounting for 48% of the variance, is likely indicative of a distinction between size-related characteristics and other morphological traits, as it exhibits the highest variability across the axes. The second main component (Dim2) captures additional variance (18.1%) that is perpendicular to the first component, potentially expressing other independent changes in traits such as color or texture.

The color scheme applied to the vectors depicting the squared cosine of the variable indicates the degree to which each variable is accurately represented in the principal components. The presence of darker hues on vectors indicates that those variables are accurately depicted by the two shown components.

The vectors of CSI, CSH, and CCI align in the same direction, it suggests that these traits tend to change together within the samples and may form a cluster. From this perspective, it is suggested that larger cotyledons may have a certain form and higher color intensity.

LL, LW, PL, LS, and LL/W are all parameters that pertain to the dimensions and proportions of the leaves. The vectors of these traits were aligned, they exhibit correlation. LC, LDoL, and LB exhibit contrasting patterns compared to the size-related features, it indicates that color and texture are not influenced by leaf size and shape. The association between LC, LDoL, and LB with the size-related characteristics does not necessarily indicate that color and texture are unrelated to leaf size and shape, as there may still be other variables influencing these qualities. The weight of the fruit and traits linked to its size, such as FLS, FDB, and FAS, may exhibit a correlation if they indicate similar tendencies.

The surface properties of the fruit are described with FDA, FGC, FG, FVC, and FPS. If these vectors exhibit proximity, it is probable that these qualities exhibit co-variation. There is a possibility that there is no correlation between fruit weight and size-related qualities such as FLS, FDB, and FAS. This could be due to

the presence of other factors that independently influence these features. Conversely, the surface attributes of the fruit, as defined by FDA, FGC, FG, FVC, and FPS, may not always exhibit similar variations simply because their vectors are in close proximity. Additionally, the color trait FC is not directly related to structural features.

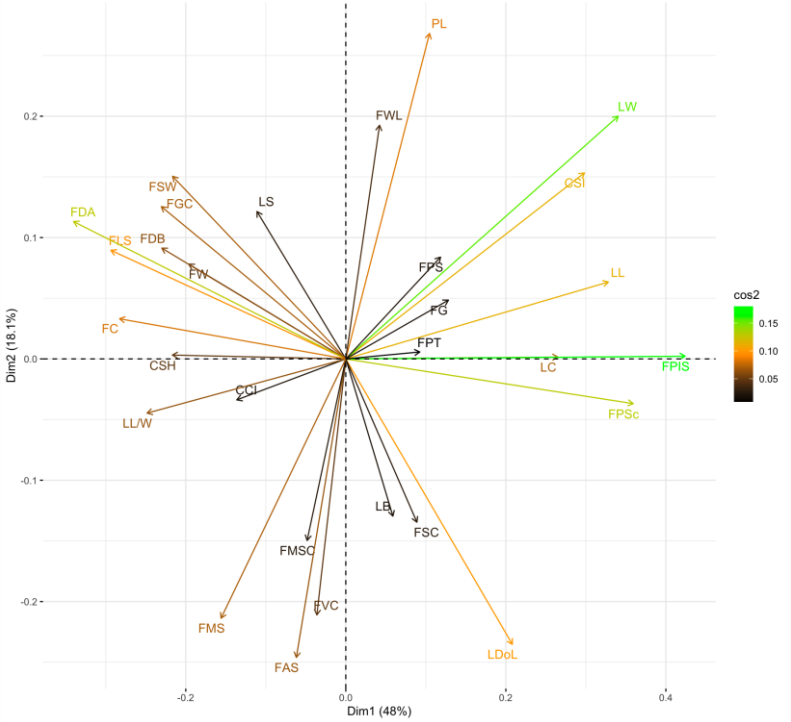

Fig 2 Principal component analysis of variables

CSI; Cotyledon: Size, CSH; Cotyledon: Shape, CCI; Cotyledon: Intensity of Green Color, LL; Leaf: Length, LW; Leaf: Width, PL; Leaf: Peduncule Length, LS; Leaf: Size, LL/W; Leaf: Blade Ratio Length/Width, LC; Leaf: Color, LDoL; Leaf: Degree of Lobing, LB; Leaf: Degree of Blistering, FW; Fruit: Weight, FLS; Fruit: Shape in Longitudinal Section, FDB; Fruit: Depression at Base, FAS; Fruit: Shape of Apical Part, FDA; Fruit: Depression at Apex, FGC; Fruit: Ground Color of Skin, FG; Fruit: Grooving, FVC; Fruit: Conspicuousness of Veining, FPS; Fruit: Pattern of Stripes, FSW; Fruit: Width of Stripes, FMSC; Fruit: Main Color of Stripes, FSC; Fruit: Conspicuousness of Stripes, FMS; Fruit: Margin of Stripes, FPIS; Fruit: Size of Insertion of Peduncle, FPSc; Fruit: Size of Pistil Scar, FWL; Fruit: Waxy Layer, FPT; Fruit: Thickness of Pericarp, FC; Fruit: Main Color of Flesh [13.69 cm (H) x 15.01 cm]

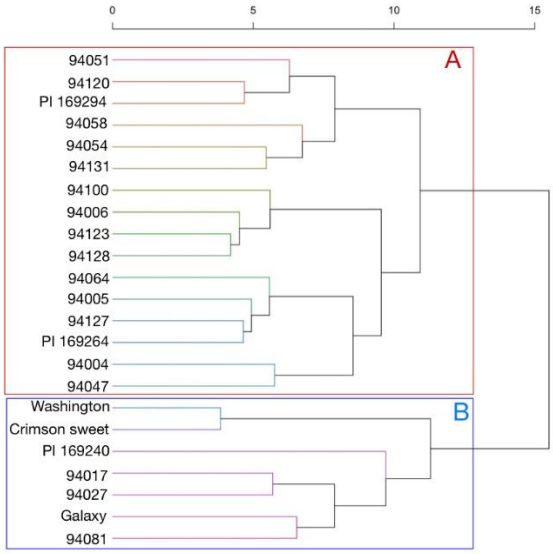

Fig 3 Hierarchical cluster analysis dendrogram of genotypes [15.34 cm (H) x 15.01 cm]

Regarding to hierarchical clustering analysis there were two main clusters (A, B) (Figure 3). According to this segregation in the first main cluster (A) there are 16 genotypes and in the second cluster (B) 7 genotypes.
PI 169294, PI169264, 94051, 94120, 94058, 94054, 94131, 94100, 94006, 94123, 94128, 94064, 94005, 94127, 94004, and 94047 genotypes were placed in the first main cluster. All of three commercial varieties placed at cluster B and PI 169240, 94017, 94027, and 94081 were placed together at cluster B.
This study provides a comprehensive analysis of the morphological characteristics of watermelon genotypes, particularly focusing on cotyledons, leaves, and fruits. Our findings suggest a diverse range of shapes, sizes, and colors within these characteristics, which contribute significantly to the distinctiveness and identification of varieties. The cotyledon characteristics observed in our study closely align with the findings of Choudhary, Pandey [38] and contrast with Solmaz, Sarı [55], highlighting the influence of different ecological conditions on morphological traits.
In comparison with previous studies, our research noted a greater prevalence of larger cotyledon and leaf sizes and a wider variation in the intensity of green color. These differences may stem from the varied geographic sampling of genotypes or the inherent genetic diversity within our study group. Similarly, leaf characteristics such as size, color, and degree of lobing showed notable variability, which may serve as additional descriptors for genotype identification and classification.
Our analysis of fruit characteristics revealed a high degree of variation, particularly in size, shape, and color traits, suggesting a rich genetic diversity within the examined genotypes. This diversity is crucial for breeding programs aimed at improving specific traits, as it provides a larger pool of characteristics from which to select. The findings also support previous research by Soltani, Ebadi [30] and Gichimu, Owuor [20] on the importance of morphological characteristics in assessing genetic variation and selection within watermelon genotypes.
The correlation matrix and principal component analysis provided in Figures 1 and 2 illustrate the relationships between different characteristics, suggesting that certain traits may have a tendency to cluster together. These patterns are essential for understanding the morphological structure of watermelon genotypes and for the potential prediction of other traits based on observed correlations.
Hierarchical clustering analysis identified two main clusters, suggesting a clear differentiation among the genotypes based on the measured morphological characteristics. The distribution of commercial varieties in a separate cluster from local varieties could indicate distinct selective breeding practices that have influenced their morphological traits.

Conclusion

Despite the lack of genetic diversity in watermelon breeding lines because of the narrow genetic base, there are many opportunity aspects of biotechnology tools for crop improvement. Underutilized crops, like local varieties or local genotypes, could be answer for lack of genetic diversity. Using biotechnology tools with those valuable underutilized crops also leads crop improvement studies one step further for the resistance of biotic and abiotic stress vectors. Overall, our study underscores the complexity of morphological characteristics in watermelon genotypes and provides valuable insights for breeding and conservation efforts. The observed variability and correlations between traits offer a resource for future research aiming to understand the underlying genetic basis of these morphological differences and their potential exploitation in the development of new varieties with desired characteristics. Since we present detailed morphological background information for those local genotypes, our further goal is to understand their resistance to biotic/abiotic stressors and combining abilities for gene pyramiding studies.

Abbreviations

CSI; Cotyledon: Size, CSH; Cotyledon: Shape, CCI; Cotyledon: Intensity of Green Color, LL; Leaf: Length, LW; Leaf: Width, PL; Leaf: Peduncule Length, LS; Leaf: Size, LL/W; Leaf: Blade Ratio Length/Width, LC; Leaf: Color, LDoL; Leaf: Degree of Lobing, LB; Leaf: Degree of Blistering, FW; Fruit: Weight, FLS; Fruit: Shape in Longitudinal Section, FDB; Fruit: Depression at Base, FAS; Fruit: Shape of Apical Part, FDA; Fruit: Depression at Apex, FGC; Fruit: Ground Color of Skin, FG; Fruit: Grooving, FVC; Fruit: Conspicuousness of Veining, FPS; Fruit: Pattern of Stripes, FSW; Fruit: Width of Stripes, FMSC; Fruit: Main Color of Stripes, FSC; Fruit: Conspicuousness of Stripes, FMS; Fruit: Margin of Stripes, FPIS; Fruit: Size of Insertion of Peduncle, FPSc; Fruit: Size of Pistil Scar, FWL; Fruit: Waxy Layer, FPT; Fruit: Thickness of Pericarp, FC; Fruit: Main Color of Flesh

Acknowledgments

The article is a part of studies previously published in the Ph.D. thesis of the author (Sahin, N. Morphological and molecular characterization of some local watermelon genotypes. Ph.D. thesis, Tekirdağ Namık Kemal University, Institute of Natural and Applied Sciences, Department of Horticulture, 2021). Data in this article was merged, and the text was critically reviewed. Thank Dr. Polat (Tekirdağ Namık Kemal University) for providing part of the plant material for the study.

Funding
The authors did not receive support from any organization for the submitted work.
Data Availability statement
The author confirms that the data supporting this study are cited in the article.
Compliance with ethical standards
Conflict of interest
The authors declare no conflict of interest.
Ethical standards
The study is proper with ethical standards.
Authors' contributions
All authors contributed equally to the study.

References

1. Sarı, N., et al. Watermelon genetic resources in Turkey and their characteristics. in III International Symposium on Cucurbits 731. 2005. https://doi.org/10.17660/ActaHortic.2007.731.59.
2. Karagöz, A., K. Özbek, and N. Sarı, Türkiye'nin bitkisel biyolojik çeşitliliğinin korunması ve sürdürülebilir kullanımına ilişkin sorunlar ve çözüm önerileri. Tarla Bitkileri Merkez Araştırma Enstitüsü Dergisi, 2016: p. 88-99https://doi.org/10.21566/tbmaed.91136.
3. Hashizume, T., I. Shimamoto, and M. Hirai, Construction of a linkage map and QTL analysis of horticultural traits for watermelon [Citrullus lanatus (THUNB.) MATSUM & NAKAI] using RAPD, RFLP and ISSR markers. Theor Appl Genet, 2003. 106(5): p. 779-85https://doi.org/10.1007/s00122-002-1030-1.
4. Liu, S., et al., Development of cleaved amplified polymorphic sequence markers and a CAPS-based genetic linkage map in watermelon (Citrullus lanatus [Thunb.] Matsum. and Nakai) constructed using whole-genome re-sequencing data. Breed Sci, 2016. 66(2): p. 244-59https://doi.org/10.1270/jsbbs.66.244.
5. Paudel, L., J. Clevenger, and C. McGregor, Chromosomal Locations and Interactions of Four Loci Associated With Seed Coat Color in Watermelon. Front Plant Sci, 2019. 10: p. 788https://doi.org/10.3389/fpls.2019.00788.
6. Bang, H., et al., Flesh Color Inheritance and Gene Interactions among Canary Yellow, Pale Yellow, and Red Watermelon. Journal of the American Society for Horticultural Science, 2010. 135(4): p. 362-368https://doi.org/10.21273/jashs.135.4.362.
7. Barham, W. A study of the Royal Golden watermelon with emphasis on the inheritance of the chlorotic condition characteristic of this variety. in Proc. Amer. Soc. Hort. Sci. 1956.
8. Dou, J., et al., Genetic mapping reveals a marker for yellow skin in watermelon (Citrullus lanatus L.). PLoS One, 2018. 13(9): p. e0200617https://doi.org/10.1371/journal.pone.0200617.
9. Gama, R.N., et al., Microsatellite markers linked to the locus of the watermelon fruit stripe pattern. Genet Mol Res, 2015. 14(1): p. 269-76https://doi.org/10.4238/2015.January.16.11.
10. Gao, L., et al., Comparative transcriptome analysis reveals key genes potentially related to soluble sugar and organic acid accumulation in watermelon. PLoS One, 2018. 13(1): p. e0190096https://doi.org/10.1371/journal.pone.0190096.
11. Guner, N. and T.C. Wehner, Gene list for watermelon. Cucurbit Genet Coop Rpt, 2003. 26: p. 76-92
12. Gusmini, G. and T.C. Wehner, Qualitative inheritance of rind pattern and flesh color in watermelon. J Hered, 2006. 97(2): p. 177-85https://doi.org/10.1093/jhered/esj023.
13. Gusmini, G. and T.C. Wehner, Polygenic inheritance of some vine traits in two segregating watermelon families. Cucurbit Genetics Cooperative Report, 2003. 26: p. 32-35
14. Hawkins, L.K., F. Dane, and T.L. Kubisiak, Molecular Markers Associated with Morphological Traits in Watermelon. Hortscience, 2001. 36(7): p. 1318–1322https://doi.org/10.21273/HORTSCI.36.7.1318.
15. McGregor, C., Citrullus lanatus germplasm of southern Africa. Israel Journal of Plant Sciences, 2012. 60(4): p. 403-413https://doi.org/10.1560/IJPS.60.1.403.
16. Alimari, A., A. Zaid, and Z. Fadda, Genetic diversity in local Palestinian watermelon (Citrullus lanatus) accessions. International Journal of Agricultural Policy and Research, 2017. 5(10): p. 157-162https://doi.org/10.15739/IJAPR.17.018.
17. Goda, M., Diversity of local genetic resources of watermelon Citrullus lanatus (Thunb.) Matsum and Nakai, in Sudan, in Sc Thesis. Swedish Biodiversity Centre, Uppsala, Sweden. 2007.
18. Achigan-Dako, E.G., et al., Phenetic characterization of Citrullus spp. (Cucurbitaceae) and differentiation of egusi-type (C. mucosospermus). Genetic Resources and Crop Evolution, 2015. 62(8): p. 1159-1179https://doi.org/10.1007/s10722-015-0220-z.
19. Choudhary, B.R., S. Pandey, and P.K. Singh, Morphological diversity analysis among watermelon (Citrullus lanatus (Thunb) Mansf.) genotypes. Progressive Agriculture, 2015. 44(2): p. 321-326
20. Gichimu, B.M., et al., Morphological characterization of some wild and cultivated watermelon (Citrullus sp.) accessions in Kenya. Journal of Agricultural and Biological Science, 2009. 4(2): p. 10-18
21. Gürcan, K., et al., A study of genetic diversity in bottle gourd [Lagenaria siceraria (Molina) Standl.] population, and implication for the historical origins on bottle gourds in Turkey. Genetic Resources and Crop Evolution, 2015. 62(3): p. 321-333https://doi.org/10.1007/s10722-015-0224-8.
22. Hakimi, F. and S. El Madidi, Variability of agro-morphological traits in some Moroccan watermelon landraces (Citrullus lanatus Thunb. Matsum & Nakai). International Journal of Current Sciences, 2015. 17: p. 90-6
23. Huh, Y.C., İ. Solmaz, and N. Sarı, Morphological characterization of Korean and Turkish watermelon germplasm, in IXth EUCARPIA, Cucurbitaceae 2008 P. M., Editor. 2008, INRA: Avignon (France).
24. Lima Neto, I.d.S., et al., Morphological characterization and genetic diversity among watermelon accessions. Magistra (Brazil), 2008
25. Silva, M.L.d., et al., Morphological and molecular characterization of watermelon. Horticultura Brasileira, 2006. 24(4): p. 405-409https://doi.org/10.1590/S0102-05362006000400002.

26. Singh, D., Morphological and molecular characterization of watermelon [Citrullus lanatus (Thunb.) Matsum and Nakai] genetic resources. 2016, Punjab Agricultural University, Ludhiana.
27. Singh, D., et al., Morphological and genetic diversity analysis of Citrullus landraces from India and their genetic inter relationship with continental watermelons. Scientia Horticulturae, 2017. 218: p. 240-248https://doi.org/10.1016/j.scienta.2017.02.013.
28. Soghani, Z.N., et al., Grouping and genetic diversity of different watermelon ecotypes based on agro-morphological traits and ISSR marker. Iheringia. Série Botânica., 2018. 73(1): p. 53-59https://doi.org/10.21826/2446-8231201873107.
29. Solmaz, İ. and N. Sarı, Characterization of watermelon (Citrullus lanatus) accessions collected from Turkey for morphological traits. Genetic Resources and Crop Evolution, 2008. 56(2): p. 173-188https://doi.org/10.1007/s10722-008-9353-7.
30. Soltani, F., et al. Evaluation of phenotypic variation of Iranian watermelon (Citrullus sp.) accessions by morphological markers. in International Symposium on Biotechnology and Other Omics in Vegetable Science 1145. 2012. 10.17660/ActaHortic.2016.1145.20.
31. Szamosi, C., et al., Morphological characterization of Hungarian and Turkish watermelon (Citrullus lanatus (Thunb.) Matsum. et Nakai) genetic resources. Genetic Resources and Crop Evolution, 2009. 56(8): p. 1091-1105https://doi.org/10.1007/s10722-009-9432-4.
32. Şahin, N., Bazı yerel karpuz genotiplerinin morfolojik ve moleküler karakterizasyonu, in Fen Bilimleri Enstitüsü. 2021, Tekirdağ Namık Kemal Üniversitesi: Tekirdağ. p. 134.
33. Levi, A., et al., Genetic Resources of Watermelon, in Genetics and Genomics of Cucurbitaceae. 2017. p. 87-110https://doi.org/10.1007/7397_2016_34.
34. Thies, J.A. and A. Levi, Characterization of watermelon (Citrullus lanatus var. citroides) germplasm for resistance to root-knot nematodes. HortScience, 2007. 42(7): p. 1530-1533https://doi.org/10.21273/HORTSCI.42.7.1530.
35. Levi, A., et al., Genetic diversity among watermelon (Citrullus lanatus and Citrullus colocynthis) accessions. Genetic Resources and Crop Evolution, 2001. 48(559-566)https://doi.org/10.1023/A:1013888418442.
36. Maggs-Kölling, G.L. and J.L. Christiansen, Variability in Namibian landraces of watermelon (Citrullus lanatus). Euphytica, 2003. 132: p. 251-258https://doi.org/10.1023/A:1025053331528.
37. Hakimi, F. and S.E. Madidi, Variability of agro-morphological traits in some Moroccan watermelon landraces (Citrullus lanatus Thunb. Matsum. and Nakai). International Journal of Current Science, 2015. 17(E): p. 90-96
38. Choudhary, B.R., et al., Characterization of variability in watermelon (Citrullus lanatus) for DUS testing. Current Horticulture, 2016. 4(2): p. 30-34
39. Pandey, A., et al., Genetic diversity and population structure of watermelon (Citrullus sp.) genotypes. 3 Biotech, 2019. 9(6): p. 210https://doi.org/10.1007/s13205-019-1736-2.
40. Jaiswal, S., et al., Putative Microsatellite DNA Marker-Based Wheat Genomic Resource for Varietal Improvement and Management. Front Plant Sci, 2017. 8: p. 2009https://doi.org/10.3389/fpls.2017.02009.
41. Ay, T. and A. Erkılıç, Çukurova'da karpuz Fusarium solgunluğu etmeni Fusarium oxysporum f.sp. niveum'un ırklarının ve bu ırklara karşı bazı karpuz çeşitlerinin reaksiyonlarının belirlenmesi. Bitki Koruma Bülteni, 2008. 48(1): p. 49-58
42. Bağ, M., et al., Çekirdekli mini karpuz melezlerinin bazı tarımsal özelliklerinin belirlenmesi. Akademik Ziraat Dergisi, 2017. 6(Özel Sayı): p. 137-144
43. Karipcin, M.Z., N. Sarı, and H. Kırnak, Effects of drought on yield and pomological features of wild and domestic turkish watermelon genotypes. Acta horticulturae, 2010(871): p. 259-266https://doi.org/10.17660/ActaHortic.2010.871.34.
44. Karipcin, M.Z., N. Sarı, and H. Kırnak, Preliminary research on drought resistance of wild and domestic Turkish watermelon accessions, in Cucurbitaceae 2008, Proceedings of the IXth EUCARPIA meeting on genetics and breeding of Cucurbitaceae. 2008: INRA, Avignon, France. p. 493-499.
45. Karipcin, M.Z., N. Sarı, and H. Kırnak, Yerli ve yabani karpuz genotiplerinde kuraklığa toleransın belirlenmesi. 2009: Şanlıurfa.
46. Solmaz, İ., et al. Seed characteristics and seed-fruit correlation of Turkish watermelon germplasm. in Cucurbitaceae 2012. Proceedings of the Xth EUCARPIA Meeting on Genetics and Breeding of Cucurbitaceae, Antalya, Turkey, 15-18 October, 2012. 2012. University of Cukurova, Ziraat Fakultesi
47. Süyüm, K., Karpuz genetik kaynaklarının tuzluluk ve kuraklığa tolerans seviyelerinin belirlenmesi, in Fen Bilimleri Enstitüsü. 2011, Çukurova Üniversitesi: Adana. p. 145.
48. Szamosi, C., et al., Morphological evaluation and comparison of Hungarian and Turkish melon (Cucumis melo L.) germplasm. Scientia Horticulturae, 2010. 124(2): p. 170-182https://doi.org/10.1016/j.scienta.2009.12.024.
49. Yağcıoğlu, M., et al., Preliminary studies of genom-wide association mapping for some selected morphological characters of watermelons. Scientia Horticulturae, 2016. 210: p. 277-284https://doi.org/10.1016/j.scienta.2016.08.001.
50. Sahin, N. and S. Polat. Morphological characterizations of some watermelon seeds. in XXX International Horticultural Congress IHC2018: V International Symposium on Plant Genetic Resources and International 1297. 2018. https://doi.org/10.17660/ActaHortic.2020.1297.27.
51. Şalk, A., et al., Cucurbitaceae (Kabakgiller) Familyası Sebzeleri, in Özel Sebzecilik. 2008, Onur Grafik Matbaa ve Reklam Hizmetleri: Tekirdağ. p. 488
52. UPOV, Watermelon Guidelines for The Conduct of Tests for Distinctness, Uniformity and Stability, in CTRLS_LAN, I.U.f.T.P.o.N.V.o. Plants, Editor. 2013, International Union for The Protection of New Varieties of Plants: Geneva. p. 39.
53. Lê, S., J. Josse, and F. Husson, FactoMineR: an R package for multivariate analysis. Journal of statistical software, 2008. 25(1): p. 1-18https://doi.org/10.18637/jss.v025.i01.
54. Solmaz, İ., Bazı karpuz genotiplerinin ssr ve srap markörleri ile karakterizasyonu ve fusarıum solgunluğu (Fusarium oxysporum f.sp. niveum)'na dayanımlarının klasik ve moleküler yöntemlerle araştırılması, in Fen Bilimleri Enstitüsü. 2010, Çukurova Üniversitesi: Adana. p. 140.
55. Solmaz, İ., et al., The genetic characterization of Turkish watermelon (Citrullus lanatus) accessions using RAPD markers. Genetic resources and crop evolution, 2010. 57(5): p. 763-771https://doi.org/10.1007/s10722-009-9515-2.

International Journal of Life Sciences and Biotechnology
Syahidah N.A., et al., Prevalence of *Edwardsiella ictaluri* in Cage Cultured *Pangasius spp* in Pahang River and Their Risk Factors. International Journal of Life Sciences and Biotechnology, 2024 7(2): p. 37-45.
https://doi.org/10.38001/ijlsb.1414371
Araştırma Makale/ Research article

Prevalence of *Edwardsiella ictaluri* in Cage Cultured *Pangasius spp* in Pahang River and Their Risk Factors

N Amira-Syahidah [1], M Nur-Nazifah [1*], R Rimatulhana [2], AA Sabuti [1], Mohamad Shafiq Mohd Ibrahim [3]

ABSTRACT
Striped catfish, *Pangasianodon hypophthalmus* is a native species to most Asian countries, including Malaysia which faced series of bacterial disease such as edwardsiellosis caused by *E.ictaluri*. *Edwardsiella ictaluri* is a Gram-negative intracellular bacterial pathogen which had caused mortalities in farmed or wild fish in lots of countries and accountable for large economic losses. This study was conducted to determine disease status of Pangasius spp due to *Edwardsiella ictaluri* and to determine the risk factors of *E.ictaluri* in striped catfish in Pahang River, Malaysia. Four sampling sites were chosen, two sites in Pekan (Kampung Belimbing and Kampung Tanjung Pulai) and two sites in Temerloh (Kampung Teluk Ira and Kampung Bintang). Thirty samples were collected from each farm for 6 months consecutively and four organ tissues were taken which were liver, spleen, kidney, and brain. External and internal clinical signs were recorded accordingly. DNA was extracted from all tissues and pursued for PCR to detect the presence of *Edwardsiella ictaluri*. Results show that the infected fish has gross internal clinical signs such as patchy liver, white nodular spleen, and congested kidney. The prevalence rate of *E.ictaluri* was highest at Kampung Tanjung Pulai in June with 16.67% compared to all farms. No infection of *E.ictaluri* shown at Kampung Belimbing during the whole sampling session. Spearman's rho correlation showed that the prevalence of *E.ictaluri* has strong correlation with temperature in Kampung Tanjung Pulai ($p > 0.05$). Meanwhile those bacteria prevalence have strong relationship with ammonia, sulfide and total suspended solid (TSS) with $p< 0.05$. The susceptible size for this bacterium in striped catfish is between 1 to 50g. To our knowledge, this paper is the first report for *Edwardsiella ictaluri*in cage cultured *P.hypopthalmus* in Pahang River, Malaysia.

ARTICLE HISTORY
Received
05 January 2024
Accepted
01 March 2024

KEYWORDS
Prevalence,
Edwardsiella ictaluri,
Pangasius hypophthalmus,
risk factor, PCR

Introduction

Pangasius hypophthalmus or striped catfish is classified into Pangasidae family and is one of the most popular species raised through aquaculture. Primarily, striped catfish are native to the Mekong Delta in Vietnam and recent years are extending most to Asian continent [1]. In Malaysia, the production of Pangasius spp showed tenfold increase from 10,891.51 tons in 2011 to 20, 861.9 tons in 2022 [2]. The culture of Pangasius spp in Malaysia become one of the primary activities for locals as their source of income, especially in Pahang River which located at Peninsular of Malaysia.

Despite the positive contribution of aquaculture, it is still an intensive agricultural practice and health-related problems that hinder both economic and socio-economic expansion of the sector. The primary constraint to many aquaculture species is the emergence of infectious diseases caused by pathogens such as bacteria, viruses, fungi, and infestations caused by parasites [3]. The majority of disease-related deaths in the catfish industry emanate from bacterial diseases, with the most common bacteria are caused by Edwardsiella ictaluri, Flavobacterium columnare, and Aeromonas hydrophila in channel catfish [4,5].

[1] Department of Marine Science, Kulliyyah of Science, International Islamic University Malaysia, Bandar Indera Mahkota, 25200 Kuantan, Pahang, Malaysia
[2] National Fish Health Research Centre, Department of Fisheries Malaysia, 11960 Batu Maung, Penang, Malaysia
[3] Kulliyyah of Dentistry, International Islamic University Malaysia, Bandar Indera Mahkota, 25200 Kuantan, Pahang, Malaysia
*Corresponding author: nurnazifah@iium.edu.my

Edwardsiella ictaluri is a Gram-negative and rod-shaped bacterium, emerging from the family of Enterobacteriaceae. It had become one of the most threatening bacteria which had caused massive loss to the catfish industry. This bacterium is the aetiological agent of Enteric Septicaemia of Catfish (ESC) in channel catfish (Ictalurus punctatus) and Bacillary Necrosis of Pangasius in striped catfish (Pangasianodon hypophthalmus) [1,6]. The external part of infected fish possessed swollen abdomen and petechial haemorrhages on the tail, fins, and occasionally over the rest of the body while internally presenting pinpoint white spot at the liver, kidney and spleen [7].

According to [8], a five years of survey study conducted in the Tama River, Japan, results indicate that mortality of ayu due to Edwardsiella ictaluri was driven by large water temperature fluctuations and low streamflow during unusual hot summer. Clinically sick fish were emaciated, and several had internally, white 1±3 mm diameter miliary lesions were observed under the capsular surface and throughout the parenchyma in the liver, kidney and spleen of diseased fish. Meanwhile, another in vitro challenge study showed that a pH value of 6.5 and NaCl concentration of 0.5% was optimal for the growth of bacteria E.ictaluri on striped catfish [9]. Given the importance of environmental conditions on the host-pathogen interaction, the aim of this study is to determine the disease status of E.ictaluri and to determine their risk factors in cage cultured striped catfish in Pahang River, Malaysia.

Material and Methods

Sampling sites

This study was carried out at Pahang River, Malaysia. Two different districts were chosen for this study which were at Pekan and Temerloh. Temerloh located upstream than Pekan which located more towards downstream. In Temerloh, two sampling sites were chosen which were Kampung Teluk Ira and Kampung Bintang, meanwhile in Pekan were at Kampung Belimbing and Kampung Tanjung Pulai. (Figure 1). These two districts are well known with their aquaculture activities especially for *Oreochromis* and *Pangasius* industry among local.

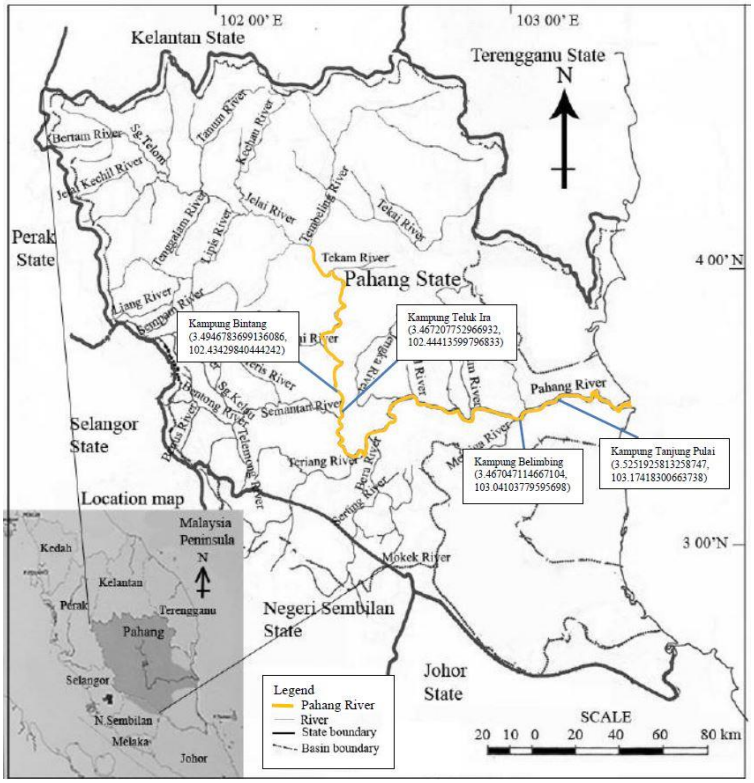

Fig 1 The map of Pahang State. Yellow line indicates Pahang River. Kampung Bintang and Kampung Teluk Ira were in Temerloh. Kampung Belimbing and Kampung Tanjung Pulai are located in Pekan

Fish sampling

Enteric septicemia of catfish (ESC), caused by the Gram-negative bacterium *Edwardsiella ictaluri*, is one of the most important diseases of farm-raised channel catfish (*Ictaluruspunctatus*), and now known to occur throughout the geographic range of the catfish industry. The source of the striped catfish fingerlings was obtained from the same supplier. On average, the size of the fish is about 3.5 inches to 4 inches during the

restocking phase. Early screeningfor each batch was done to detect the presence of *E.ictaluri* bacterium to ensure no infection occurred before the experiment. The total of samples throughout the study were 480 fish. At each farm, 30 samples were taken monthly from the two cages. Each sample was measured for their length and weight before examined for the external clinical signs. Fish were then pithed between its head and body segment to immobilize and kill the fish. Any internal clinical signs were observed and recorded. Spleen, liver, kidney, and brain were removed carefully and stored in -20°C for further used.

In Pekan at Kampung Tanjung Pulai, the size of the cage is 10x15x4 feet stocked with 4000 fingerlings. At Kampung Belimbing, the cage size was 10x9x5 feet were stocked with 3000 fish. In Temerloh, both Kampung Teluk Ira and Kampung Bintang were stocked with 4000 fisheach farm with cage size of 10x12x5 ft. These fish were reared until they were harvested at marketable size which consumed within seven to nine months.

Detection and identification of *E.ictaluri*

The collected tissue organ then were then proceeds with DNA extraction using DNA extraction kit (PrimeWay Genomic DNA extraction kit, Apical Scientific Sdn. Bhd., Malaysia).DNA fragment was checked qualitatively and quantitatively by using gel electrophoresis and Nanodrop. Polymerase chain reaction technique was used to confirm *E.ictaluri* as described inprevious study [11].

The primer set used are stated in the Table 1 below:

Table 1 Primers used to detect *Edwardsiella ictaluri*

Type	Primers	Size
Species specific for *Edwardsiella ictaluri* [11]	IVS (5'- TTA AAG TCG AGT TGG CTT AGG G-3')	2000bp
	IRS (5'-TAC GCT TTC CTC AGT GAG TGT C -3')	

The PCR mixture used were as in following Table 2:

Table 2 PCR reagents used

Reagent	Amount	Concentration
PCR buffer (Thermo Scientific)	2 µL	10x
MgCl2 (Thermo Scientific)	2 µL	25 mM
dNTP (Thermo Scientific)	0.5 µL	10 mM
IVS (NHK Bioscience, Kuala Lumpur, Malaysia)	0.5 µL	100 pmol μL^{-1}
IRS (NHK Bioscience, Kuala Lumpur, Malaysia)	0.5 µL	100 pmol μL^{-1}
DNA template	1 µL	50ng/µL minimum
Taq DNA Polymerase (Thermo Scientific)	0.5 µL	5 μL^{-1}
Distilled water	43 µL	
Total volume	50 µL	

The amplification was performed in thermocycler machine (Techne TC-3000 PCR ThermalCycler, GMI, US) with minor modification from the reference data [11] as in Table 3:

Table 3 Temperature and time setting up in PCR machine.

Step	Temperature	Time
Initial denaturation	94°C	4 min
Denaturation	94°C	1 min
Annealing	50°C	1 min
Extension	72°C	1 min
Final elongation	72°C	10 min

The cycle run for 35 cycles starting from denaturation to extension phase. The amplifiedDNA were then mixed with 6x loading dye (Thermo Scientific) and were distinguished by usinggel electrophoresis with stained 1% Agarose in 1x Tris/Borate/EDTA (TBE) buffer at 100V, 400A for 30 minutes. Any band appear were compared to the 1kb standard marker (Thermo Scientific).

For validation, *Edwardsiella ictaluri* (ATCC® 33202™) strain were used as positive control for each reaction. Fish samples that appeared band on the gel which in line with the positive control were considered positive with *E.ictaluri* strain.

Water quality sampling

In this study, water samples were collected monthly. The reading of *in-situ* physical datawas taken at three different depths at three different points along the farm. For water chemicaldata, the water sample were only collected from the surface at three different point. Water samples for chemical analysis were collected in sterilized 250ml high-density polyethylene (HDPE) bottles. These samples then were kept straight away in an insulated ice box and transported to the laboratory for immediate analysis.

The physical parameters that were measured in this study were temperature, pH, dissolved oxygen (DO) and total suspended solid (TSS) using a portable multiprobe (NKEInstrumentation WiMo multi-parameter sonde) and TSS were measured by using a colorimeter(HACH DR900, HACH Company, Loveland,CO, USA).

Meanwhile, the chemical parameters observed were ammonical-nitrogen (AN), sulfide, nitriteand iron. These parameters were assessed based on the standard procedures in the laboratory. The analytical determination of ammonical-nitrogen was using salicylate method, iron was using FerroVer method, nitrite used methylene blue method and sulfide were determined according to diazotization method. These methods required the usage of powder pillow and sulfide reagents for sulfide test and were used colorimeter (HACH DR900, HACH Company, Loveland,CO, USA) for measurement according to their respective wavelength.

Data analysis

The mean prevalence of *E.ictaluri* in reared pangasius was calculated and compared with growth rate by using Excel software. All data were analyzed by using IBM SPSS Statistics(Version 26). All data variables were arranged horizontally according to the timeline and the subject which are the farms were arranged vertically. Then, screening for multivariate outliersfrom the data was performed through Mahalanobis distance where this step is essential prior toperforming data analysis. The distance of a case is analyzed from the centroid of all cases in a data set which is conducted through multidimensional statistical techniques by Malahanobis distance. The centroid is a point in multivariate space where all means from all variables intersect which determine the value of Mahalanobis distance (the bigger the value of MD, the further away from the centroid the data point is).

Then each of the chemical and physical parameters were determined for their possible association with the prevalence of *E.ictaluri* through Spearman's rank-order correlation (ρ). Spearman's correlation measures monotonic relationships (whether linear or not) and if there are no repeated data values, a perfect Spearman correlation of +1 or −1 occurs when each of the variables is a perfect monotone function of the other.

Results and Discussion

Clinical signs of *Edwardsiella ictaluri*

During the sampling session, clinical signs observed were lethargy, inflame anus, patchy liver,white nodular spleen, black and rough nodular spleen, and puss kidney (Figure 2, Figure 3, Figure 4).

Fig 2 White nodular at spleen

Fig 3 Inflame anüs

Fig 4 Puss kidney with straw-colour ascitic fluid

During the whole sampling session, there were neither acute nor chronic external clinical conditions presented rather than minor inflammation on the fin or anus. Acute externalclinical signs on affected catfish may have internal fluid accumulation that can lead to a swollen abdomen and exophthalmia, small red and white ulcers which cover the skin, pinpoint red spotsappearing under the lower jaw or belly region, and a raised or eroded red ulcer with inflammatory exudate protruding through the cranial foramen at the top of the skull, where chronic signs might show ulceration of the cranial foramen [1,7,12]. However, most of the affected fish had almost similar gross internal clinical signs such as such as pale areas of tissuedestruction (necrosis) or a general mottled red and white appearance in liver, white nodular spleen, black and rough nodular spleen, and puss kidney from the samples. Few of them showedclear, straw-colored, or bloody fluid (ascites) as per described by [12]. Liver, spleen, and kidneyare important for the defense systems in teleost. Kidney and spleen form an

extensive networkwhich is vital in trapping blood-borne substances. The populations of lymphocytes and macrophages in these organs can exhibit an immune response which is situated close to sites ofantigen trapping and frequently associated with accumulations of cell masses called melanomacrophages (MMC) [13]. The MMCs are histologically distinguishable within the tissue for presenting macrophages with distinct pigments such as melanin, hemosiderin and lipofuscins [14]. Melanin of MMC are more or less colored by yellow, brown or black pigmentswith its phagocytic characteristics which consume foreign particle, catabolic product or carbonparticle [15].

Bacteria identification from PCR

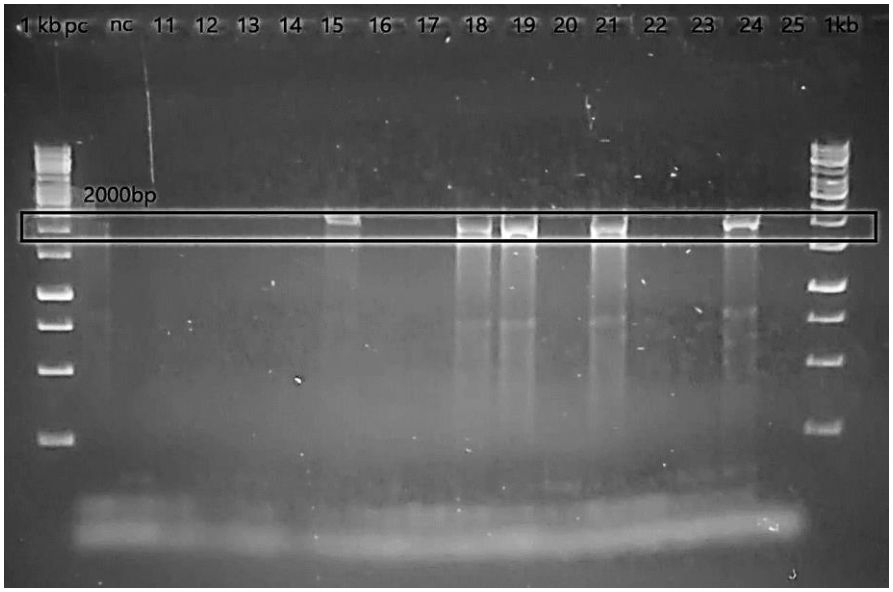

Fig 5 Samples from Kampung Tanjung Pulai during the fingerling size about 3.5 inches to 4 inches. From most left is 1kb ladder, followed by lane 2 (positive control; ATCC 33202), lane 3 (negative control), lane 4 until lane 18 (DNA samples from pooled organ), lane 19 (1 kb ladder). The positive samples with *E.ictaluri* were on the lane with sample numbered 15, 18,19,21 and lane 25 with the size of 2000bp referring to the positive control lane.

The pooled DNA of spleen, liver, kidney, and brain samples were tested with PCR by using IVS-IRS primer. Infected fish showed positive band with the size of 2000bp viewed from the gel electrophoresis of PCR product (Figure 5).

Prevalence Rate of *E.ictaluri*

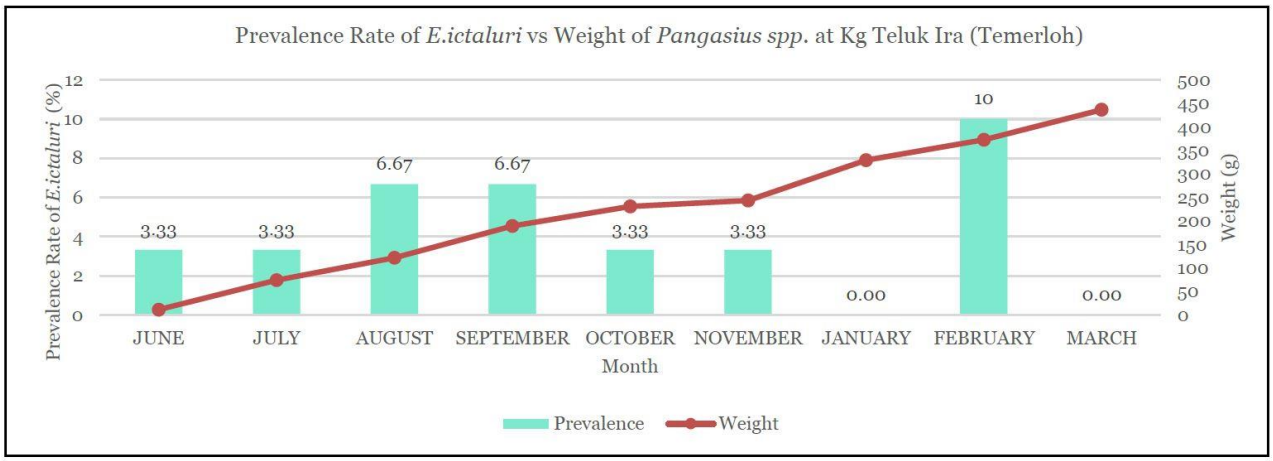

Fig 6 Prevalence Rate of *E.ictaluri* at Kampung Teluk Ira (Farm 1)

Throughout sampling session at Kampung Teluk Ira (Farm 1), *E.ictaluri* was observed in all months except in January and March. Meanwhile the highest prevalence of *E.ictaluri* (10%) was on February where the weight of the fish samples reached about 350g (Figure 6).

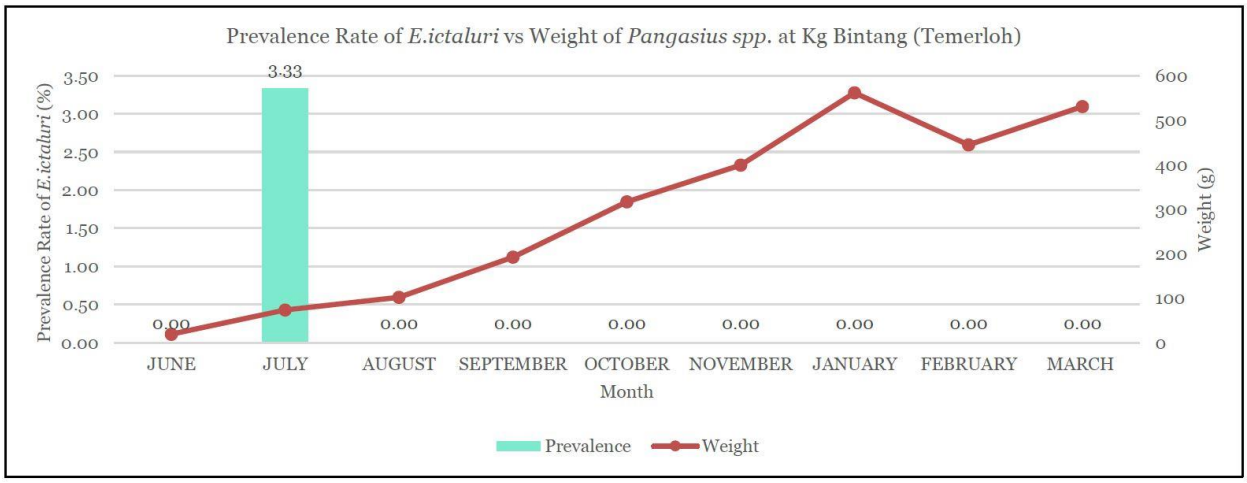

Fig 7 Prevalence Rate of *E.ictaluri* at Kampung Bintang (Farm 2)

The situation was reversible at Kampung Bintang (Farm 2) compared to Kampung Teluk Ira.Throughout the 9 months of sampling, prevalence of *E.ictaluri* was only in July with 3.33% (Figure 7).

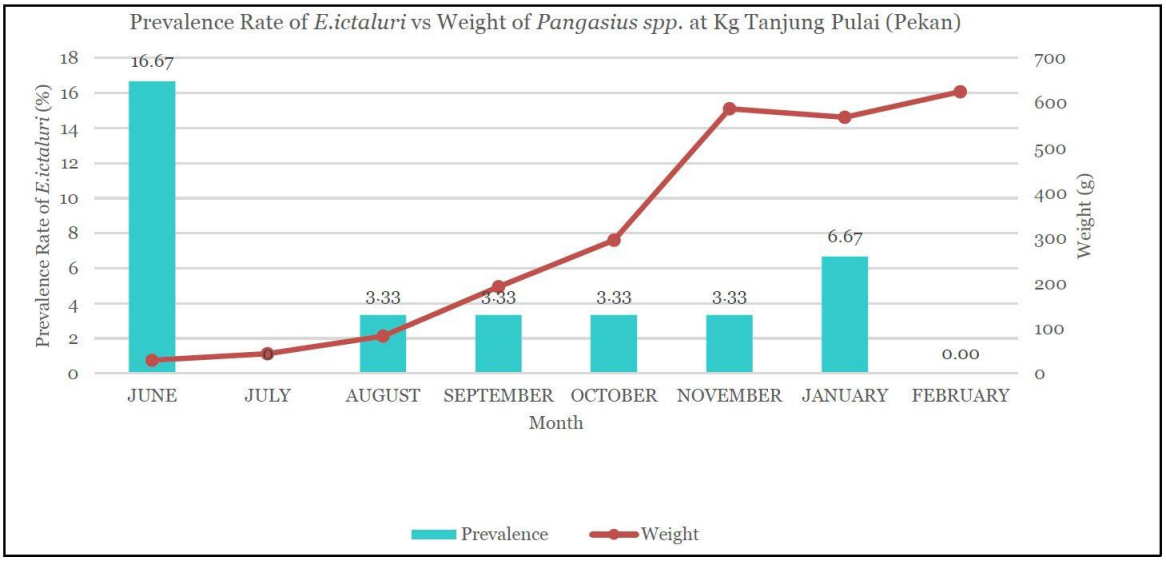

Fig 8 Prevalence Rate of *E.ictaluri* at Kampung Tanjung Pulai (Farm 3)

In Pekan at Kampung Tanjung Pulai (Farm 3), the highest prevalence was shown in June with 17.24%, where the average weight of the striped catfish at that time was less than 100g. The second highest prevalence was in January with 6.67% (Figure 8).

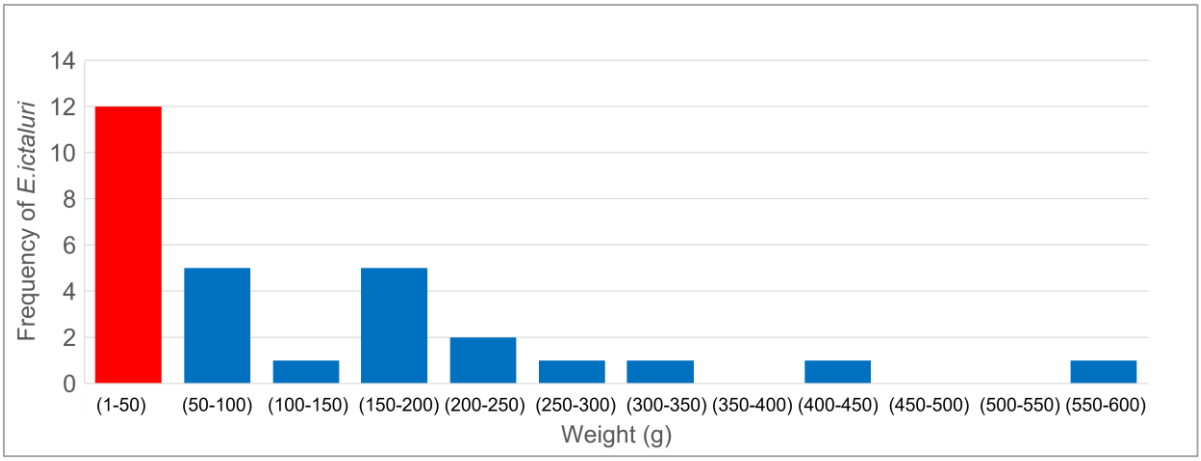

Fig 9 Susceptibility size of *E.ictaluri* in cage cultured striped catfish in Pahang River. The red bar chart indicate the most susceptible size of *Pangasius hypophthalmus* towards *E.ictaluri*. The blue bar chart show the frequency of *E.ictaluri* found in *P.hypopthalmus* according to their sizes throughout this study.

Compared to another farms, Farm 3 recorded the highest prevalence of *E.ictaluri* which obtained 16.67% where the average size of fish reached 29.5g during the first month of sampling. In overall, the susceptibility of this bacterium in stripe catfish is during the first month especially during the first restocking in the cage when the fish reach size 1g to 50g (Figure 9).

Fish are more dependent on theirnon-specific immune system for survival during the early stages of their embryonic life than higher vertebrates [16]. Several external and internal factors can influence the activity of innateimmune systems in teleost. Temperature changes, handling and crowding stress can have suppressive effects on innate parameters, whereas several food additives and immunostimulantscan enhance different innate factors [17]. In Vietnam, BNP in freshwater catfish (*Pangasianodon hypophthalmus*) may occur in fish of all ages, although especially fingerlings and juvenile fish seem to be more affected [18,19]. In general, fingerlings are high tendency to infection from *E.ictaluri* but adults may also succumb to the disease as well even though the immune status of individuals in the population may determine the outcome [12].

Edwardsiella ictaluri is susceptible to the striped catfish when environmental conditions are conducive to proliferation of the pathogen and stressful for the host. Such stressfulconditions include several factors such as netting, handling, over stocking density, improper diet and poor water quality like low oxygen or high levels of ammonia and nitrite [12]. There were significant ($p < 0.05$) positive correlations between the prevalence of *E.ictaluri* with concentration of ammonia, sulfide and total suspended solid (TSS) at Kampung Teluk Ira (Spearman's rank correlation test, rs = 0.55-0.56).

Ammonia is the main nitrogenous excretory product of aquatic animals, especially for feed-based aquaculture. Large stocking density without a proper management release more ammonia nitrogen into the culture system [20]. In tilapia, carp, and pufferfish, ammonia was found to cause tissue swelling and hydropic degeneration, increasing oxidative stress and apoptosis in liver tissues [21]. Meanwhile, the exposure of fish to high suspended solids can cause physical damage to gill structure of fish and clogging which leads to respiratory failure and mortality [22]. The same effect of total suspended solid in water may result such disturbancein migrations and spawning, movement pattern, reduced hatching rate as well as directmortality. Sulfide can be produced in the absence of oxygen in sediment by sulfate-reducing bacteria and enter the water column. Sulfide level which exceeds the optimum level may inhibitenergy metabolism by cells, which have the same effect as hypoxia. The condition in cage witha very low running water and lowered to the bottom of the riverbed might mimical to the condition in the pond which may lead to the deterioration of water quality within the cage itself. Previous study showed that striped catfish only exploited the upper-most 25% of the water column and frequently experienced severe hypoxia at night and at depths greater than 1 m belowthe surface, and with increasing hypoxia and anoxia towards the bottom [23]. Temperature values are varied at all sampling sites throughout the study, ranging from 25.88ºC to 30.43ºC which is very similar to previous study for the growth of *E.ictaluri* [24,25].

Conclusion

In conclusion, *Edwardsiella ictaluri* appear year-round in cultured *Pangasius hypopthalmus*. The factors which cause the disease are interrelated to each other. Improper stocking density adding the stress factor and thus decreasing the immune system in fish.

However, the susceptibility of this bacterium in stripe catfish is more prone during the first three month when the fish reach size 1g to 50g and 150g to 200g. The prevalence of *E.ictaluri*have strong relationship with ammonia, sulfide and total suspended solid (TSS). Deep investigation such as histology and study of cortisol level in fish is needed to determine the stress level of striped catfish with these correlated parameters. Further study on the co-infectionof *E.ictaluri* with another bacteria is also required to understand the epidemiological of this bacterium in natural environments.

Abbreviations

TSS: Total Suspended Solid; DO: Dissolved Oxygen; AN: Ammonical-nitrogen; PCR:polymerase chain reaction; ESC: enteric septicemia catfish; MMC: melanomacrophage

Funding

This study is funded by Department of Fisheries Malaysia in collaboration with Department ofMarine Science, Kulliyyah of Science, International Islamic University Malaysia.

Availability of data and material

Please contact the corresponding author for any data request.

References

1. Crumlish, M., et al., 2002. "Identification of *Edwardsiella ictaluri* from Diseased Freshwater Catfish, PangasiusHypophthalmus (Sauvage), Cultured in the Mekong Delta, Vietnam." *Journal of FishDiseases* 25 (12): 733–36. https://doi.org/10.1046/j.1365-2761.2002.00412.x.
2. Annual Fisheries Statistics 2022. Available from: https://www.dof.gov.my/en/resources/fisheries-statistics-i/ [accessed 29 Feb, 2024]
3. Klesius, P. H., and J. W. Pridgeon. "Live attenuated bacterial vaccines in aquaculture."In Proceedings of the 9th International Symposium on Tilapia in Aquaculture, pp. 18- 26. 2011.[GoogleScholar]
4. Wagner, Bruce A., et al., 2002. "TheEpidemiology of Bacterial Diseases in Food-Size Channel Catfish." *Journal of Aquatic Animal Health* 14 (4): 263–72. https://doi.org/10.1577/1548-8667(2002)014<0263:TEOBDI>2.0.CO;2.
5. Wise, A. L., et al., 2021. "A Review of Bacterial Co-infections inFarmed Catfish: Components, Diagnostics, and Treatment Directions." *Animals* 11 (11): 1–17. https://doi.org/10.3390/ani11113240.
6. Hawke, J. P, et al., 1981."*Edwardsiella ictaluri* Sp. Nov., the Causative Agent of Enteric Septicemia ofCatfish." *International Journal of Systematic Bacteriology* 31 (4): 396–400. https://doi.org/10.1099/00207713-31-4-396.
7. Ferguson, H W, et al., 2001. "Bacillary Necrosis in Farmed Pangasius Hypophthalmus (Sauvage) from theMekong Delta, Vietnam." *Journal of Fish Diseases* 24 (9): 509–13. https://doi.org/10.1046/j.1365-2761.2001.00308.x.
8. Takeuchi, H. et al., 2021. "Environmental Factors Affecting*Edwardsiella ictaluri*-Induced Mortality of Riverine Ayu, Plecoglossus Altivelis (Temminck & Schlegel)." *Journal of Fish Diseases* 44 (8): 1065–74. https://doi.org/10.1111/jfd.13368.
9. Phuoc, Nguyen Ngoc, Randolph Richards, and Margaret Crumlish. 2020. "Environmental Conditions Influence Susceptibility of Striped Catfish Pangasianodon Hypophthalmus (Sauvage) to *Edwardsiella ictaluri*." *Aquaculture* 523 (May 2019): 735226. https://doi.org/10.1016/j.aquaculture.2020.735226.
10. Towards Integrated Water Resources Management Approach in Malaysia: A Case Study in Pahang River Basin - Scientific Figure on ResearchGate. Available from: https://www.researchgate.net/publication/266872132_Towards_Integrated_Water_Resources_Management_Approach_in_Malaysia_A_Case_Study_in_Pahang_River_Basin [accessed 21 Dec, 2023]
11. Williams, M. L., and M. L. Lawrence. 2010. "Verification of an *Edwardsiella ictaluri*-Specific Diagnostic PCR." *Letters in Applied Microbiology* 50 (2): 153–57. https://doi.org/10.1111/j.1472-765X.2009.02770.x.
12. Hawke, John P. 2015. "Enteric Septicemia of Catfish." *Alabama Cooperative Extension System*, no. 477: 1–6. http://www.aces.edu/dept/fisheries/aquaculture/documents/EntericSepticemiaofCatfish.pdf.
13. Press, C. Mc L., and O. Evensen. 1999. "The Morphology of the Immune System inTeleost Fishes." *Fish and Shellfish Immunology* 9 (4): 309–18. https://doi.org/10.1006/fsim.1998.0181.
14. Agius, C., and Roberts, R. J. 2003. "Melano-Macrophage Centres and Their Role inFish Pathology." *Journal of Fish Diseases* 26 (9): 499–509. https://doi.org/10.2174/1570180815031801311027 47.
15. Kranz, H., and N. Peters. 1984. "Melano-Macrophage Centres in Liver and Spleen ofRuffe (Gymnocephalus Cernua) from the Elbe Estuary." *Helgoländer Meeresuntersuchungen* 37 (1–4): 415–24. https://doi.org/10.1007/BF01989320.
16. Sahoo, S., B. Husne, P. Abhinav, and T. Gayatri, 2021. "Immune System of Fish: An Evolutionary Perspective." *Antimicrobial Immune Response*, 1–21. https://doi.org/10.5772/intechopen.99541.
17. Magnadóttir, B. 2006. "Innate Immunity of Fish (Overview)." *Fish and Shellfish Immunology* 20 (2): 137–51. https://doi.org/10.1016/j.fsi.2004.09.006.
18. Dung, Tu Thanh. "Edwardsiella ictaluri in Pangasianodon catfish: antimicrobial resistance and the early interactions with its host." PhD diss., Ghent University, 2010. [GoogleScholar]
19. Yuasa, K., et al., 2003. "First Isolation of *Edwardsiella ictaluri* from Cultured Striped Catfish Pangasius Hypophthalmus in Indonesia." *Fish Pathology* 38 (4): 181–83. https://doi.org/10.3147/jsfp.38.181.
20. Boyd, C. E. 2017. *General Relationship between Water Quality and Aquaculture Performance in Ponds. Fish Diseases: Prevention and Control Strategies*. Elsevier. https://doi.org/10.1016/B978-0-12-804564-0.00006-5.
21. Jin, J., et al., 2017. "Transcriptomic Analysis of Liver from Grass Carp (Ctenopharyngodon Idellus) Exposed to High Environmental Ammonia Reveals the Activation of Antioxidant and Apoptosis Pathways." *Fish and Shellfish Immunology* 63: 444–51. https://doi.org/10.1016/j.fsi.2017.02.037.
22. Au, D. W.T., et al., 2004. "Chronic Effects of Suspended Solids on Gill Structure, Osmoregulation, Growth, and Triiodothyronine in Juvenile Green Grouper Epinephelus Coioides." *Marine Ecology Progress Series* 266: 255–64. https://doi.org/10.3354/meps266255.
23. Lefevre, S.,et al., 2011. "A Telemetry Study of Swimming Depth andOxygen Level in a Pangasius Pond in the Mekong Delta." *Aquaculture* 315 (3–4): 410–13. https://doi.org/10.1016/j.aquaculture.2011.02.030.
24. Crumlish, M., et al., 2010. "Experimental Challenge Studies in Vietnamese Catfish, Pangasianodon Hypophthalmus (Sauvage), Exposed to *Edwardsiella ictaluri* and *Aeromonas hydrophila*." *Journal of Fish Diseases* 33 (9): 717–22. https://doi.org/10.1111/j.1365-2761.2010.01173.x.
25. Dung, Tu T., et al., 2008. "Antimicrobial Susceptibility Pattern of *Edwardsiella ictaluri* Isolates from Natural Outbreaks of Bacillary Necrosis of Pangasianodon Hypophthalmus in Vietnam." *Microbial Drug Resistance* 14 (4): 311– 16. https://doi.org/10.1089/mdr.2008.0848.

International Journal of Life Sciences and Biotechnology
Sarı O., Effects of Different Growing Medium on Obtaining Bulblets from Bulb Scales in Oriental *Lilium* 'Siberia' Cultivar. International Journal of Life Sciences and Biotechnology, 2024 7(1): p. 46-51.
https://doi.org/10.38001/ijlsb.1385988
Araştırma Makale/ Research article

Effects of Different Growing Medium on Obtaining Bulblets from Bulb Scales in Oriental *Lilium* 'Siberia' Cultivar

Ömer Sarı [1]*

ABSTRACT
This study was carried out to determine the best medium for obtaining bulblets in the Oriental *Lilium* 'Siberia' plant using bulb scales and different media. In the research, six different growing mediums were used as growing media: soil (control), peat, soil + peat, perlite, perlite + peat, and peat + sand. In the experiment, the number of bulblets, bulblet width, bulblet length, number of healthy and infected bulb scales, and the time it took for the first bulbs to formation were measured. As a result of the study, the highest number of bulblets (110) were obtained from peat + sand. The growing medium with the highest values of bulblet width (11.38 cm) and bulblet length (16.27 cm) was determined to be peat. The highest number of healthy bulb scales (54) was obtained from perlite medium, and the highest number of infected bulb scales (20) was obtained from soil medium. In terms of the formation time of the first bulblets, perlite medium (15 days) was the growing medium where the earliest bulbs were obtained, and the latest bulblets were obtained from control (soil) and soil + peat (40 days). In general, the quality of bulblets obtained from peat medium was better than that from other mediums. In this regard, peat growing medium is recommended to obtain quality bulblets, and peat + sand is recommended if the number of bulblets is desired to be high.

ARTICLE HISTORY
Received
09 November 2023
Accepted
20 February 2023

KEYWORDS
Lilies,
bulb scales,
bulblet,
growing medium

Introduction

Lilies are a geophyte with showy and colorful flowers. Lilies, which are very important commercially, are widely grown worldwide. Lily bulbs consist of fleshy scales, which are responsible for storing nutrients. Lilies do not have a protective layer (tunic) surrounding the bulb, which is why the bulbs are white [1].
Oriental *Lilium* 'Siberia', a hybrid of the oriental group, has white and fragrant flowers. The upper part of the bulb is yellow and the lower part is white. Bulb development and size vary depending on species, cultivar and plant age. After planting the seeds, the development of the bulb reaches 4-7 cm in the first year, 12-16 cm in the second year and 16 cm in the third year. Oriental *Lilium* 'Siberia' bulbs bloom approximately 110 days after planting. 6 - 8 flowers grow on each stem, which consists of a bulb, and the plant can grow up to 90-110 cm. The best development occurs in loamy-sandy soils with good drainage [2]. Seeds used in the production of ornamental plants are mainly imported. In addition to seeds, bulbs used in the production of bulbous plants are also imported. This situation increases foreign dependency on ornamental plants and production costs, causing the country's resources to be exported [3].
The ornamental plants sector is known as the sector that provides the highest added value per unit area when compared to other areas of the agricultural sector [4]. Although Turkey's ornamental plant production and exports have increased recently, it has yet to reach the desired target. Imports of ornamental plants amounted to $37,517 and exports amounted to $114,391. Natural flower bulb production areas are quite low, 506 decares [5]. Increasing R&D studies so that the ornamental sector can develop will contribute to our country's production and therefore its economy.
Soilless growing media have been widely used in ornamental plant cultivation in recent years [6]. It has been reported that growing mediums consisting of different growing mediums and their components significantly affect plant development [7]. When Asiatic lily hybrids 'America' and 'Novecento' varieties were grown in a different growing medium, it was reported that the medium contained a mixture of soil and rice husk and a mixture of perlite and river sand gave the best results in terms of stem length and dry matter accumulation [8].

[1] Black Sea Agricultural Research Institute, Samsun, Turkey
Corresponding Author: Ömer Sarı, e-mail: omer.sari@tarimorman.gov.tr

In Asiatic and Oriental varieties 'Gronde' and 'Cassandra', flower stem length, number of leaves, number of flowers, flower diameter, flowering time, vase life and leaf chlorophyll content were measured in plants grown in cocopeat, gravel, sand, peat and perlite media. Growing mediums significantly affected only flower stem length [9]. In another study on Oriental Lilium, earliness, quality, fresh and dry weights of flowers and leaves, root length, number of roots, bud length and root length parameters were examined. It has been reported that the best results are obtained from cocopeat medium [10]. Nine different growth media consisting of soil, chicken manure, sawdust and river sand and their combinations were used in *Mussaenda philippica*. The best results were found in the soil + sawdust + chicken manure mixture [11]. In another study, nine different media were prepared using chestnut shell, perlite, peanut shell, sand, garden soil, barnyard manure, peat, coconut shell and slag for the *Lilium* LA hybrid 'Ceb Dazzle' cultivar. It has been determined that the best results are obtained from a mixture of perlite and peanut shell (1:1) [12]. Again, in the 'Connecticut King' cultivar, shrub soil, coniferous soil, perlite and field soil were used. In the research, in terms of shoot period and heading period; the best results were obtained from plants grown in 1:1:1 field soil + perlite + coniferous soil and 1:1 shrub soil + coniferous soil mortars. In terms of plant height and maximum number of bulbs, the best results were obtained from the mixture of heather soil and coniferous soil (1:1). It has been reported that as the ratio of field soil in the mixtures increases, the flowering and flower quality of the plants decrease [13].
In their studies on different species and varieties of lily, researchers have revealed that different growing mediums have different effects on plant quality and yield. Studies on lilies are mainly studies on plant development. Therefore, this study aimed to determine the effects of different growing mediums for obtaining bulblets from bulb scales in the Oriental *Lilium* 'Siberia' cultivar on the yield of bulblets and to offer suggestions to those who aim to produce bulbs from bulb scales.

Material and Methods

This research was carried out in the application greenhouse of Ünye Agriculture and Forestry Directorate (41°06'17.7"N 37°23'04.0"E) during the summer and autumn growing periods of 2014. Oriental *Lilium* 'Siberia' cultivar, used for cut flower purposes, was used in the research. Flower bulbs were obtained from a commercial company. Before removing bulb scales, diseased, injured, wrinkled and unhealthy bulbs were removed. After the outermost scales of the bulbs were removed, the remaining three rows of scales were separated to include a piece from the growth point at the bottom of the bulb. The separated bulb scales were kept in a solution containing 1% Captan for 30 minutes. Then, the stamps were kept in a cool and shaded place to dry the surface. For planting bulb scales, 60 liter plastic crates with perforated and permeable sides and dimensions of 520×365×310 mm were used. The inside of the crates is covered with black plastic mulch. After the crates were filled with growing material, 40 bulb scales were placed at equal intervals in each crate (Figure 1), and then the flakes were covered with 1 cm of growing material. Plantings were made on June 10. In the study, six different growing medium consisting of peat (0-6 mm, PH: 5.5-6.5 and 0.6 kg NPK m^{-3}), perlite (0.2- 0.5 mm) and sand were used as growing material (garden soil) (Table 1; Figure 1).

Table 1 Six different growing mediums were used as experiment factors

	Growing media	Mixing ratios
1	Soil (control)	1
2	Peat	1
3	Soil+peat	1
4	Perlite	1+1
5	Perlite+peat	1+1
6	Peat+sand	1+1

In the experiment, irrigation was done manually. The crates containing bulb scales were given only water from planting to emergence. In the experiment, number of infected bulb scales, number of healthy bulb scales, initial formation time of bulblets, number of bulblets, bulblets width and bulblets length were measured.
The experiment was set up in three repetitions according to the completely randomized plot design, and 40 bulb scales were planted in each replicate plot (case). The data obtained from the experiment were evaluated using the SPSS 20 statistical package program. After applying analysis of variance to the data, differences between growing mediums were compared using the Duncan test ($p<0.05$).

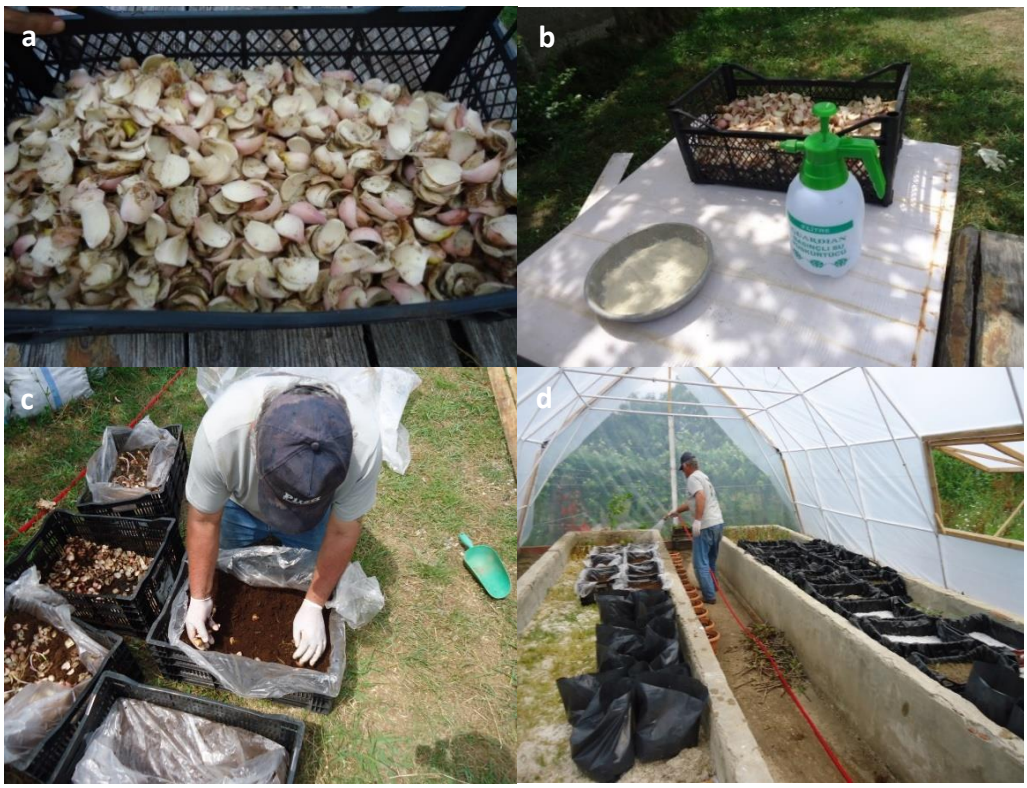

Fig 1 Stages of bulblet production from bulb scales in the Oriental *Lilium* 'Siberia' cultivars (a. Separating the scales from the mother bulbs, sorting the bulb scales, b. Preparation for the spraying process, c, d. Planting process in plastic cases containing the prepared media, placing the boxes in the greenhouse and watering process)

Results and Discussion

Effects of growing medium on the number of bulblets

According to the study findings, the number of healthy bulb scales was 54 in the perlite, while the lowest number of healthy bulb scales was 40 in the control (soil). Again, the lowest number of infected bulb scales was obtained from perlite (4), and the highest was obtained from control (soil) (20) (Table 2). No sterilization process was applied to the media used in this study. Soil and sand taken from their natural environment are less sterile mediums than perlite and peat. In the study results, it is thought that the rate of infected bulb scales was higher in mediums containing soil and sand. It is assumed that the development of infection is low due to the absence of living matter in the perlite mediums.

Table 2 Numbers of infected and healthy bulb scales in growing medium

Growing medium	Number of infected bulb scales	Number of healthy bulb scales
Soil (control)	20 a	40 b
Peat	14 b	45 ab
Soil+peat	17 ab	42 b
Perlite	4 c	54 a
Perlite+peat	12 bc	47 ab
Peat+sand	14 b	43 b

Data shown with different letters in each column are statistically significant ($p<0.05$).

In the study, when the bulblet formation times from bulb scale were compared in the growing medium, the earliest medium was perlite with 15 days, and perlite + peat medium followed with 20 days. It was determined that control and soil + peat were the slowest growing mediums with 40 days (Figure 2). Li et al. [16] in their study on *Lilium davidii* var. detected the earliest bulb formation on the 15th day, similar to this study.

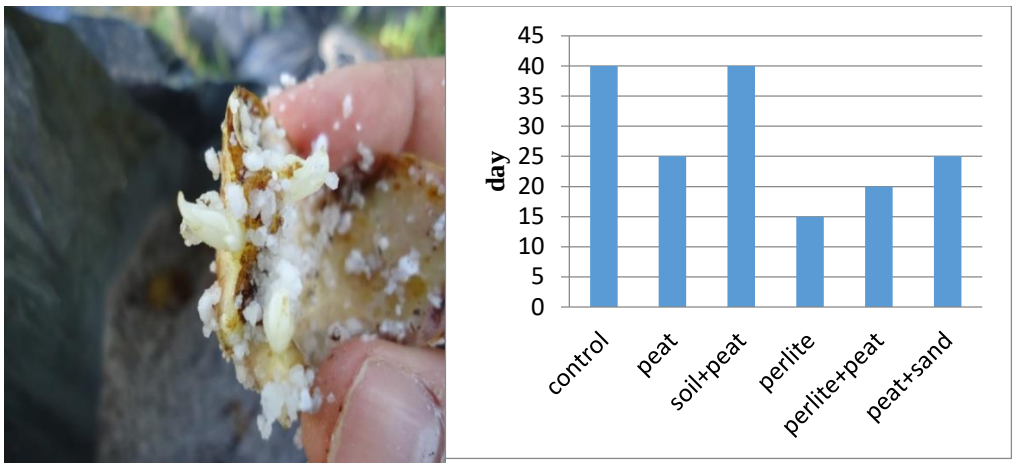

Fig 2 Initial formation time and appearance of bulblets in perlite medium (15th day)

Different growing media used to obtain bulblets statistically affected the number of bulblets. The highest value in terms of the average number of bulblets was obtained from the peat + sand (110), followed by the perlite + peat (95). The lowest value was obtained from the control growing medium (25) (Table 3; Figures 3 and 4).

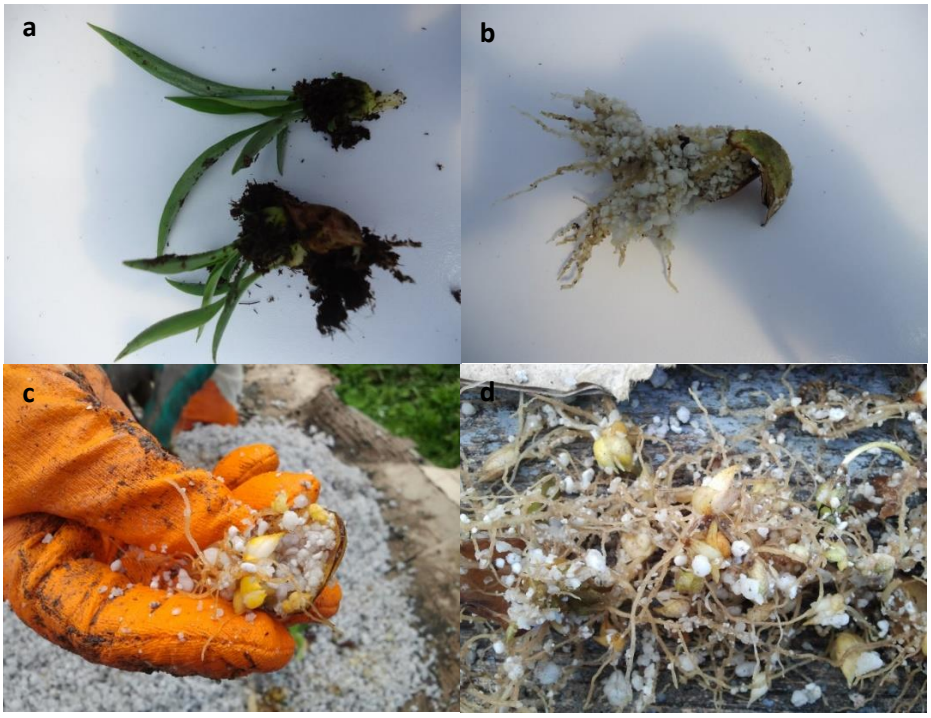

Fig 3 Obtaining bulblets from bulb scales in the Oriental *Lilium* 'Siberia' cultivar (a. Bulblets obtained from peat medium, b. Bulblets obtained from perlite medium, c. Bulblets obtained from a flake, d. A group of bulblets removed from perlite medium)

In the study, it was seen that the peat and sand mixture was more effective on bulblet formation than other applications. This may be associated with the nutrition provided by the peat, the water permeability provided by the sand, and the possible mineral content in the sand. The results of this study are compatible with the results of some previous studies showing that a mixture of organic matter and sand is more effective. Thus, it has been reported that in the Oriental *Lilium* 'Siberia' cultivar, the highest value in the number of bulblets was obtained in the peat and sand, and the lowest value was obtained in the sheep manure and sand [14]. In the study conducted by Eken and Şirin [12] on the *Lilium* LA hybrid "Ceb Dazzle" cultivar, although the effect of the media on the number of bulblets was found to be insignificant, the highest results were obtained from the peanut shell and sand medium, with 17.50. In a study on bulb development, the highest bulblet rate (43.8%) was obtained in a Taurus snowdrop grown in coconut [17]. In addition, in another study conducted on lilies, it was stated that the best values in terms of the number of mother bulbs and bulblets were obtained from the soil-rice husk mixture and river sand-perlite mixture [8]. Again, in the *Oriental* Lilium 'Siberia' cultivar, the growing medium using sheep manure reduced the number of bulblet but increased their size [14].

Table 3 Effects of growing medium on average yield of bulblet

Growing medium	Bulblet width (mm)	Bulblet length (mm)	Number of bulblets
Soil (control)	8.62 c	12.00 c	25 e
Peat	11.38 a	16.27 a	60 d
Soil+peat	10.30 b	14.02 b	50 d
Perlite	8.22 c	13.36 bc	81 c
Perlite+peat	9.45 b	14.10 b	95 b
Peat+sand	8.00 c	12.33 c	110 a

Data shown with different letters in each column are statistically significant ($p<0.05$)

In this study, the different media used to obtain bulblets from bulb scales affected the bulblet length statistically significantly (Table 3; Figures 3 and 4). The best result for bulblet length (16.27 mm) was obtained in peat medium, while a lower result (12.00 mm) was obtained in soil (control) medium. In the study conducted on the Oriental *Lilium* 'Siberia' cultivar, the length of the bulblets formed on the mother bulb was found to be between 12.15 mm - 14.91 mm. The biggest bulblets were obtained from sheep manure and sand medium, and the smallest ones were obtained from perlite medium [14]. In the *Lilium* LA hybrid "Ceb Dazzle" cultivar, the lengths of the bulblets vary between 10.90 mm and 14.54 mm, and the bulblets with the largest length values were obtained from peanut shell + sand, and the smallest ones were obtained from volcanic slag [12]. In a study conducted based on the basal part sizes of *Lilium longiflorum*, the average bulb length was found to be 28.67 mm [15].

In the study, the different media used to obtain bulblets from bulb scales affected the bulblet width statistically significantly (Table 3; Figures 3 and 4). The best result for bulblet width (11.38 mm) was obtained in peat, while a lower result (8.22 mm) was obtained in perlite. In the study conducted on the Oriental *Lilium* 'Siberia' cultivar, the width of the bulblets formed from the mother bulb was found to be between 8.45 mm - 13.85 mm. Bulblet yields were highest in sheep manure + sand and lowest in peat + sand [14]. In addition, in the *Lilium* LA hybrid "Ceb Dazzle" cultivar, the highest values of bulblet width were obtained in peanut shell + sand medium with 14.34 mm, followed by peat + sand with 13.31 mm. The lowest value in terms of bulblet width, 10.11 mm, was determined from the volcanic slag medium [12]. In *Lilium longiflorum*, the bulb width was found to be 11.3 mm [15]. In study, values close to those found by the researchers were obtained. Bulbs and bulblets grow well in growing media with high organic matter content. As a matter of fact, in this study, the best bulblet length and width were obtained from the peat medium. However, good humidity control is required to reduce bulb losses.

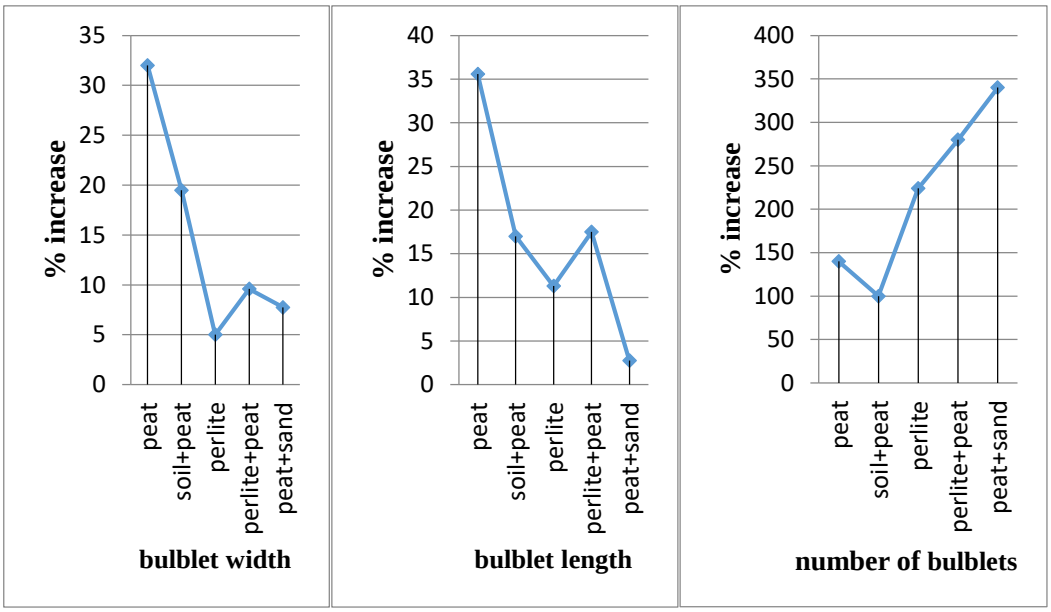

Fig 4 Effects of different growing mediums on bulblet yield, bulblet width and length obtained from bulb scales

Conclusion

In lily cultivation, it is extremely important for producers to determine the methods by which they can produce their own bulbs. In this study, which was conducted to determine the best growing medium for obtaining bulblets and to reduce the costs of supplying bulbs for cultivation, different growing mediums significantly affected bulblet length, width and number of bulblets. Peat + sand growing mediums gave better results in terms of the number of bulblets obtained. According to the measurements made between the growing mediums, the best values in terms of obtaining quality bulblets were obtained from the peat. As a result of the research, it is revealed that if the bulblet quality is desired to be high, peat can be preferred, and if the number of bulblets is desired to be high, peat + sand can be preferred. For this reason, peat + sand can be recommended for bulblet production. However, it should not be forgotten that these results may vary depending on species and varieties. For this reason, it would be beneficial to conduct more detailed studies using different types and varieties of different media to obtain bulbs.

Acknowledgments

The experiments in this article were carried out in the application greenhouse of Ünye Agriculture and Forestry District Directorate.

Funding

The author did not receive support from any organization for the submitted work.

Data Availability statement

The author confirms that the data supporting this study are cited in the article.

Compliance with ethical standards

Conflict of interest

The author declare no conflict of interest.

Ethical standards

The study is proper with ethical standards.

References

1. Lazare, S., et al, The proof is in the bulb: glycerol influences key stages of lily development. The Plant Journal, 2019. 97(2), 321-340. https://doi.org/10.1111/tpj.14122
2. Johannes, A., Lily plant named 'Siberia'. 1996, https://www.google.com/patents. [accessed 05.Feb, 2023].
3. Çelikel, F. G., Bahçe bitkileri tohumluğu üretimi ve kullanımında değişimler ve yeni arayışlar., Türkiye Ziraat Mühendisliği VIII. Teknik Kongresi Bildiriler Kitabı, 2015. 2: 1004-1006, 12-16 Ocak 2015, Ankara.
4. SÜSBİR., Süs Bitkileri Sektör Raporu. 2016, http://www.susbir.org.tr/index.php/raporlar. [accessed 05 Jan, 2023].
5. TÜİK., https://data.tuik.gov.tr/Kategori/GetKategori?p=tarim-111&dil=1. 2022. [accessed 29 Feb, 2023]
6. Maloupa, E., et al, Study of substrates use in gerbera soilless culture grown in plastic greenhouses., Acta Horticulturae, 1993. 323:139-144. https://doi.org/10.17660/ActaHortic.1993.323.12
7. Hussain, R., et al, Evaluating sustainable and environment friendly substrates for quality production of potted *Caladium*., International Journal of Recycling of Organic Waste in Agriculture, 2016. 6:13-21. https://doi.org/10.1007/s40093-016-0148-0
8. Klasman, R., Moreira, D., Benedetto, A, Cultivation of asiatichybrids of *Lilium* sp. in three different substrates. Catedra de Floricultura, Facultad de Agronomia (U.B.A.), 2002. Volume: 22, Issue: 1, pp. 79-83. Av. San Martin 4453 (1417), Buenos Aires, Argentina.
9. Tehranifar, A., Y. Selahvarzi, and B. Alizadeh, Effect of different growing media on growth and development of two *Lilium* (Oriental and Asiatic Hybrids) types in soilless conditions. Department of Horticulture Science. II International Symposium on the Genus Lilium. Acta Horticulturae, 2011. 900:139-141. https://doi.org/10.17660/ActaHortic.2011.900.16

10. Treder, J., The effects of cocopeat and fertilization on the growth and flowering of *Oriental lily* 'Star Gazer'. Journal of Fruit and Ornamental Plant Research, 2008. 16:361-370.
11. Okanlawon, S. O., et al, Jmoh, Effects of different growth media on propagation of horticultural plant, *Mussaenda philippica* (Queen of Philippines). International Journal of Current Research in Biosciences and Plant Biology, 2016. 3: 4-10.
12. Eken, L. and U. Şirin, Lilyum zambaklarında (*Lilium* sp.) farklı yetiştirme ortamlarının yavru soğan oluşumu ve gelişimi üzerine etkisi. Anadolu Tarım Bilimleri Dergisi. 2018. 33(2), 85-91. https://doi.org/10.7161/omuanajas.322340
13. Yılmaz, R. and A. Korkut, Zambak (*Lilium* L.) Yetiştiriciliğinde değişik harç kullanımının çiçeklenmeye etkileri, 1998. I Ulusal Süs Bitkileri Kongresi, 6–9 Ekim, Yalova.
14. Sarı, Ö. and F. G. Çelikel, Effects of different growing medium on flower quality and bulb yield of Oriental *Lilium* 'Siberia', International Journal of Agricultural and Wildlife Sciences, 2017. 3(2), 54-60. https://doi.org/10.7161/10.24180/ijaws.317210
15. Marinangeli, P. A., et al, Bulblet differentiation after scale propagation of *Lilium longiflorum*, Journal of the American society for Horticultural science, 2003. 128(3), 324-329.
16. Li, X., et al, Lilium davidii var.'da soğancık oluşumu ve gelişimi sırasında karbonhidrat metabolizmasının transkriptom analizi . tek renkli BMC Plant Biol, 2014. 14, 358 https://doi.org/10.1186/s12870-014-0358-4
17. Kahraman, Ö., Farklı yetiştirme ortamlarının toros kardeleni (*Galanthus elwesii* Hook.)'nin soğan performansı üzerine etkileri. ÇOMÜ Zir. Fak. Derg. (COMU J. Agric. Fac.), 2015. 3(1): 109–114.

International Journal of Life Sciences and Biotechnology
Pulat, C. C. and S. Ilhan, *Feijoa sellowiana*: A Natural Extract with Cytotoxic Effects on Breast Cancer Cells, International Journal of Life Sciences and Biotechnology, 2024 7(1): p. 52-59.
https://doi.org/10.38001/ijlsb.1370006
Araştırma Makale/ Research article

Feijoa sellowiana: A Natural Extract with Cytotoxic Effects on Breast Cancer Cells

Cisil Camli Pulat[1*] **Suleyman Ilhan**[2]

ABSTRACT
Breast cancer remains a leading cause of mortality among women, necessitating heightened attention and innovative treatment approaches. Given the heterogeneous nature of breast cancer, exploring novel therapeutic avenues is crucial. Natural products, with their potential to offer less aggressive alternatives to conventional chemotherapy, have garnered interest. In this study, the potential cytotoxic effect of *Feijoa sellowiana* fruit extract (FE) was investigated on a panel of human breast cancer cells. GC-MS analysis was performed to identify the active constituents present in the FE extract and MTT analysis was conducted to evaluate the cytotoxicity of FE against breast cancer cells. Results showed a strong efficacy of FE against MDA-MB-453 and MDA-MB-231 cell lines. The cytotoxicity was evident after a 24-hour treatment duration for both lines. It was observed that the two cell lines in which the FE extract was most effective belonged to the triple-negative breast cancer category. The viability of MCF-7 cells decreased to 23.2% after 72 hours of exposure to 1000 µg/mL FE, and this decline was also noticeable at lower concentrations. Conversely, the BT-474 cell line displayed the least susceptibility, with a viability of 43.9% even at the highest concentration of 1000 µg/mL FE. These findings underscore FE's targeted efficacy against triple-negative breast cancer cells, indicating its promise as an alternative avenue to tackle this formidable cancer subtype.

ARTICLE HISTORY
Received
03 October 2023
Accepted
28 November 2023

KEYWORDS
cytotoxicity,
GC-MS,
breast cancer,
pineapple guava,
anti-cancer

Introduction

Cancer occurrence and cancer-related death rates over the world continue to increase. Among women, breast cancer holds the top position in terms of cancer diagnoses with 2.26 million cases according to GLOBOCAN cancer statistics in 2020 [1]. It was also shown that breast cancer-related death rates were increasing over time. Reoccurrence rates were also shown at relatively high rates [2, 3].
Breast cancer is a heterogeneous disease from both genetic and clinical aspects [4]. There are different classification approaches to breast cancer subtypes. These classifications can be made based on the origin or their receptor types [5-9]. One of these classification strategies uses the hormone receptors of estrogen receptor, ER (+/-), progesterone receptor, PR (+/-) along with the human epidermal growth factor receptor2, HER2 (+/-) [10]. Thus, the treatment approaches also change based on these molecular subtypes of breast cancer. Hormone therapies can be used against hormone receptor-positive breast cancers. Nevertheless, the primary treatment approach for triple-negative breast cancer remains aggressive chemotherapy. As a result, it is crucial to find different treatment options for more effective treatment approaches.
*Feijoa sellowiana (*O. Berg*)* O. Berg *(*synonym, *Acca sellowiana)* [11], represents a small tree displaying distinct cultivars, commonly identified as pineapple guava. It belongs to the Myrtaceae family. Feijoa, originally indigenous to South America, has experienced both natural and commercial cultivation in various countries, including Brazil, Argentina, Chile, Colombia, Uruguay, and New Zealand. This tree bears a resemblance to the olive tree in terms of its appearance and thrives under comparable environmental conditions and growth patterns. Feijoa was introduced to Turkey in 1989, subsequent to which dedicated adaptation orchards were established in Sakarya, Antalya, Mersin, and İzmir [12, 13].
The feijoa fruit has a distinctive aromatic flavor. Due to the rich bioactive compounds of feijoa, it has significant pharmacological potential. As demonstrated by various studies, feijoa fruit extract and its essential oil exhibit notable antimicrobial properties [14-16]. It was also shown that the feijoa plant has antioxidant,

[1] Manisa Celal Bayar University, Applied Science Research Center (DEFAM), Manisa, Türkiye
[2] Manisa Celal Bayar University, Faculty of Science and Letters, Department of Biology, Manisa, Türkiye
*Correspondence: cisil.camli@cbu.edu.tr

anti-inflammatory, immune-stimulating and anti-cancer activities [12, 17, 18]. Several studies reported that the feijoa extracts are effective tools for anti-cancer activities as well as to fight against multidrug resistance [19-21]. However, screening of the cytotoxic activity of the feijoa extract has not been examined in detail in different breast cancer cell lines with different properties.

This study aimed to provide a screening of the effect of feijoa fruit extract (FE) on different breast cancer cell types. Along with the volatile compound composition of FE, the potential relationship between the breast cancer types and the chemical compounds was observed. Thus, this study could provide a basis for further research on latent alternative treatment approaches for different breast cancer types.

Material and Methods

Collection and Extraction of Feijoa fruit

Feijoa fruit was collected from a local garden in Özdere-İzmir/Turkey at the end of the October since its harvest time is in the second week of October and ended in the last week of November [13]. The whole fruit including the fruit peel and seeds was used for extraction. First, 10 gr fruit was mixed in 50 mL absolute ethanol at room temperature using a homogenizer. Then the solution was ultrasonically extracted for 30 minutes. After waiting for cooling down to room temperature, it was stored at 4ºC. Before use, 0.45µm sterile filters were used to filter the feijoa fruit extract [22].

Cell culture conditions

Four distinct breast cancer cell lines were employed to assess the cytotoxicity of FE. These cell lines were MCF-7 (mammary gland adenocarcinoma, ATCC HTB-22), MDA-MB-231, mammary gland adenocarcinoma, ATCC HTB-26), BT-474, mammary gland ductal carcinoma, ATCC HTB-20) and MDA-MB-453, mammary gland carcinoma, ATCC HTB-131). All four cell lines were cultured in RPMI-1640 (Roswell Park Memorial Institute medium 1640) with 10% fetal bovine serum, 1% L-glutamine and 1% penicillin-streptomycin [23]. Cells were maintained in 75 cm^2 polystyrene filtered cap flasks (Corning Life Sciences, UK) in a 37°C incubator with 5% CO_2. Cell growth rates, confluence, and morphologies were observed daily with an inverted microscope (Zeiss Primovert, Germany).

Cell viability assay

The cytotoxic effects of FE were assessed using the MTT assay, which measures metabolic activity through a colorimetric approach. For each cell line, a seeding density of $5x10^4$ cells per well in 96-well plates was maintained during the 24, 48, and 72-hour experimental time points. Cell counts were determined by staining with trypan blue and employing an automated cell counter (Countess, Invitrogen). Following cell seeding, plates were incubated in a CO_2 incubator for 24 hours, after which varying concentrations of FE were introduced into the wells. All the concentrations were added as triplets. After the incubation period of the plates, MTT was added to each plate as 10% of the final volume. Plates were further incubated for 4h after MTT treatment. Upon completion of the incubation period, the culture medium was aspirated, and DMSO (Sigma-Aldrich) was introduced into each well [24]. Absorbance readings at 570 nm, with a reference wavelength set at 690 nm, were recorded using a microplate reader. (Tecan Infinite M200 PRO, Switzerland).

Gas chromatography-mass spectrometry (GC-MS) analysis

For GC-MS analysis of FE a gas chromatography system (Agilent Technologies 7890A) with a mass spectrometer (5975 C mass spectrometer) was used in electron-ionization (EI) mode as described in previous studies [25, 26]. To begin with, FE ethanol extract was centrifuged at 15,000 rpm, the pellet was removed, and the supernatant of the extract was transferred to the vial for GC-MS analysis. Agilent HP-5 MS capillary column with 0.25 µm film thickness was used as the chromatographic column. Helium was used as a carrier gas at a flow rate of 1 mL min^{-1}. The database of the National Institute of Standard and Technology (NIST) was used as the source database to comment on the results.

Statistical analysis

The statistical analyses of the MTT assay results were performed with Graph Pad Prism 5 (USA) [27, 28]. The one-way ANOVA (Dunnett's t-test) was used for data analysis. Values with $p \leq 0.05$ (*) were considered statistically significant. Biosoft CalcuSyn 2.1 (USA) was used to calculate the IC_{50} values for each treatment [29].

Results and Discussion

Plant extracts are widely recognized for their bioactivities, which stem from their remarkable selectivity and, in many cases, their ability to biodegrade into non-toxic substances. This enables their application like conventional chemical drugs but in a less harmful manner. Numerous studies have documented the significant biological characteristics of Feijoa fruit extracts, highlighting their potent antimicrobial properties and remarkable antioxidant activity [14, 30]. It is also shown to have strong anticancer properties and display

tumor-selective activity in several studies [14, 21, 31-33]. Some studies also show the anti-cancer effect of feijoa-derived silver nanoparticles on MCF-7 [21, 34].

Nevertheless, no research has been conducted to study and compare the cytotoxic impact of FE on various breast cancer cells. Due to the distinct nature of various types of breast cancers, different treatment approaches are necessary to address their responses. Therefore, this study established a framework to comprehend the diverse effects of FE on distinct types of breast cancer cells.

First, the cell viability was determined. For this aim, MCF-7, MDA-MB-231, MDA-MB-453, and BT-474 breast cancer cell lines were treated with increasing concentrations (50-1000 µg/mL) of FE for 24h, 48h, and 72h. Then MTT assay was performed. As shown in Figure 1.a, the highest decrease in the cell viability of MCF-7 cells was observed in 72h as compared to the untreated control. The cell viability for 1000 µg/mL was 67.4%, 53.1%, and 23.2% in 24, 48, and 72h, respectively. The IC_{50} value of the MCF-7 at 72h was 139.3 µg/mL (Figure 2). The viability of the MDA-MB-231 cells was decreased starting from the 24h treatment and the IC_{50} value was 121.1 µg/mL at 72h (Figure 1.b, Figure 2). For the 1000 µg/mL FE, the cell viability was measured as 16% even at the end of the 24h.

The least effect of the FE on the cell viability was observed on BT-474 (Figure 1.c). Although the cell viability was 43.9% for the 1000 µg/mL FE, the overall effect was lower as compared to the other breast cancer cell lines. Conversely, the effect of FE was already significant for 200 µg/mL in all 24, 48, and 72h treatments of MDA-MB-453. The viability was measured as 31.7%, 26.3%, and 25.2% and the IC_{50} values were 277.4, 286.0, and 121.1 µg/mL respectively (Figure 1.d, Figure 2).

The volatile compound composition was identified by GC-MS analysis of the whole fruit extract. GC-MS analysis results were listed in Table 2 including the molecular formula and NIST scores. The obtained results were compared with the previous studies on feijoa.

Overall, the results showed that the FE was highly effective on MDA-MB-453 and MDA-MB-231 cell lines. Its effect was apparent starting from the 24h treatment for both cell lines. This similarity draws attention that both cell lines are triple-negative breast cancer cell lines. So, it shows that FE holds great potential as an alternative to aggressive chemotherapy treatment. However, FE was not only effective on MDA-MB-453 and MDA-MB-231 cell lines. It has a time-increasing level of cytotoxicity for the MCF-7 cell line as well.

It was observed that the cell viability of the MCF-7 cell line at 72h was dropped to 23.2% with 1000 µg/mL FE but it decreased the viability even at the lower concentrations. It was also shown in another study with Crystal violet assay that, feijoa extract showed an anti-proliferative effect on MCF-7 and MDA-MB-231 cell lines. However, cell cycle analysis between these two cell lines was different and the effect on MCF-7 cells was in S or G2/M phases [31]. Other studies showed the effect of feijoa extract as green-synthesized nanoparticles on MCF-7 cells as well [21, 34].

MCF-7

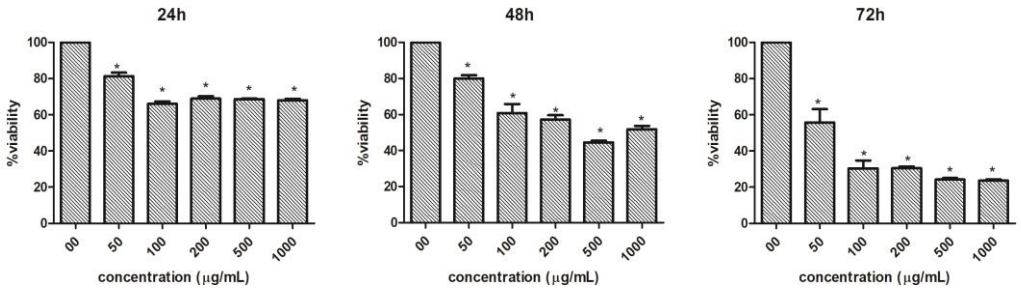

1.a

MDA-MB-231

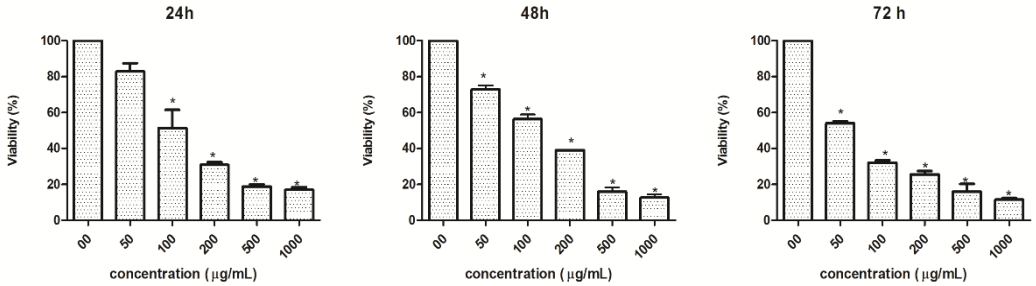

1.b

BT-474

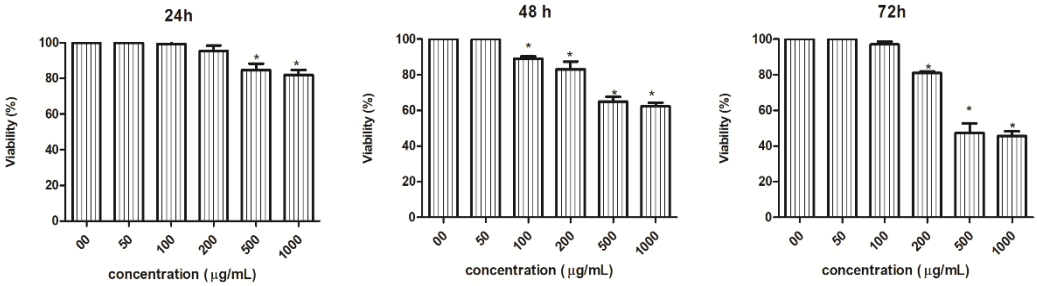

1.c

MDA-MB-453

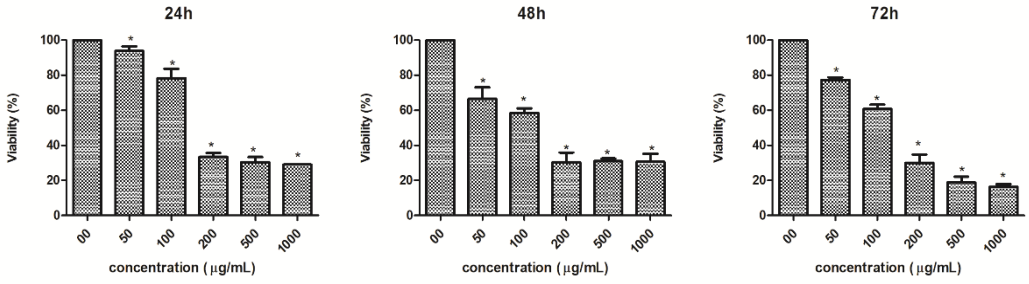

1.d

Fig 1 Time and concentration-dependent effect of FE extract on the viability of 1.a, MCF-7; 1.b, MDA-MB-231; 1.c, BT-474; and 1.d, MDA-MB-453 cells (*P < 0.05 compared to untreated control)

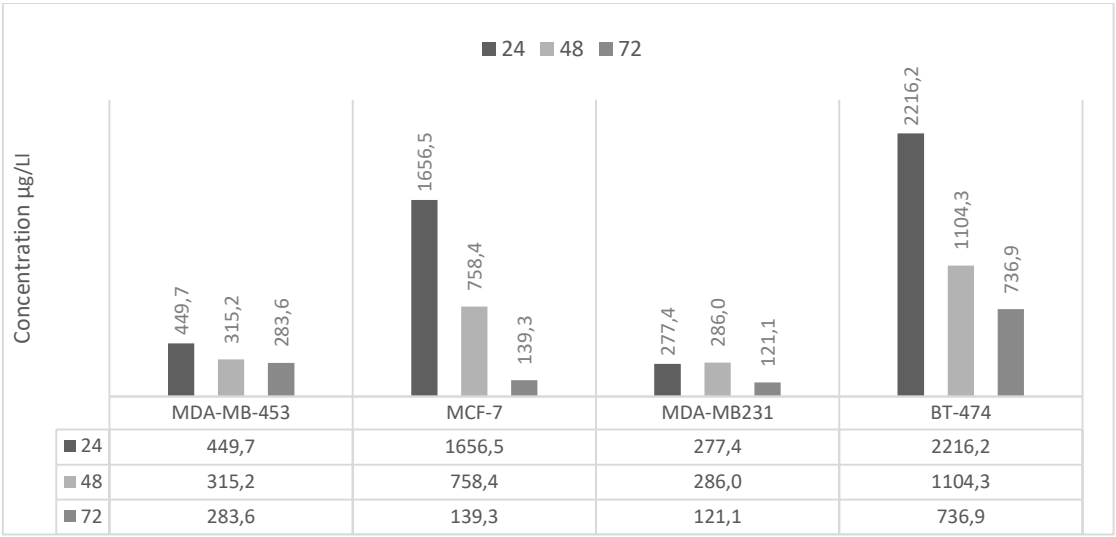

	MDA-MB-453	MCF-7	MDA-MB231	BT-474
24	449,7	1656,5	277,4	2216,2
48	315,2	758,4	286,0	1104,3
72	283,6	139,3	121,1	736,9

Fig 2 IC_{50} results in µg/mL for the four different breast cancer cell lines in 24, 48, and 72 h.

The least effect on cell viability was shown against the BT-474 cell line. Then again, the cell viability was 43.9% for the 1000 µg/mL FE. The main difference was while the cytotoxicity of FE was observable even at the lower doses and/or early treatment times, it was only evident for the high doses and 72h treatment for the BT-474 cell line.

It is important to understand the relation between the cytotoxic effect of the FE and the breast cancer cell lines. Therefore, as seen in earlier research, the use of GC-MS analysis served as a foundation for establishing this connection [25, 26, 35]. For instance, there are furane derivates found in FE. Furan derivatives, known for their antibacterial, antifungal, anti-inflammatory, and anticancer properties, are currently under development as potential treatments for drug-resistant infections [36, 37].Eugenol, with its potential uses in cancer and Alzheimer's treatment, serves as an antiseptic against bacteria, fungi, and viruses, offers local anesthesia as an analgesic, reduces inflammation for conditions like arthritis, and provides antioxidant protection to cells. It's also under investigation for antimicrobial applications in infection treatment [38, 39]. While methyl benzoate is known for its contribution to the fruity aroma, 9-octadecenamide, and its derivatives are being investigated for a variety of potential applications including sleep-inducing and skin-care products [39, 40]. In the context of previous investigations into feijoa, the observed results align consistently with the potential utility of these compounds.

Also in other studies, it was shown that the active compound found in feijoa was flavone. Flavonoids are known to exhibit a broad range of anticancer effects. These impacts include the regulation of ROS-scavenging enzyme functions, cell cycle, prompting apoptosis and autophagy, and controlling the growth and invasiveness of cancer cells. The flavonoids have a twofold function in preserving ROS balance. In typical circumstances, they act as antioxidants, but in cancer cells, they demonstrate robust pro-oxidant characteristics, initiating apoptotic processes and diminishing pro-inflammatory signaling pathways [41]. Also, flavonoids induce excessive and prolonged autophagy. This suggests that flavonoids hold promise for treating individuals with cancer that are resistant to apoptosis [42]. As an active compound of FE, flavone is known to induce apoptosis through caspase, p16, p21, and TRAIL [31].

The responsiveness to TRAIL-induced apoptosis was influenced by the molecular phenotype of breast cancer. It was demonstrated that TRAIL exhibits a preferential ability to induce cell death in triple-negative cells [43]. Considering this information, it was consistent to observe that FE demonstrated greater efficacy against the MDA-MB-453 and MDA-MB-231 cell lines. TRAIL-mediated apoptosis is ineffective in inducing cell death in MCF7 cells, indicating their resistance to this mechanism. BT-474 cells have likewise exhibited resistance to TRAIL [43-45]. This information explains the increased impact of FE on MDA-MB-231 and MDA-MB-453 cells while demonstrating a lowered effect on MCF-7 and BT-474 cell lines. However, despite a lesser impact compared to triple-negative cell lines, a noticeable effect was still observed, particularly during the 72-hour treatment. This suggests that other active compounds present in the extract also play a significant role in breast cancer.

Table 1 GC-MS results of the FE extract. RT, Retention time. National Institute Standard and Technology (NIST) (Wiley7Nist05.L) was used as a database

Compound Name	**Molecular Formula**	**Score (NIST, similarity %)**	**RT**
2(5H)-Furanone	C4H4O2	90.33	8.879
Cyclohexanone	C6H10O	84.94	9.038
1,2-Cyclopentanedione	C5H6O2	96.58	9.158
2,5-Furandione	C5H4O3	96.78	9.683
2-Furancarboxaldehyde, 5-methyl-	C6H6O2	94.36	10.166
2,4-Dihydroxy-2,5-dimethyl-3(2H)-furan-3-one; 2,4-Dihydroxy-2,5-dimethyl-3(2H)-furanone #	C6H8O4	95.96	10.698
Butanedial; Succinaldehyde; Succindialdehyde; Succinic aldehyde; Succinic dialdehyde;	C4H6O2	84.84	10.898
Benzenemethanol	C7H8O	93.63	12.109
1,3-Cyclopentanedione, 2,2-dimethyl-	C7H10O2	75.96	12.67
Pentanoic acid, 4-oxo-	C5H8O3	71.56	12.751
2,5-Furandicarboxaldehyde; 2,5-Furandicarbaldehyde	C6H4O3	88.77	13.596
2-Furancarboxylic acid, methyl ester	C6H6O3	96.73	13.768
2,3-Dihydro-5-hydroxy-6-methyl-4H-pyran-4-one	C6H8O3	81.16	13.853
Pentanal	C5H10O	82.3	13.86
1,2-Butanediol, 3,3-dimethyl-; 3,3-Dimethyl-1,2-butanediol	C6H14O2	81.23	14.193
4H-Pyran-4-one, 2,3-dihydro-3,5-dihydroxy-6-methyl-	C6H8O4	81.03	15.298
(+/-)bis(2-aminobut-3-enyl) disulphide	C8H16N2S2	84.24	15.597
2,3-Dihydro-3,5-dihydroxy-6-methyl-4H-pyran-4-one	C6H8O4	91.93	15.858
1-cyano-5-benzoyloxy-.beta.-D-ribofuranose	C13H13NO5	91.93	16.47
Dianhydromannitol	C6H10O4	89.14	17.18
2(3H)-Furanone, dihydro-4-hydroxy-	C4H6O3	59.56	17.702
D-Erythro-Pentose, 2-deoxy-	C5H10O4	80.16	17.987
2-Bromo-4,4-Di-N-Propylcyclobutanone; Cyclobutanone, 4-bromo-2,2-dipropyl-	C10H17OBr	77.63	18.66
(bistrifluoromethylamino-oxy)cyclopentane	C7H9NOF6	86.01	18.891
Soleron; 2(3H)-Furanone, 5-acetyldihydro-; .delta.-oxo-.gamma.-hexalactone; solerone	C6H8O3	82.9	18.926
1,5-dibromo-2,4-dimethyl-pentane; Pentane, 1,5-dibromo-2,4-dimethyl-	C7H14Br2	77.4	19.128
3-Hexyn-2-ol, 5-methyl-	C7H12O	70.6	19.157
3-Hydroxy-2,5,5-trimethylcyclopentanone	C8H12D2O2	65.17	19.183
Ketone, methyl 2-methyl-1,3-oxothiolan-2-yl	C6H10O2S	82.63	19.383
Methyl 1-Methyl-d3-2-propenyl Ether	C5H7D3O	69.71	20.113
Methyl 11-Acetoxy-5-methyl-4-oxoundecanoate	C15H26O5	61.62	21.09
Eugenol	C10H12O2	90.4	21.181
Methyl benzoate	C6H5CO2CH5	98.7	22.04
1,2(S)-Epoxyheptane	C7H14O	67.99	22.935
Naphthalene, 1,2,3,4-tetrahydro-1,6-dimethyl-4-(1-methylethyl)-, (1S-cis)-	C15H22	88.05	25.737
3-Pentanone	C5H10O	76.06	25.874
Dodecyl acrylate	C15H28O2	95.55	29.529
Butylphosphonic acid, dihexyl ester	C16H35O3P	50.11	30.877
n-Hexadecanoic acid	C16H32O2	89.15	35.008
5,5'-Oxy-Dimethylene-Bis(2-Furaldehyde); 2-Furancarboxaldehyde, 5,5'-[oxybis(methylene)]bis-	C12H10O5	85.54	35.631
Oleic Acid	C18H34O2	93.89	38.024
4H-1-Benzopyran-4-one, 2-phenyl-	C15H10O2	96.13	39.775
9-Octadecenamide, (Z)-	C18H35NO	78.96	42.122
Hexadecanoic acid, 2-hydroxy-1-(hydroxymethyl)ethyl ester; Palmitin, 2-mono-; Palmitic acid .beta.-monoglyceride; 2-Hexadecanoyl glycerol; 2-Monopalmitin; 2-Monopalmitoyl-sn-glycerol; 1,2,3-Propanetriol 2-hexandecanoyl ester; Glycerol .beta.-palmitate; 2-	C19H38O4	88.5	44.441
Octadecanoic acid, 2,3-dihydroxypropyl ester	C21H42O4	90.53	47.521
13-Docosenamide, (Z)-	C22H43NO	82.68	48.433

Conclusion

Feijoa fruit extracts (FE) exhibit significant cytotoxic effects on breast cancer cell lines, with the highest efficacy observed in triple-negative cells, MDA-MB-453 and MDA-MB-231. FE also demonstrates potential by showing time-dependent cytotoxicity against hormone receptor-positive MCF-7 cells. While the effect on BT-474 cells is less pronounced, the study highlights the diverse potential of FE in breast cancer treatment. Chemical GC-MS analysis reveals the presence of compounds like furan derivatives, eugenol, and flavone, all with known anticancer properties. The objective was to establish a foundational framework for future investigations into alternative latent treatments for various breast cancer subtypes. This study underscores FE's promise as a novel therapeutic agent for breast cancer treatment, warranting further investigation.

Abbreviations
FE: *Feijoa sellowiana* fruit extract; DMSO: Dimethyl sulfoxide; GC-MS: Gas chromatography-mass spectrometry; EI: electron-ionization; NIST: National Institute of Standard and Technology; RT: Retention time; ROS: Reactive oxygen species; TRAIL: TNF-Related Apoptosis Inducing Ligand; TNF: Tumor necrosis factor.

Acknowledgements
The experiments in this paper were performed at Manisa Celal Bayar University (Turkey) – Applied Science and Research Center (DEFAM). Part of this work was presented as an Oral Presentation in 1st International Congress on Solutions in Science (INSCORE).

Funding
The authors did not receive support from any organization for the submitted work.

Data Availability statement
The author confirms that the data supporting this study are cited in the article.

Compliance with ethical standards
Conflict of interest
The authors declare no conflict of interest.

Ethical standards
The study is proper with ethical standards.
Authors' contributions
All authors contributed equally to the study.

References

1. Sung, H., et al., Global Cancer Statistics 2020: GLOBOCAN Estimates of Incidence and Mortality Worldwide for 36 Cancers in 185 Countries. CA: A Cancer Journal for Clinicians, 2021. 71(3): p. 209-249.
2. Richie, R.C. and J.O. Swanson, Breast cancer: a review of the literature. Journal of insurance medicine, 2003. 35 2: p. 85-101.
3. Schapira, D.V. and N. Urban, A Minimalist Policy for Breast Cancer Surveillance. JAMA, 1991. 265(3): p. 380-382.
4. Riaz, M., et al., miRNA expression profiling of 51 human breast cancer cell lines reveals subtype and driver mutation-specific miRNAs. Breast Cancer Research, 2013. 15(2): p. R33.
5. Dai, X., et al., Breast cancer intrinsic subtype classification, clinical use and future trends. American journal of cancer research, 2015. 5 10: p. 2929-43.
6. Kao, J., et al., Molecular profiling of breast cancer cell lines defines relevant tumor models and provides a resource for cancer gene discovery. PLoS One, 2009. 4(7): p. e6146.
7. Charafe-Jauffret, E., et al., Gene expression profiling of breast cell lines identifies potential new basal markers. Oncogene, 2006. 25(15): p. 2273-2284.
8. Hollestelle, A., et al., Distinct gene mutation profiles among luminal-type and basal-type breast cancer cell lines. Breast Cancer Research and Treatment, 2010. 121(1): p. 53-64.
9. Neve, R.M., et al., A collection of breast cancer cell lines for the study of functionally distinct cancer subtypes. Cancer Cell, 2006. 10(6): p. 515-27.
10. Vuong, D., et al., Molecular classification of breast cancer. Virchows Arch, 2014. 465(1): p. 1-14.
11. Online, P.o.t.W. *Feijoa sellowiana* (O.Berg) O.Berg. Available from: https://powo.science.kew.org/taxon/urn:lsid:ipni.org:names:596467-1
12. Weston, R.J., Bioactive products from fruit of the feijoa (*Feijoa sellowiana*, Myrtaceae): A review. Food Chemistry, 2010. 121(4): p. 923-926.
13. Beyhan, Ö. and S.P. Eyduran, Determination of promising native Feijoa (*Feijoa sellowiana* Berg.) genotypes from Sakarya Region in Turkey. Scientific Research and Essays, 2011. 6: p. 4104-4108.
14. Vuotto, M.L., et al., Antimicrobial and antioxidant activities of *Feijoa sellowiana* fruit. Int J Antimicrob Agents, 2000. 13(3): p. 197-201.
15. Saj, O.P., R.K. Roy, and S.V. Savitha, Chemical composition and antimicrobial properties of essential oil of *Feijoa sellowiana* O. Berg. (Pineapple guava). 2008. 2: p. 227-230.
16. Motohashi, N., et al., Biological activity of feijoa peel extracts. Anticancer Res, 2000. 20(6b): p. 4323-9.
17. Lapčík, O., et al., Identification of isoflavones in *Acca sellowiana* and two Psidium species (Myrtaceae). Biochemical Systematics and Ecology, 2005. 33(10): p. 983-992.

18. Germano, G., et al., Role of Macrophage Targeting in the Antitumor Activity of Trabectedin. Cancer Cell, 2013. 23(2): p. 249-262.
19. Dell'Olmo, E., et al., Fighting multidrug resistance with a fruit extract: anti-cancer and anti-biofilm activities of *Acca sellowiana*. Nat Prod Res, 2021. 35(10): p. 1686-1689.
20. Russi, S., et al., Effect of *Feijoa sellowiana* Acetonic Extract on Proliferation Inhibition and Apoptosis Induction in Human Gastric Cancer Cells. Applied Sciences, 2020. 10(21): p. 7756.
21. Hashemi, Z., et al., Green Synthesized Silver Nanoparticles Using *Feijoa sellowiana* Leaf Extract, Evaluation of Their Antibacterial, Anticancer and Antioxidant Activities. Iran J Pharm Res, 2020. 19(4): p. 306-320.
22. Gambin, L.D.B., et al., Phenolic compounds from feijoa (*Acca sellowiana*) fruits: Ultrasound-assisted extraction and antiproliferative effect on cutaneous melanoma cells (SK-MEL-28). Food Bioscience, 2023. 55: p. 103078.
23. Erten, C., et al., Regulation of growth factors in hormone- and drug-resistant prostate cancer cells by synergistic combination of docetaxel and octreotide. BJU Int, 2009. 104(1): p. 107-14.
24. Kumar, P., A. Nagarajan, and P.D. Uchil, Analysis of Cell Viability by the MTT Assay. Cold Spring Harb Protoc, 2018. 2018(6).
25. Atmaca, H., C. Camli Pulat, and M. Cittan, *Liquidambar orientalis* Mill. gum extract induces autophagy via PI3K/Akt/mTOR signaling pathway in prostate cancer cells. Int J Environ Health Res, 2022. 32(5): p. 1011-1019.
26. Oguz, F., et al., GC-MS Analysis and Potential Apoptotic Effect of *Paliurus spina-christi* Mill. Leaf and Flower Extracts against Breast Cancer Cells. Sakarya University Journal of Science, 2022. 26(2): p. 357-364.
27. GraphPad. GraphPad Prism 7 Statistics Guide - The essential concepts of statistics. Available from: https://www.graphpad.com/guides/prism/7/statistics/index.htm
28. Guide, G.S. GraphPad Statistics Guide. 1995; Available from: www.graphpad.com
29. Chou, T.C., Theoretical basis, experimental design, and computerized simulation of synergism and antagonism in drug combination studies. Pharmacol Rev, 2006. 58(3): p. 621-81.
30. Basile, A., et al., Antibacterial and antifungal properties of acetonic extract of *Feijoa sellowiana* fruits and its effect on *Helicobacter pylori* growth. J Med Food, 2010. 13(1): p. 189-95.
31. Bontempo, P., et al., *Feijoa sellowiana* derived natural Flavone exerts anti-cancer action displaying HDAC inhibitory activities. Int J Biochem Cell Biol, 2007. 39(10): p. 1902-14.
32. Peng, Y., et al., Characterization of phenolic compounds and aroma active compounds in feijoa juice from four New Zealand grown cultivars by LC-MS and HS-SPME-GC-O-MS. Food Research International, 2020. 129: p. 108873.
33. Rossi, A., et al., Inhibition of Inducible Nitric Oxide Synthase Expression by an Acetonic Extract from *Feijoa sellowiana* Berg. Fruits. Journal of Agricultural and Food Chemistry, 2007. 55(13): p. 5053-5061.
34. Hashemi, Z., et al., Biogenic Silver and Zero-Valent Iron Nanoparticles by Feijoa: Biosynthesis, Characterization, Cytotoxic, Antibacterial and Antioxidant Activities. Anticancer Agents Med Chem, 2020. 20(14): p. 1673-1687.
35. Ilhan, S., Essential Oils from *Vitex agnus* castus L. Leaves Induces Caspase-Dependent Apoptosis of Human Multidrug-Resistant Lung Carcinoma Cells through Intrinsic and Extrinsic Pathways. Nutr Cancer, 2021. 73(4): p. 694-702.
36. Li, Y.-S., et al., Synthesis and biological evaluation of 2,5-disubstituted furan derivatives as P-glycoprotein inhibitors for Doxorubicin resistance in MCF-7/ADR cell. European Journal of Medicinal Chemistry, 2018. 151: p. 546-556.
37. Banerjee, R., H. Kumar, and M. Banerjee, Medicinal significance of furan derivatives: a review. International Journal of Research in Phytochemistry and Pharmacology, 2015. 5(3): p. 48-57.
38. Abdou, A., et al., Recent advances in chemical reactivity and biological activities of eugenol derivatives. Medicinal Chemistry Research, 2021. 30(5): p. 1011-1030.
39. Patterson, J.E., et al., Inhibition of Oleamide Hydrolase Catalyzed Hydrolysis of the Endogenous Sleep-Inducing Lipid cis-9-Octadecenamide. Journal of the American Chemical Society, 1996. 118(25): p. 5938-5945.
40. Shaw, G.J., et al., Volatile flavour constituents of feijoa (*Feijoa sellowiana*)—analysis of fruit flesh. Journal of the Science of Food and Agriculture, 1990. 50(3): p. 357-361.
41. Kopustinskiene, D.M., et al., Flavonoids as Anticancer Agents. Nutrients, 2020. 12(2).
42. Zhang, Z., et al., The Multifaceted Role of Flavonoids in Cancer Therapy: Leveraging Autophagy with a Double-Edged Sword. Antioxidants (Basel), 2021. 10(7).
43. Rahman, M., et al., TRAIL induces apoptosis in triple-negative breast cancer cells with a mesenchymal phenotype. Breast Cancer Res Treat, 2009. 113(2): p. 217-30.
44. Sanlioglu, A.D., et al., Surface TRAIL decoy receptor-4 expression is correlated with TRAIL resistance in MCF7 breast cancer cells. BMC Cancer, 2005. 5: p. 54.
45. Chandrasekaran, S., et al., TRAIL-mediated apoptosis in breast cancer cells cultured as 3D spheroids. PloS one, 2014. 9(10): p. e111487.

International Journal of Life Sciences and Biotechnology
Caf, et al., Smartphone-Based Point-of-Care Urinalysis Vivoo App: A Validation Study. International Journal of Life Sciences and Biotechnology, 2024 7(1): p. 60-73.
https://doi.org/10.38001/ijlsb.1371191
Araştırma Makale/ Research article

Smartphone-Based Point-of-Care Urinalysis Vivoo App: A Validation Study

Balım Bengisu Caf[1,2*], Gizem Cebi[1,3], Haluk Çelik[1,4], Aliasghar Noroozi[1], Ali Atasever [1], Miray Tayfun[1]

ABSTRACT
Point-of-care (POC) analysis has emerged as a pivotal approach in providing rapid and convenient medical diagnostics. Smartphone-based solutions further augment the accessibility and ease of POC, enabling efficient on-the-go analysis. The integration of smartphone technology with POC has paved the way for innovative applications such as the Vivoo App, which empowers users to monitor various health parameters conveniently. Our study validated the accuracy and reliability of the smartphone-based POC urinalysis Vivoo mobile application. A comparative approach was followed wherein artificial urine samples were analyzed using both the Vivoo and traditional laboratory methods. A diverse range of health parameters were assessed. A total of 2618 strips were used over the course of this study to evalate the accuracy of Vivoo. The test strips results appeared to match exactly the expected measurement results. In addition, when the ±1 color block acceptance criterion was applied, 2608 of 2618 measurements of the tested strips were found to have met the expected measurement results completely. Based on the results, the 95% confidence interval for the exact match agreement proportion of Vivoo is 87.55% ± 1.27% and 99.62% ± 0.24%. As a wellness product, this study thus concludes that the Vivoo is appropriate in terms of both device reliability and performance. The app's ability to provide accurate and timely health results offers promising opportunities to improve individual health management.

ARTICLE HISTORY
Received
05 October 2023
Accepted
20 December 2023

KEYWORDS
Point of care,
urinalysis,
artificial intelligence,
wellness,
healthcare

Introduction

Point-of-care (POC) analysis is a form of testing that allows for the immediate testing of medical samples at the point of care without the need for conventional laboratory analysis [1]. Point-of-care testing is described as conducting tests at the patient care site or in its nearby vicinity [2]. This method offers several benefits, such as rapid results, reduced costs, and improved patient outcomes [3]. In recent years, one emerging trend in POC analysis has been the use of smartphone-based technology for diagnostics, including through urine analysis [4]. Point-of-care technology delivers relevant data directly at the location of treatment, facilitating quick clinical judgments. As the healthcare focus moves towards precision medicine, overall population well-being, and the effective handling of chronic conditions, the significance of its potential is on the rise. Over the past ten years, various notable trends in POC have surfaced or gained more prominence.
Urine analysis is one of the most common diagnostic tests in clinical practice, providing valuable information about kidney function, urinary tract infections, and other medical conditions [5, 6, 7, 8]. Urine analysis, a fundamental diagnostic tool in medical practice, plays a pivotal role in assessing and monitoring various health conditions [9]. Urine analysis provides crucial insights into an individual's health, revealing information about kidney function, hydration levels, and potential underlying medical conditions [2, 10]. This non-invasive method provides critical insights into an individual's metabolic, renal, and systemic health. Analyzing components such as pH, specific gravity, and the presence of proteins, glucose, ketones, and blood cells can help in the early detection and management of conditions like diabetes, kidney disease, urinary tract infections,

[1] Vivosens Inc., 44 Tehama Street, Suite 409, San Francisco, CA, US 94105
[2] Program of Bioengineering, Faculty of Chemical and Metallurgical Engineering, Yildiz Technical University, 34210, Istanbul, Türkiye
[3] Program of Chemical Engineering, Faculty of Chemical and Metallurgical Engineering, Istanbul Technical University, 34469, Istanbul, Türkiye
[4] Program of Stem Cell and Tissue Engineering, Institute of Health Sciences, Istinye University, 34010, Istanbul, Türkiye
*Corresponding Author: Balım Bengisu Caf, e-mail: bengisu.caf@std.yildiz.edu.tr

and liver problems. The advent of home urine test kits has further revolutionized this field, enabling patients to conduct preliminary assessments in the comfort of their homes. These test, which often use dipsticks with color-changing pads, offer a convenient and rapid means to track health indicators. By allowing for frequent monitoring, home urine analysis can facilitate early intervention and timely consultation with healthcare professionals [4]. This not only empowers individuals in their health management but also aids in reducing the burden on healthcare systems by preventing the escalation of untreated conditions. Thus, urine analysis, especially when accessible at home, stands as a cornerstone in preventive healthcare and patient empowerment. Traditional urine analysis involves laboratory-based testing, which can be both time-consuming and expensive. However, smartphone-based urine analysis offers a rapid and cost-effective alternative that typically utilizes a disposable test strip that is dipped into a urine sample [11, 12, 13]. The smartphone app provides a visual readout of the test results, which can be used by healthcare professionals for diagnosis and treatment of different diseases, medical conditions, and overall health and wellness [14, 15, 16, 17].

Smartphone-based POC urinalysis is a rapidly growing field that has the potential to revolutionize the ways in which patients are diagnosed and treated for various conditions. It is a promising technology due to its rapid and low-cost diagnosis of urine biomarkers [18, 19]. Smartphone-based urine analysis typically involves the use of mobile devices equipped with high-resolution cameras and specialized software applications. The purpose of these applications is to evaluate images of urine test strips and calculate the concentration of different analytes in the urine. This process is done by comparing color changes to a pre-calibrated colorimetric scale. This process becomes more complex when AI algorithms are used. AI significantly improves accuracy and makes it possible to identify small variations that might be overlooked by the human eye. The idea assumes that smartphones which are widely available and equipped with advanced imaging software, can be used for rapid and cost-effective urine analysis. This approach has significant implications for healthcare, especially in the diagnosis and management of medical conditions [20, 21]. The process typically involves dipstick preparation, image capture, image analysis, and results. This system has several advantages, such as rapid results, cost-effectiveness, remote monitoring, and accessibility. Smart-phone based POC systems can be applied to chronic disease management, infection detection, pregnancy testing, and wellness-associated parameter testing. Advancements in artificial intelligence and machine learning could further enhance the accuracy and capabilities of smartphone-based urine analysis. Integration with electronic health records and telehealth platforms could also broaden its impact [22, 23]. Traditionally, urinalysis has been performed in laboratory settings using specialized equipment, which can be time-consuming and require patients to travel to a healthcare facility [24, 25]. With the increasing ubiquity of smartphones and the development of innovative POC diagnostic technologies, it is now possible for patients to perform their own urinalysis at home or in a healthcare facility by using their smartphone as a diagnostic platform [25].

The widespread accessibility of smartphones and tablets offers several significant prospects for the integration of point-of-care testing (POCT) [26]. Incorporating POCT with these platforms also facilitates the storage of data on a cloud-based server for telemedicine purposes. While a standardized approach for seamlessly integrating this data into regular medical records is yet to be established, enabling the sharing of this information beyond the limitations of a specific hospital or device will set the stage for future advancements. Numerous POCTs under development have capitalized on the optical sensing functionalities of the integrated complementary metal oxide semiconductor cameras found in smartphones and tablets [28, 29]. These cameras can be employed for tasks such as capturing images or spectra and subsequently analyzing them.

The accuracy and reliability of smartphone-based POC analysis rely heavily on artificial intelligence (AI) and image processing algorithms [30, 31]. AI algorithms can detect subtle changes in color or intensity that may be difficult for the human eye to discern. Image processing algorithms can help reduce noise and improve the signal-to-noise ratio, leading to more accurate and reliable results [32, 33]. AI and image processing can also be used to develop predictive models for diagnosing and treating diseases based on large datasets of POC analysis results [34, 35].

In recent years, machine learning (ML) techniques have been increasingly used for the analysis of POC urinalysis test results [36, 37]. ML algorithms can be trained to analyze images of urine test strips captured by smartphone cameras and provide diagnostic information based on test results [38, 39, 40]. This approach has the potential to significantly improve the accuracy and speed of POC urinalysis, as well as increase its accessibility and affordability [41, 42]. However, the development of ML algorithms for POC urinalysis requires extensive validation studies to ensure their accuracy and reliability [43].

Due to advancements in POC, urinalysis has evolved into a trustworthy and efficient diagnostic method. Recent progress in AI technology has enhanced the precision, reliability, and efficiency of urine analysis diagnostics. These tools now have the capacity to recognize various medical issues and deliver precise insights into an individual's health by examining the physical and chemical attributes of urine. Urine test strips provide a rapid

and convenient means of initial urinalysis, swiftly detecting substances such as glucose, nitrite, urobilinogen, bilirubin, protein, ketone, albumin, creatinine, pH, and leukocyte esterase. The development of multi-component test strips enables the simultaneous identification of these substances using just one urine sample. The focus of this study is on the accuracy and reliability of smartphone-based POC urinalysis, particularly the use of AI and ML algorithms for analyzing test results. The aim of the study is to validate the accuracy of the Vivoo urine analysis platform for measuring different chemical components found on the Vivoo test strip. In this study, artificial urine solutions were used to test the accuracy of the Vivoo results. The results of our study suggest that the Vivoo urine analysis is a reliable method for measuring various chemical components in urine. The use of AI and image processing algorithms in POC urinalysis has the potential to significantly improve the accuracy and speed of diagnosis and increase its accessibility and affordability to consumers.

Material and Methods

The Vivoo App processes each strip image in three steps: 1) sensor and reference detection, 2) color correction, and 3) sensor value prediction.

Detecting the strip through sensors and references

In our patented process, named "Analysis of urine test strips with mobile camera analysis and providing recommendation by customizing data" (patent number: US20220405973A1) [44], we first began by employing an object detection model to localize the Vivoo test strip and its sensors and reference boxes. Next, we used segmentation to extract the sensors and references. With the extracted references and object detection results, we conducted a series of checks, including on strip position, distance, movement, perspective, and lighting conditions.

We then positioned the strip carefully to achieve optimal test results. To do this, we used the strip's bounding box as a reference for its position, defined edge margins to the screen, and hit the test bounding box. Although it was not necessary for the strip to be positioned exactly, we were conscious of the possibility of the strip failing the check if positioned at an angle or too close, even if it is centered correctly. We also took into account the appropriate strip distance, as this was crucial for improved test outcomes. We ensured that the strip was not too far away, which would present challenges in extracting sensor colors accurately, or too close, which can cause blurriness or shadow interference. The width and height of the strip bounding box helped determine the distance, and we ensured they were within a predefined range. During testing, we also maintained the strip's movement and stability, recognizing that if the strip moved, the resulting image could become blurry, leading to incorrect test results. To maintain stability during the image-capturing process, we used the strip's bounding box as a reference for its position and ensured that its movement speed was slower than its predefined value. Overall, these steps were critical for ensuring the secure positioning of the strip and producing accurate results during testing.

We recognized the importance of having the strip's face parallel to the camera to obtain accurate test results and proper strip perspective. To achieve this, we calculated the distance between all corner boxes, compared these distances to calculate differences, and used them to determine the strip's vertical and horizontal perspectives. Accurately determining the strip's perspective was a crucial step in achieving reliable test results, as it ensured that the strip was viewed correctly by the camera, allowing for accurate readings during testing. Additionally, consistent lighting conditions were essential to achieving accurate test results, as inconsistent lighting could cause partial dark regions over sensors, and shadows could also cause color changes on some regions of the strip surface. To maintain consistent lighting, we calculated the overall brightness and checked for deviations, as well as calculated the overall color changes and analyzed deviations. These steps helped identify any discrepancies in the lighting conditions and allowed for corrections to be made to achieve consistent lighting. Throughout testing, we monitored and adjusted the lighting to maintain consistency, recognizing its importance for achieving accurate and reliable test results.

Color correction

In this step, a dominant color is calculated for each extracted reference box. These reference colors are used to perform color correction on extracted sensors. Color correction normalizes the environment light by comparing extracted reference colors with the original printed reference colors.

Fig 1 depicts a flowchart of how color correction functions in the Vivoo App. 8-bit RGB refers to integer values of color channels R, G, and B, which are between the range of 0 to 255. Float linear RGB refers to float values in range [0, 1]. Precision of float linear values are higher than integer 8-bit values. The inherent component in Fig 1 is Root Polynomial Regression [45], in which a correction matrix is computed from the original reference colors and the observed (extracted) reference colors using least-squares regression. Fig 2 presents the result of applying the color correction to the entire image.

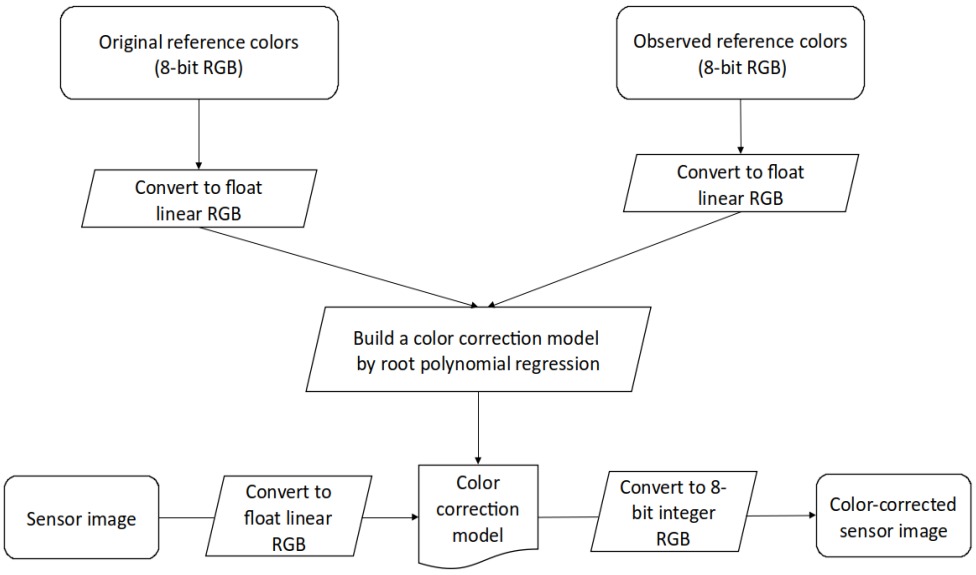

Fig 1 Color correction functioning in the Vivoo App [44]

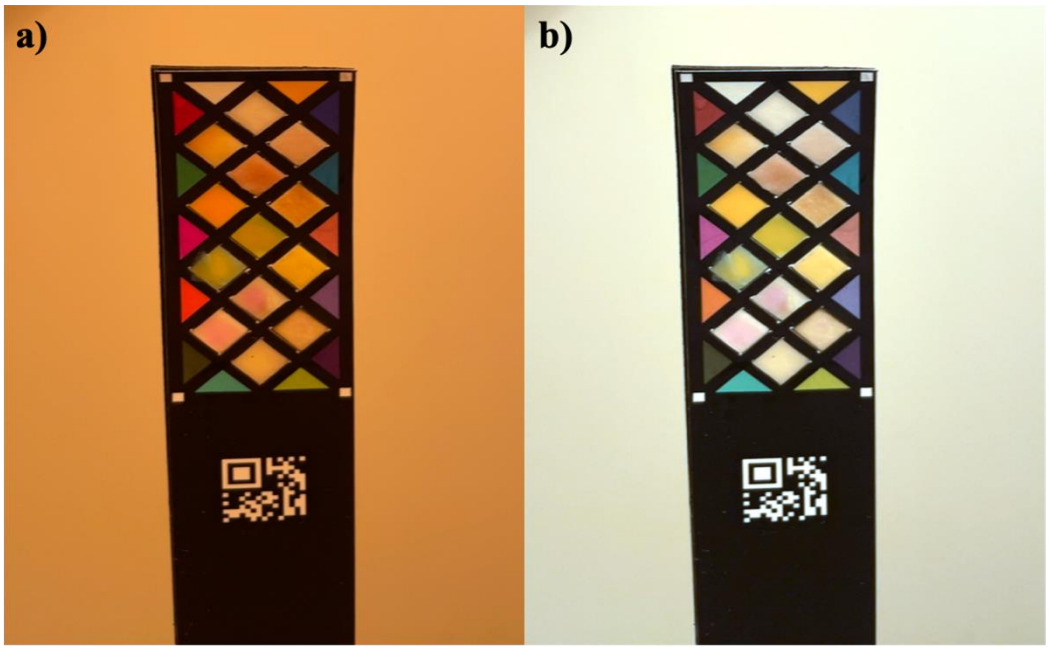

Fig 2 Color correction: (a) the detected Vivoo urine test strip, (b) the Vivoo urine test strip after color correction

Sensor value prediction

The Vivoo App contains an ML model for each sensor called sensor models. They predict the value of each sensor. We used Convolutional Neural Networks (CNNs) [46] as the architectural basis for these models. The models are trained with thousands of lab images, and these lab images are created using urine samples with values that are already established.

While training a sensor model, the CNN automatically learns the features that are crucial for differentiating images of each sensor value. The most important features are the color ranges, the extent of color change in the sensor image, the possible shapes created by sensor reaction to the urine sample, etc. These features are different for each sensor value.

Vivoo app validation

The experimental design covers the validation studies of Vivoo App produced by Vivosens Biotechnology R&D, Ind. And Trade Co. Ltd. This analytical validation study was conducted in the True Testing Services

between October and December 2022. To evaluate the accuracy of the Vivoo, this study employed the use of artificial urine samples. Potential factors that may affect the product's performance include ambient light during scanning, image resolution of the phone camera, and partial shading. To eliminate the effects of these factors, all tests were conducted using the same phone in the same environment, and under the same lighting conditions.

Preparation of urine solutions

This study used the following materials to prepare artificial urine solutions for testing: BIORAD Urinalysis Control 1 and 2, distilled water, Gündüz Kimya Buffer Solutions (pH: 10/pH: 7/pH: 4), sodium chloride salt, Sunlife Vitamin C Tablet, Aromel Kimya Calcium Chloride, MAGNORM tablet, Cayman Chemical Creatinine, and Supelco Malondialdehyde tetrabutylammonium (MDA) salt. We conducted chemical analyses of the BIORAD Urinalysis Control 1 and 2 obtained by the Roche Cobas U-411 Analyzer.

Vivoo was designed to with the purpose of examining the existence and/or quantification of the subsequent chemical constituents in urine: bilirubin, ketones, leukocytes, nitrites, protein, specific gravity, pH, creatinine, calcium, vitamin C, magnesium, sodium, and MDA. As such, we did not consider blood, glucose, and urobilinogen specified in the BIORAD Urinalysis Control solutions when preparing the artificial urine solutions. Additionally, since the BIORAD Urinalysis Control solutions did not account for creatinine, calcium, vitamin C, magnesium, sodium, and MDA, we prepared additional stock solutions using sodium chloride salt, Sunlife Vitamin C Tablet, Aromel Kimya Calcium Chloride, MAGNORM tablet, Supelco MDA, and Cayman Chemical Creatinine (Supplementary file 1).

Verification of urine solutions

We prepared 41 artificial urine solutions for this study, which were verified as follows: the Roche Cobas U-411 Urine Analyzer was used to verify the solutions for testing bilirubin, ketone, leukocyte, nitrite, protein, and specific gravity; the Ohaus ST 2100 F Benchtop pH Meter was used to verify the solutions for testing pH; the enzymatic photometric methodology with the Abbott/Architect C8000 was used to verify the solutions for testing creatinine, calcium, magnesium, and sodium; the Urine Analyzer BC401 (Contec Medical Systems Co., Ltd.) was used to verify the solutions for testing vitamin C; and the solutions for testing MDA were verified visually at the Vivosens Biotechnology laboratory. All solutions used for conducting tests were stored at 4°C.

Experimental procedure and statistical analysis

We performed the following procedure to test the Vivoo test strips. First, we downloaded the Vivoo App from the Apple Store and created a user account. We then applied artificial urine solutions onto the Vivoo test strips and waited for 90 seconds before scanning the test strip onto the Vivoo App via a smartphone (iPhone 13 IOS 15.6.1) (Fig 3). After scanning, we discarded the test strip. We repeated these steps to obtain experimental replicates. We then saved the results that we obtained in a datasheet (Ref. Attachment 11.14 Vivoo). Finally, we conducted a statistical analysis of the results of the Vivoo test strips by using IBM SPSS Statistics Version 26. We performed a two-sided confidence intervals analysis. The sample size for bilirubin, ketones, leukocytes, nitrites, proteins, calcium, creatinine, vitamin C, and MDA solutions was 200. The sample size for pH, specific gravity, magnesium, and sodium solutions were 207, 203, 204, and 204 respectively.

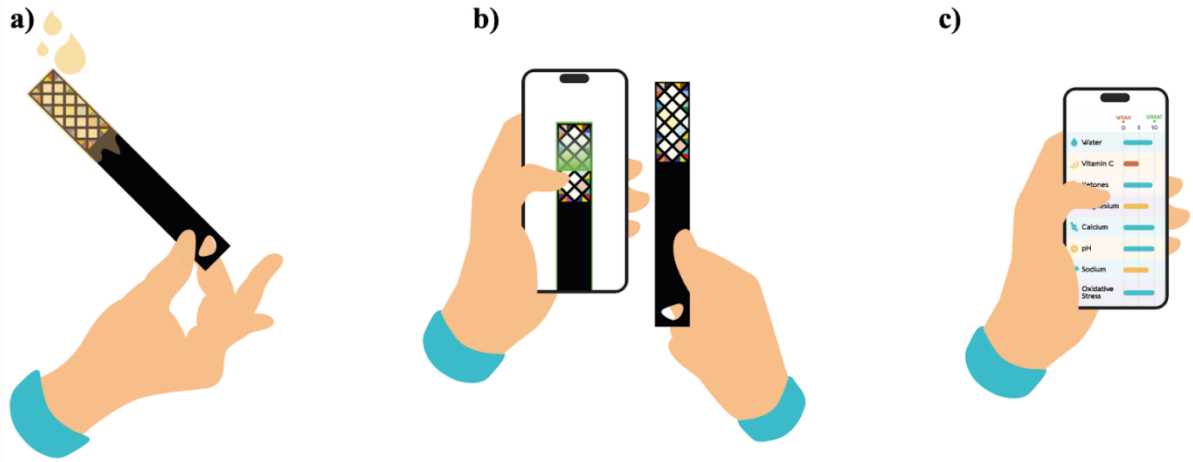

Fig 3 Illustration of the urine test strip analysis process using the smartphone-based reader Vivoo App. a) apply urine to the Vivoo test strip, b) capture the image of the test strip using the Vivoo, c) obtain the results for each artificial urine solution used for this study

Results

Chemical analysis of urinalysis solutions

The results from the chemical analysis conducted on BIORAD Urinalysis Control 1 show that the sample tested negative for bilirubin, blood, ketones, leukocytes, nitrite, and protein (total). The glucose level was within the normal range, and the pH was slightly acidic between 5 - 6.5. The specific gravity was also within the normal range of 1.005 - 1.020, and the urobilinogen level was normal.

In contrast, the BIORAD Urinalysis Control 2 created significantly different results. Bilirubin was present in the sample at a concentration of 3 - 6 mg/dL (50 -100 umol/L) (2+ - 3+), and blood was present at a concentration of 150 - 250 Ery/uL (4+ - 5+). The glucose level was high, ranging from 250 -1000 mg/dL (14 - 56 mmol/L) (3+-4+), and ketones were also present in the sample at a concentration of 50 - 150 mg/dL (5 - 15 mmoI/L) (3+ - 4+). The leukocyte concentration was elevated, ranging between 100 - 500 Leu/uL (2+ - 3+), and nitrite was present in the sample. The pH was alkaline within a range of 7 - 8, and protein (total) concentration was high, ranging between 100 - 500 mg/dL (1.0 - 5.0 g/L) (3+ - 4+). The specific gravity was within the normal range of 1.000 - 1.020, and urobilinogen was present at a concentration of 8 - 12 mg/dL (135 - 203 umol/L) (3+ - 4+) (Table 1).

Table 1 Chemical analysis of the BIORAD Urinalysis Control 1 and 2 measured by the Roche Coban U 411 Analyzer

Parameter	BIORAD Urinalysis Control 1	BIORAD Urinalysis Control 2
Bilirubin	Negative	3 - 6 mg/dL (50 -100 umol/L) (2+ - 3+)
Blood	Negative	150 - 250 Ery/uL (4+ - 5+)
Glucose	Normal	250 -1000 mg/dL (14 - 56 mmol/L) (3+-4+)
Ketones	Negative	50 - 150 mg/dL (5 - 15 mmoI/L) (3+ - 4+)
Leukocytes	Negative - 25	100 - 500 Leu/uL (2+ - 3+)
Nitrite	Negative	Positive
pH	5 - 6.5	7 - 8
Protein (total)	Negative	100 - 500 mg/dL (1.0 - 5.0 g/L) (3+ - 4+)
Specific gravity	1.005 - 1.020	1.000 - 1.020
Urobilinogen	Normal	8 - 12 mg/dL (135 - 203 umol/L) (3+ - 4+)

It is important to note that BIORAD Urinalysis Control 1 and 2 are quality control solutions used for monitoring the performance of urinalysis tests in medical laboratories. These solutions contain various substances that simulate the properties of human urine and can be used to assess the accuracy and precision of urinalysis tests. The results from our analysis indicate that BIORAD Urinalysis Control 1 and 2 had significantly different properties in its chemical composition. We have thus demonstrated that the artificial urine solutions used in this experiment are suitable for use in validating the accuracy of the Vivoo App.

Verification of artificial urine solutions

The results obtained from various verification methods for the artificial urine solutions prepared for testing different parameters were determined to be within the desired value ranges. The verification results of the artificial urine solutions prepared for testing provided in Supplementary file 2.

Descriptive statistics

Descriptive statistics on the test results into the accuracy of Vivoo for measuring each of the 13 chemical components found on the Vivoo test strip are provided as a tables in Supplementary file 3. The Vivoo App was used to analyze various components in artificial urine samples. The app analyzed the levels of bilirubin, ketones, leukocytes, nitrites, pH, specific gravity, protein, magnesium, sodium, calcium, creatinine, vitamin C, and MDA. The analysis was conducted using a total of 200 strips each for bilirubin, ketones, leukocytes, nitrites, protein, calcium, creatinine, vitamin C, and MDA. Additionally, pH, specific gravity, protein, magnesium, and sodium were analyzed using 207, 203, 204, 204, and 204 strips, respectively.

Vivoo categorized bilirubin measurements into four potential outcomes: 0 mg/dL, 1 mg/dL, 3 mg/dL, and 5 mg/dL. To assess Vivoo's bilirubin readings, we employed artificial urine solutions (specifically, solutions 1, 7, 2, and 5) corresponding to these measurements. Our findings revealed that when using solution 1, all tested strips achieved the anticipated bilirubin measurement, with a 100% accuracy rate. For Solution 2, accuracy stood at 98%, while solution 5 demonstrated 92% accuracy, and solution 7 yielded an 86% accuracy rate.

When applying the ±1 color block acceptance criterion, all bilirubin solutions displayed 100% agreement with the expected bilirubin measurement.

Vivoo categorized ketone measurements into five potential outcomes: 0 mg/dL, 5 mg/dL, 15 mg/dL, 50 mg/dL, and 150 mg/dL. To assess the accuracy of Vivoo's ketone readings, we utilized artificial urine solutions (specifically, solutions 1, 7, 3, 2, and 5) corresponding to these measurements. Our findings indicated that solution 1 yielded the expected ketone measurement in 100% of the tested strips, while solution 2 achieved a 97.5% accuracy rate. Solution 5 demonstrated an 80% accuracy rate, solution 3 showed 75% accuracy, and solution 7 resulted in a 70% accuracy rate. When applying the ±1 color block acceptance criterion, all ketone solutions exhibited 100% agreement with the expected ketone measurement.

Vivoo categorized leukocyte measurements into four potential outcomes: 0 Leu/uL, 25 Leu/uL, 100 Leu/uL, and 500 Leu/uL. To assess the accuracy of Vivoo's leukocyte readings, we employed artificial urine solutions (specifically, solutions 1, 2, 4, and 5) corresponding to these measurements. Our findings indicated that when using solution 1 and solution 5, all tested strips achieved the anticipated leukocyte measurement, resulting in a 100% accuracy rate. For solution 4, accuracy stood at 90%, while solution 2 exhibited a 64% accuracy rate. Applying the ±1 color block acceptance criterion, all leukocyte solutions exhibited a 100% agreement with the expected leukocyte measurement.

Vivoo categorized nitrite measurements into two potential outcomes: either positive or negative. To assess the accuracy of Vivoo's nitrite readings, we utilized artificial urine solutions (specifically, solutions 1 and 5) corresponding to these categories. Our findings revealed that all tested strips precisely identified the presence or absence of nitrites in the designated artificial urine solutions for nitrite testing.

Vivoo categorized pH measurements into nine possible outcomes: 5, 5.5, 6, 6.5, 7, 7.5, 8, 8.5, and 9. Artificial urine solutions (solutions 1, 9, 10, 3, 11, 12, 13, 14, and 15, respectively) with these measurements were used to test the accuracy of Vivoo readings of pH. Our results indicated that the Vivoo accurately measured their expected pH values. More specifically, solution 1 was measured accurately by 52.2% of the strips; solution 9 was measured accurately by 69.6% of the strips; solution 10 was measured accurately by 78.3% of the strips; solution 3 was measured accurately by 100% of the strips; solution 11 was measured accurately by 95.7% of the strips; solution 12 was measured accurately by 95.7% of the strips; solution 13 was measured accurately by 82.6% of the strips; solution 14 was measured accurately by 47.8% of the strips; and solution 15 was measured accurately by 95.7% of the strips. Furthermore, when applying the ±1 color block acceptance criterion, it was evident that, except for solutions 1 and 11, all solutions exhibited a complete agreement, reaching 100%, with their anticipated pH values.

Vivoo categorized specific gravity measurements into seven possible outcomes: 1.000, 1.005, 1.010, 1.015, 1.020, 1.025, and 10.30. Artificial urine solutions (solutions 1, 2, 16, 8, 17, 18, and 19, respectively) with these measurements were used to test the accuracy of Vivoo readings of specific gravity. Our results demonstrated that the Vivoo accurately measured their expected specific gravity values. More specifically, solution 1 was measured accurately by 100% of the strips; solution 2 was measured accurately by 75.9% of the strips; solution 16 was measured accurately by 96.6% of the strips; solution 8 was measured accurately by 100% of the strips; solution 17 was measured accurately by 93.1% of the strips; solution 18 was measured accurately by 65.5% of the strips; and solution 19 was measured accurately by 86.2% of the strips. Moreover, when applying the ±1 color block acceptance criterion, it was evident that all solutions exhibited a complete agreement, reaching 100%, with their anticipated specific gravity values.

Vivoo categorized protein measurements into five potential outcomes: 0 mg/dL, 25 mg/dL, 75 mg/dL, 150 mg/dL, and 500 mg/dL. To evaluate the accuracy of Vivoo's protein readings, we employed artificial urine solutions (specifically, solutions 1, 7, 2, 6, and 5) corresponding to these measurements. The strips precisely measured their anticipated protein values, with solution 5 achieving 100% accuracy, and solutions 1, 2, 6, and 7 reaching 97.5%, 77.5%, 95%, and 80% accuracy, respectively. When applying the ±1 color block acceptance criterion, all protein solutions exhibited 100% agreement with their expected protein measurements.

Vivoo categorized magnesium measurements into four potential outcomes: 0.5 mg/dL, 3.6 mg/dL, 6-7.2 mg/dL, and 10.8-14.4 mg/dL. To assess the precision of Vivoo's magnesium readings, we employed artificial urine solutions (specifically, solutions 1, 34, 35, 36, 37, and 38) corresponding to these measurements. The Vivoo accurately measured their expected magnesium measurements, with solution 35 showing 100% accuracy, and solutions 1, 34, 36, 37, and 38 showing 61.8%, 61.8%, 73.5%, 79.4%, and 88.2% accuracy, respectively. When applying ±1 color block acceptance condition, solutions 35, 36, 37, and 38 showed 100% agreement with their expected magnesium measurements, and solutions 1 and 34 showed 97.1% agreement.

Vivoo categorized sodium measurements into four possible results: 0 mg/dL, 100 mg/dL, 200-400 mg/dL, and 500 mg/dL. We employed artificial urine solutions (specifically, solutions 1, 39, 10, 8, 6, and 16) corresponding to these measurements to assess the precision of Vivoo's sodium readings. The results showed

that the strips tested using solution 1 had a 100% accuracy rate. Strips tested using solution 39 had a 91.2% accuracy rate, strips tested using solution 10 had a 64.7% accuracy rate, strips tested using solution 8 had a 97.1% accuracy rate, strips tested using solution 6 had a 94.1% accuracy rate, and strips tested using solution 16 had a 79.4% accuracy rate. When applying the ±1 color block acceptance criterion all strips tested using solutions 1, 39, 10, 8, 6, and 16 exhibited 100% agreement with their expected sodium measurements.

Vivoo categorized calcium measurements into five potential outcomes: 4 mg/dL, 10 mg/dL, 20 mg/dL, 30 mg/dL, and 40 mg/dL. To assess the precision of Vivoo's calcium readings, we utilized artificial urine solutions (specifically, solutions 1, 25, 26, 27, 28, and 29) corresponding to these measurements. The outcomes revealed that strips tested with solutions 1 and 25 achieved a perfect accuracy rate of 100%. Strips tested with solution 26 displayed a 72.5% accuracy rate, while those with solution 27 had a 77.5% accuracy rate. Strips tested using solution 28 showed a 90% accuracy rate, and those tested with solution 29 reached a 67.5% accuracy rate. When applying the ±1 color block acceptance criterion, all calcium solutions exhibited 100% agreement with their anticipated calcium measurements.

Vivoo categorized creatinine measurements into five potential outcomes: 10 mg/dL, 50 mg/dL, 100 mg/dL, 200 mg/dL, and 300 mg/dL. We utilized artificial urine solutions (specifically, solutions 20, 21, 22, 23, and 24) corresponding to these measurements to evaluate the precision of Vivoo's creatinine readings. The outcomes indicated that 60% of strips measuring solution 20, 60% of strips assessing solution 21, 87.5% of strips analyzing solution 22, 85% of strips examining solution 23, and 80% of strips testing solution 24 accurately measured their expected creatinine levels. When applying the ±1 color block acceptance criterion, all creatinine solutions demonstrated 100% agreement with their anticipated creatinine measurements, underscoring the accuracy of Vivoo's creatinine readings, particularly when employing the ±1 color block acceptance criterion.

Vivoo categorized vitamin C measurements into five potential outcomes: 0 mmol/L, 0.6 mmol/L, 1.4 mmol/L, 2.8 mmol/L, and 5 mmol/L. We utilized artificial urine solutions (specifically, solutions 1, 30, 31, 32, and 33) corresponding to these measurements to assess the precision of Vivoo's vitamin C readings. The outcomes indicated that the Vivoo accurately measured their expected vitamin C levels for 97.5% of strips tested with solution 1, 87.5% of strips tested with solution 30, 82.5% of strips tested with solution 31, 97.5% of strips tested with solution 32, and 100% of strips tested with solution 33. Moreover, when applying the ±1 color block acceptance criterion, all vitamin C solutions exhibited a 100% agreement with their anticipated vitamin C measurements, highlighting the high accuracy of Vivoo's vitamin C readings, particularly when employing the ±1 color block acceptance criterion.

Vivoo categorized MDA measurements into two potential outcomes: either positive or negative. We utilized artificial urine solutions (specifically, solutions 1 and 40 without MDA, and 41 with MDA) corresponding to these categories to assess the precision of Vivoo's MDA readings. The outcomes revealed that all strips precisely detected the absence of MDA for solutions 1 and 40, while 99.5% of Vivoo accurately identified the presence of MDA for solution 41. Moreover, when applying the +1 color block acceptance criterion, all MDA solutions demonstrated 100% agreement with their expected results, emphasizing the high accuracy of Vivoo's MDA readings, especially when employing the +1 color block acceptance criterion.

Confidence intervals

The analysis evaluated 2618 strip measurements, of which 2292 measurements were consistent with their expected values. With the ±1 color block acceptance criterion, 2608 strip measurements met their expected values.

When applying the ±1 color block acceptance criterion, all values aligned with their anticipated measurement outcomes, with a 95% confidence interval for the exact match agreement proportion of Vivoo at 94% ± 3.29% for bilirubin, 81.5% ± 5.38% for calcium, 84.5% ± 5.02% for ketones, 74.5% ± 6.04% for creatinine, 88.5% ± 4.42% for leukocytes, 99.5% ± 0.98% for MDA, 90% ± 4.16% for protein, 87.75% ±4.51% for sodium, and 88.18% ± 4.44% for specific gravity. In the case of magnesium, when we employed the ±1 color block acceptance criterion, the 95% confidence interval for Vivoo's exact match agreement proportion is 77.45% ± 5.74%, and the agreement proportion falls within a 95% confidence interval of 97.06% ± 2.31%. As for pH, with the same ±1 color block acceptance criterion, Vivoo's exact match agreement proportion has a 95% confidence interval of 79.71% ± 5.48%, while the agreement proportion is within a 95% confidence interval of 98.07% ± 1.88%.

Out of the total number of tested strips (2618), 2292 exhibited an exact match with their expected measurement results. Furthermore, when we applied the ±1 color block acceptance criterion, 2608 out of 2618 measurements conformed entirely to the expected results. We conducted a 95% confidence interval calculation for Vivoo's exact match agreement proportion, resulting in 87.55% ± 1.27%. Upon the application of the ±1 color block acceptance criterion, Vivoo's exact match agreement proportion's 95% confidence interval was 99.62% ±

0.24%. When we individually assessed each of Vivoo's 13 components, the 95% confidence interval for the exact match agreement proportion varied between 74.50% and 99.50%, depending on the specific component. Following the application of the ±1 color block acceptance criterion, 11 out of 13 components on Vivoo displayed results that perfectly aligned with the expected measurement values.

We observed a lack of exact match percentages for 2 out of the 13 components on Vivoo, namely magnesium and pH. However, in terms of Vivoo's presentation of its results to users, magnesium exhibited an exact match percentage of 77.45%. While this component didn't achieve a 100% match, the exact match percentage remains relatively high. When considering the confidence intervals for these components under the ±1 color block acceptance criterion, magnesium, and pH yielded values of 97.06% and 98.07%, respectively (Table 2).

Table 2 Confidence intervals results of Vivoo

Chemical Component	frequency	n	proportion	95% Confidence Interval Lower Bound	95% Confidence Interval Upper Bound	Standard Error of the Estimate	±
Total	2292[a]	2618	87.55 %	86.28 %	88.81 %	0.65 %	1.27 %
	2608[b]	2618	99.62 %	99.38 %	99.85 %	0.12 %	0.24 %
Bilirubin	188[a]	200	94.00 %	90.71 %	97.29 %	1.68 %	3.29 %
Ketone	169[a]	200	84.50 %	79.48 %	89.52 %	2.56 %	5.02 %
Leukocyte	177[a]	200	88.50 %	84.08 %	92.92 %	2.26 %	4.42 %
pH	165[a]	207	79.71 %	74.23 %	85.19 %	2.80 %	5.48 %
	203[b]	207	98.07 %	96.19 %	99.94 %	0.96 %	1.88 %
Specific gravity	179[a]	203	88.18 %	83.74 %	92.62 %	2.27 %	4.44 %
Protein	180[a]	200	90.00 %	85.84 %	94.16 %	2.12 %	4.16 %
Magnesium	158[a]	204	77.45 %	71.72 %	83.19 %	2.03 %	5.74 %
	198[b]	204	97.06 %	94.74 %	99.38 %	1.18 %	2.31 %
Sodium	179[a]	204	87.75 %	83.25 %	92.24 %	2.30v	4.51 %
Calcium	163[a]	200	81.50 %	76.12 %	86.88 %	2.75 %	5.38 %
Creatinine	149[a]	200	74.50 %	68.46 %	80.54 %	3.08 %	6.04 %
Vitamin C	186[a]	200	93.00 %	89.46 %	96.54 %	1.80 %	3.54 %
MDA	199[a]	200	99.50 %	98.52 %	100.00 %	0.50 %	0.98 %

a: True/False (Exact Match), **b:** True/False (± 1 Color Block)

The experiment conducted aimed to validate the accuracy of Vivoo urine analysis for measuring 13 different chemical components found on the Vivoo test strip. The study used artificial urine solutions to test the accuracy of the Vivoo readings for bilirubin, ketones, leukocytes, nitrites, pH, specific gravity, protein, magnesium, sodium, calcium, creatinine, vitamin C, and MDA. Overall, the results show that the Vivoo provided accurate measurements for all chemical components tested.

The results of this study suggest that the Vivoo urine analysis is an accurate method for measuring various chemical components in urine. These findings are in line with previous studies that have demonstrated the reliability of urine analysis as a diagnostic tool [32]. In addition, the use of artificial urine solutions allowed

for controlled testing conditions, ensuring that the results were not influenced by other factors. Ho wever, it should be highlighted that this study successfully demonstrated the accuracy of the Vivoo in measuring chemical components in artificial urine solutions, indicating its potential effectiveness for testing real human urine samples.

Discussion

In the realm of medical diagnostics, the integration of smartphone technology with urinalysis presents a transformative approach, revolutionizing how urine analysis is conducted and interpreted. This integration leverages the ubiquity and advanced capabilities of smartphones to offer a convenient, rapid, and user-friendly means of conducting urine tests. By utilizing smartphone cameras and specialized apps, individuals can perform self-testing, where the smartphone interprets the results from urine test strips [47]. Furthermore, the advent of smartphone and AI-based technologies has revolutionized the landscape POC diagnostics of urine analysis. This innovative approach combines the accessibility of smartphones with the advanced analytical capabilities of AI, paving the way for rapid, accurate, and user-friendly urine testing methods [17]. Our study presents a comprehensive analysis of the accuracy of Vivoo App which is a AI integrated urine analysis app, which are designed to measure various chemical components in urine. The methodology involved using 2618 strips with artificial urine solutions to measure 13 different chemical components by Vivoo App, including bilirubin, ketones, leukocytes, nitrites, pH, specific gravity, protein, magnesium, sodium, calcium, creatinine, vitamin C, and MDA.

The chemical analysis of BIORAD Urinalysis Control 1 and 2 provides insightful data for understanding the efficacy and reliability of urinalysis testing, particularly in relation to the Vivoo App, a health monitoring tool. Control 1's results are indicative of a normal urinary profile.

In contrast, Control 2's results simulate a pathological urinary state. The presence of bilirubin and blood at significant levels suggests hepatic pathology or hematuria, potentially indicative of liver dysfunction or urinary tract damage [48]. Elevated glucose and ketones are hallmarks of uncontrolled diabetes mellitus [49]. The elevated leukocyte count and the presence of nitrite are suggestive of a urinary tract infection. The alkaline pH (7 - 8) can be associated with certain renal tubular acidosis or urinary tract infections [50]. High protein concentration points towards possible kidney damage or disease [51]. The presence of urobilinogen at elevated levels could indicate liver disease or hemolytic conditions [52].

The contrast between Control 1 and Control 2 is crucial for validating the Vivoo App. It demonstrates the app's ability to differentiate between normal and pathological conditions, a key feature for a reliable urinalysis tool. This differentiation is essential for users relying on the app for health monitoring, as it can guide them in seeking professional medical advice when abnormal results are detected. Tchemical analysis of BIORAD Urinalysis Control 1 and 2 highlights their suitability as quality control solutions for urinalysis tests. Their distinct chemical compositions, simulating both normal and pathological conditions, provide a robust platform for validating the accuracy and precision of the Vivoo App. This analysis underscores the importance of comprehensive quality control in the development and maintenance of digital health monitoring tools.

The comprehensive analysis of the Vivoo App's performance in measuring various chemical components in artificial urine solutions presents a robust picture of its accuracy and reliability. The study meticulously evaluated the App's ability to quantify 13 distinct chemicals, including bilirubin, ketones, leukocytes, nitrites, pH, specific gravity, protein, magnesium, sodium, calcium, creatinine, vitamin C, and MDA. The initial verification of the artificial urine solutions, as outlined in Supplementary file 2, confirmed that the preparations were within the desired value ranges. This step was critical to ensuring the validity of subsequent tests and analyses.

The accuracy assessment of bilirubin, ketones, leukocytes, nitrites, pH, specific gravity, protein, magnesium, sodium, calcium, creatinine, vitamin C and MDA are demonstrated high accuracy, The findings from this study underscore the reliability and accuracy of the Vivoo App in measuring a range of chemical components in artificial urine. The use of the ±1 color block acceptance criterion significantly enhanced the agreement rates, highlighting the importance of considering minor variations in color readings. The study's methodology, involving a large number of strips for each test, lends credibility to the results.

A significant portion of the analysis focuses on the assessment of exact match agreement proportions, both with and without the ±1 color block acceptance criterion. Our results show that a high percentage of measurements were consistent with their expected values. Notably, with the ±1 color block acceptance criterion, the vast majority of strip measurements aligned with anticipated outcomes, as evidenced by the 95% confidence intervals calculated for each component. These confidence intervals provide a quantitative measure of the accuracy of Vivoo App’s readings, indicating a high level of precision across most of the tested components.

The overall exact match agreement proportion of Vivoo, considering all 13 components, falls within a 95% confidence interval of 87.55% ± 1.27%. However, this proportion dramatically increases to 99.62% ± 0.24% when the ±1 color block

acceptance criterion is applied. This criterion's application seems to significantly enhance the match agreement, demonstrating the potential flexibility and reliability of Vivoo App in different analytical settings.

In conclusion, our study robustly demonstrates the accuracy of Vivoo App in measuring a range of chemical components. The high exact match percentages and narrow confidence intervals indicate the reliability of Vivoo App. Our study aligns with previous research underscoring the reliability of urine analysis apps as a diagnostic tool, adding to the growing body of evidence supporting the use of such non-invasive testing methods with potential applications in medical diagnostics, research, and personal health monitoring.

Conclusion

Smartphone-based POC urinalysis is a rapidly evolving field that has the potential to revolutionize health monitoring and disease prevention. With the widespread availability of smartphones and their ability to integrate various sensors and devices, it is now possible to perform a range of medical tests using just a smartphone and a urine sample. One of the most promising applications of smartphone-based POC is the detection of various biomarkers in urine, which can provide valuable insight into a person's health status and risk of developing certain diseases.

Despite the promising results of smartphone-based POC urine analysis, there are still some limitations that must be addressed before this technology can be widely adopted. One of the main challenges is the lack of standardization in urine analysis methods and the potential for user error. The accuracy of urine analysis can be affected by factors such as the timing of the sample collection, the sample volume, and the user's technique in using the smartphone app. Therefore, it is essential to develop standardized protocols and guidelines for smartphone-based POC urine analysis to ensure consistency and accuracy across different users and devices.

Another limitation of smartphone-based POC urine analysis is the need for further validation and testing to ensure the accuracy and reliability of the results. While the Vivoo App has shown promising results in smartphone-based POC urinalysis, there is a need to develop more sophisticated urine analysis technology that can measure a wider range of biomarkers with higher accuracy and sensitivity.

Looking to the future, there are many exciting possibilities for the development of smartphone-based POC urine analysis. One such possibility is the integration of AI and machine learning algorithms for improving the accuracy and reliability of urine analysis results. AI can aid in identifying patterns and correlations in urine analysis data that may not be visible to the human eye, which can in turn enable more precise and personalized health recommendations. Another direction for future research is the development of new sensors and devices that can measure a wider range of biomarkers in urine. In conclusion, smartphone-based POC urine analysis has the potential to transform the way we monitor our health and prevent diseases. The validation of the Vivoo Application is thus a significant step forward in this field, but there are still many challenges and opportunities that need to be addressed. By collaborating with healthcare providers, technology companies, and regulatory bodies, we can ensure that smartphone-based POC urine analysis is safe, effective, and accessible to all. With continued research and innovation, we can unlock the full potential of this technology to improve our health and well-being.

Abbreviations

POC: Point-of-care; POCT: Point-of-care testing; AI: Artificial Intelligence; ML: Machine Learning; CNN: Convolutional Neural Networks; MDA: Malondialdehyde tetrabutylammonium.

Acknowledgements

We would like to express our sincere gratitude to C. Balkı Germinter for her invaluable guidance and support throughout the process of preparing this manuscript. Also, we would like to express our sincere gratitude to Senay Tayfun and Ece Unal for their exceptional contributions in designing the figures presented in this manuscript.

Funding

This study received no external funding but the all analysis was carried out by Vivosens Biotechnology.

Data availability statement

Please contact the corresponding author for any data request. The authors declare that the data supporting the findings of this study are available within the paper and its Supplementary files.

Compliance with ethical standards

Conflict of interest

The authors declare no conflicts of interest.

Ethical standards
The study is proper with ethical standards.

Authors' contributions
BBKC and GC designed the experiments. GC performed the experiments. Writing—original draft preparation HÇ, GC, and AN; review and editing by HÇ, AA, MT, and BBKC. All authors contributed to the final version of the manuscript. All authors contributed equally to the study.

References

1. Liu, D., et al., Trends in miniaturized biosensors for point-of-care testing. TrAC Trends in Analytical Chemistry, 2020. 122, 115701. https://doi.org/10.1016/j.trac.2019.115701.
2. Hou, Y., et al., Recent advances and applications in paper-based devices for point-of-care testing. Journal of Analysis and Testing, 2022. 6(3), 247-273. https://doi.org/10.1007/s41664-021-00204-w.
3. Trenti, T., Synergy between point-of-care testing and laboratory consolidations. The electronic Journal of the International Federation of Clinical Chemistry and Laboratory Medicine, 2021. 32(3):328.
4. Lei, R., Huo, R., Mohan, C., Current and emerging trends in point-of-care urinalysis tests. Expert review of molecular diagnostics, 2020. 20(1):69-84. https://doi.org/10.1080/14737159.2020.1699063.
5. Mahoney, E., et al., Point-of-care urinalysis with emerging sensing and imaging technologies. Journal of The Electrochemical Society, 2019. 167(3), 037518. https://doi.org/10.1149/2.0182003JES.
6. Echeverry, G., Hortin, G.L., Rai, A.J., Introduction to urinalysis: historical perspectives and clinical application. Methods Molecular Biology, 2010. 641:1-12. https://doi.org/10.1007/978-1-60761-711-2_1.
7. Boon, H. A., et al., Point-of-care tests for pediatric urinary tract infections in general practice: a diagnostic accuracy study. Family Practice, 2022. 39(4), 616-622. https://doi.org/10.1093/fampra/cmab118.
8. Zhang, Z., et al., Urine analysis has a very broad prospect in the future. Frontiers in Analytical Science, 2022. 1, 812301. https://doi.org/10.3389/frans.2021.812301.
9. Kavuru, V., et al., Dipstick analysis of urine chemistry: benefits and limitations of dry chemistry-based assays. Postgraduate Medicine, 2020. 132(3), 225-233. https://doi.org/10.1080/00325481.2019.1679540.
10. Rysz, J., et al., Novel biomarkers in the diagnosis of chronic kidney disease and the prediction of its outcome. International journal of molecular sciences, 2017. 18(8), 1702. https://doi.org/10.3390/ijms18081702.
11. Kutter, D., The urine test strip of the future. Clinica chimica acta, 2000. 297(1-2):297-304. https://doi.org/10.1016/s0009-8981(00)00255-2.
12. Lepowsky, E., et al., Paper-based assays for urine analysis. Biomicrofluidics, 2017. 11(5):051501. https://doi.org/10.1063%2F1.4996768.
13. Rink, S., & Baeumner, A.J., Progression of paper-based point-of-care testing toward being an indispensable diagnostic tool in future healthcare. Analytical Chemistry, 2023, 95(3), 1785-1793. https://doi.org/10.1021/acs.analchem.2c04442.
14. Ventola, C.L., Mobile devices and apps for health care professionals: uses and benefits. Pharmacy and Therapeutics, 2014. 39(5):356.
15. Baxter, C., et al., Assessment of mobile health apps using built-in smartphone sensors for diagnosis and treatment: systematic survey of apps listed in international curated health app libraries. JMIR mHealth and uHealth. 2020;8(2):e16741. https://doi.org/10.2196/16741.
16. Yeasmin, S., et al., Current trends and challenges in point-of-care urinalysis of biomarkers in trace amounts. TrAC Trends in Analytical Chemistry, 2022. 157, 116786. https://doi.org/10.1016/j.trac.2022.116786.
17. De Bruyne, S., De Kesel, P., & Oyaert, M., Applications of Artificial Intelligence in Urinalysis: Is the Future Already Here?. Clinical Chemistry, 2023. 69(12), 1348-1360. https://doi.org/10.1093/clinchem/hvad136.
18. Karlsen, H., Dong, T., Smartphone-based rapid screening of urinary biomarkers. IEEE transactions on biomedical circuits and systems, 2017. 11(2):455-463. https://doi.org/10.1109/TBCAS.2016.2633508.
19. Ra, M., et al., Smartphone-based point-of-care urinalysis under variable illumination. IEEE journal of translational engineering in health and medicine, 2017. 6:1-11. https://doi.org/10.1109/JTEHM.2017.2765631.
20. Zhang, S., Tis, T.B., & Wei, Q., Smartphone-based clinical diagnostics. In Precision Medicine for Investigators, Practitioners and Providers, 2020. (pp. 493-508). Academic Press. https://doi.org/10.1016/B978-0-12-819178-1.00048-4.
21. Shi, Z., et al., Smartphone-based portable photoelectrochemical biosensing system for point-of-care detection of urine creatinine and Albümin. Lab on a Chip, 2023. 23(15), 3424-3432. https://doi.org/10.1039/D3LC00238A.
22. Shrivastava, S., Trung, T.Q., & Lee, N.E., Recent progress, challenges, and prospects of fully integrated mobile and wearable point-of-care testing systems for self-testing. Chemical Society Reviews, 2020. 49(6), 1812-1866. https://doi.org/10.1039/C9CS00319C.
23. Yang, M., et al., SARS-CoV-2 point-of-care (POC) diagnosis based on commercial pregnancy test strips and a palm-size microfluidic device. Analytical Chemistry, 2021. 93(35), 11956-11964. https://doi.org/10.1021/acs.analchem.1c01829.
24. Kibria, I. E., Ali, H., & Khan, S. A., Smartphone-based point-of-care urinalysis assessment. In 2022 44th Annual International Conference of the IEEE Engineering in Medicine & Biology Society (EMBC), 2022. (pp. 3374-3377). IEEE. https://doi.org/10.1109/embc48229.2022.9870917.
25. Oyaert, M., and Delanghe, J., Progress in automated urinalysis. Annals of laboratory medicine, 2019. 39(1):15-22. https://doi.org/10.3343/alm.2019.39.1.15.

26. Zayed, B. A., Ali, A. N., Elgebaly, A. A., Talaia, N. M., Hamed, M., & Mansour, F. R. (2023). Smartphone-based point-of-care testing of the SARS-CoV-2: A systematic review. Scientific African, e01757. https://doi.org/10.1016/j.sciaf.2023.e01757.
27. Christodouleas, D.C., Kaur, B., and Chorti, P., From point-of-care testing to eHealth diagnostic devices (eDiagnostics). ACS Central Science, 2018. 4(12), 1600-1616. https://doi.org/10.1021/acscentsci.8b00625.
28. Gove, R.J., Complementary metal-oxide-semiconductor (CMOS) image sensors for mobile devices, High performance silicon imaging, Daniel Durini, 2014, Woodhead Publishing. p. 191-234. https://doi.org/10.1533/9780857097521.2.191.
29. Kandasamy, K., et al., Complementary metal-oxide-semiconductor (CMOS) image sensor: an insight as a point-of-care label-free immunosensor. Analytical Sciences, 2010. 26(12):1215-1217. https://doi.org/10.2116/analsci.26.1215.
30. Gani, M.O., et al., A light weight smartphone based human activity recognition system with high accuracy. Journal of Network and Computer Applications, 2019. 141:59-72. https://doi.org/10.1016/j.jnca.2019.05.001.
31. Susanto, A.P., et al., Building an artificial intelligence-powered medical image recognition smartphone application: What medical practitioners need to know. Informatics in Medicine Unlocked, 2022. 101017. https://doi.org/10.1016/j.imu.2022.101017.
32. White, P., Baumann, O., and De Stefano, A., On improving the noise reduction algorithms using image segmentation. In: 2004 12th European Signal Processing Conference. IEEE, 2004. p. 501-504.
33. Shi, W., et al., Change detection based on artificial intelligence: State-of-the-art and challenges. Remote Sensing, 2020. 12(10):1688. http://dx.doi.org/10.3390/rs12101688.
34. Kumar, Y., et al., Artificial intelligence in disease diagnosis: a systematic literature review, synthesizing framework and future research agenda. Journal of Ambient Intelligence and Humanized Computing, 2022. 1-28. https://doi.org/10.1007/s12652-021-03612-z.
35. Undru, T.R., et al., Integrating Artificial Intelligence for Clinical and Laboratory Diagnosis–a Review. Maedica, 2022. 17(2):420. https://doi.org/10.26574/maedica.2022.17.2.420.
36. Wang, H.Y., et al., Increase Trichomonas vaginalis detection based on urine routine analysis through a machine learning approach. Scientific reports, 2019. 9(1):11074. https://doi.org/10.1038/s41598-019-47361-8.
37. Xie, Q., et al., Deep learning for image analysis: Personalizing medicine closer to the point of care. Critical Reviews in Clinical Laboratory Sciences, 2019. 56(1):61-73. https://doi.org/10.1080/10408363.2018.1536111.
38. Downing, H., et al., The diagnosis of urinary tract infections in young children (DUTY): protocol for a diagnostic and prospective observational study to derive and validate a clinical algorithm for the diagnosis of UTI in children presenting to primary care with an acute illness. BMC infectious diseases, 2012. 12(1):1-15. https://doi.org/10.1186/1471-2334-12-158.
39. St-Louis, P., Status of point-of-care testing: promise, realities, and possibilities. Clinical biochemistry, 2000. 33(6):427-440. https://doi.org/10.1016/s0009-9120(00)00138-7.
40. Suarez-Ibarrola, R., et al., Current and future applications of machine and deep learning in urology: a review of the literature on urolithiasis, renal cell carcinoma, and bladder and prostate cancer. World journal of urology, 2020. 38:2329-2347. https://doi.org/10.1007/s00345-019-03000-5.
41. Davenport, M., et al., New and developing diagnostic technologies for urinary tract infections. Nature Reviews Urology, 2017. 14(5):296-310. https://doi.org/10.1038/nrurol.2017.20.
42. Faidah, N., et al., Detection of voluntary dehydration in paediatric populations using non-invasive point-of-care saliva and urine testing. Journal of Paediatrics and Child Health, 2021. 57(6):813-818. https://doi.org/10.1111/jpc.15325.
43. Park, S.M., et al., A mountable toilet system for personalized health monitoring via the analysis of excreta. Nature biomedical engineering, 2020. 4(6):624-635. https://doi.org/10.1038/s41551-020-0534-9.
44. Tayfun, M., Noroozi, A., Atasever, A., Karacaoglu, B.B., Radman, G., Buyukacaroglu, G., U.S. Patent Application No. 17/821,936.
45. Finlayson, G.D., Mackiewicz, M., and Hurlbert, A., Color correction using root-polynomial regression. IEEE Transactions on Image Processing, 2015. 24(5):1460-1470. https://doi.org/10.1109/TIP.2015.2405336.
46. Gu, J., et al., Recent advances in convolutional neural networks. Pattern recognition, 2018. 77:354-377. https://doi.org/10.1016/j.patcog.2017.10.013.
47. Flaucher, M., et al., Smartphone-based colorimetric analysis of urine test strips for at-home prenatal care. IEEE Journal of Translational Engineering in Health and Medicine, 2022. 10, 1-9. https://doi.org/10.1109/JTEHM.2022.3179147.
48. Parker, J. L., et al., Reliability of urinalysis for identification of proteinuria is reduced in the presence of other abnormalities including high specific gravity and hematuria. In Urologic Oncology: Seminars and Original Investigations 2020. (Vol. 38, No. 11, pp. 853-e9). Elsevier. https://doi.org/10.1016/j.urolonc.2020.06.035.
49. Saasa, V., et al., Blood ketone bodies and breath acetone analysis and their correlations in type 2 diabetes mellitus. Diagnostics, 2019. 9(4), 224. https://doi.org/10.3390%2Fdiagnostics9040224
50. Suresh, J., et al., Diagnostic accuracy of point-of-care nitrite and leukocyte esterase dipstick test for the screening of pediatric urinary tract infections. Saudi Journal of Kidney Diseases and Transplantation, 2021. 32(3), 703-710. https://doi.org/10.4103/1319-2442.336765.
51. Kamińska, J., et al., Diagnostic utility of protein to creatinine ratio (P/C ratio) in spot urine sample within routine clinical practice. Critical reviews in clinical laboratory sciences, 2020. 57(5), 345-364. https://doi.org/10.1080/10408363.2020.1723487.
52. Guerra Ruiz, A.R., et al., Measurement and clinical usefulness of bilirubin in liver disease. Advances in Laboratory Medicine/Avances en Medicina de Laboratorio, 2021. 2(3), 352-361. https://doi.org/10.1515/almed-2021-0047.

Bir sonraki sayıda görüşmek ümidiyle..
Hope to see you in the next issue..

Author Guidelines

General Principles

1. The article should be submitted by the responsible author responsible as Microsoft Word (Doc, Docx).

2. The responsible author is responsible for monitoring all the processes of the article.

3. The main section headings should be bold and the first letter in capital letters, the first letter of the first word in the 2nd-degree headings should be large. If a third-degree title is required, the title should be in italics and only the first letter of the first word should be capitalized. If possible, articles with fourth-degree titles should not be used in our journal.

4. The main headings and sub-headings should not be numbered.

5. Turkish and English titles of the articles should be short, descriptive, and not more than fourteen words (except prepositions).

6. In the Pre-Control and Evaluation processes, the authors must submit the proposed corrections within 30 days at the latest. Otherwise, the article will be rejected.

7. Please click here to see the article written according to tothe rules of our journal.

Note: The general similarity rate should not exceed 20% except the bibliography part of the submitted articles. It is necessary to inform the journal editor if the rate specified in the necessary cases is exceeded. All articles submitted to the journal are screened with ithenticate plagiarism program.

8. Except for the Turkish and English titles of the work, all remaining parts should be written on the right side.

9. The text should be written on an A4-size page, in 12-font size Times New Roman, and double-spaced.

10. There should be 3 cm margin on the left, right, and top of the page.

11 Text should be written in a single column, all pages should be given a page number.
There is no page limit in publishing an article in our journal.

Names Section

A double-blind peer reviewer system is applied in our journal. Therefore, the names and addresses of authors should not be given in the main text when loading the Manuscript to the system. Author names and contact information should be written on a separate cover page. The cover page is available in the article submission section of our journal.

Abstract

The article can be written in Turkish and English. English and Turkish abstracts should be written at the beginning of the Turkish manuscripts.
The abstract should contain brief and clear information about the purpose, method , and results of the article. 10 font size, single line spacing and maximum 300 words should be written. No reference should be made to the "Abstract".
Keywords: Keywords should be 10 font sizes, minimum 3, and maximum of 5 words. Keywords must be separated with a comma (,) sign and should be in lowercase.

Introduction

The sections of the main part of the study should be written in 14 font sizes; Bold and the first letter should be capitalized; Article should have Introduction, Methods, Results, Discussion, and Conclusion sections. The second level titles should be written in the left, in 12 font sizes, the first letter of the first word should be capitalized, bold, and numbered. A line in the previous paragraph must be separated by a space.

Figures and Tables

In the Turkish article for Figures and Tables;" Şekil", "Tablo"; whereas in The English article "Fig", "Table" should be used (Table 1, Fig 1).

Figure and Table words should be written in bold, and at the end of the description of figures and tables should not have a dot (.)

Figures, graphics, photographs and the like should be written under Figures and written with 11 fonts. Figure and Table should be given in the main document in the relevant places, should not be uploaded as separate files or should not be added to the end of the text.

Examples;

Table 1 Possible effects of genetically modified organisms

Table 2 Methods of tissue culture in tomato plants

Fig. 1 Amount of GMO products in the world

Fig. 2 Countries with the highest number of GM cultivation in the world

Citation Inside the Text

In the text, the author should be numbered. Name and year should not be specified.

Example: Potatoes produced on a global scale are used in many basic areas [1, 2, 3]. Fifty percent of primarily produced potatoes are used for fresh consumption, such as baking, frying, boiling [4, 5, 6, 7].

References

The references section should be written in 10 font sizes and without hanging indentations. In the references section, italics should not be written except in italic words such as "in vivo, in vitro, ex-situ" and species names. References should be written according to the "Chicago style". Besides, there is an endnote style preparing for "International Journal of Life Sciences and Biotechnology". You can prepare your references using that style. For Endnote style, you can reach it by clicking on the endnote at the bottom right part of the main page of the journal. Examples

Example of an article with 1 author;

Marakli, S., A Brief Review of Molecular Markers to Analyze Medicinally Important Plants. International Journal of Life Sciences and Biotechnology, 2018. 1 (1): p. 29-36.

Example of an article with 2 authors;

Kocacaliskan, I. and I. Tailor, Allelopathic effects of walnut leaf extracts and juglone on seed germination and seedling growth. The Journal of Horticultural Science and Biotechnology, 2001. 76 (4): p. 436-440.

Example of an article with 3 authors;

Segura-Aguilar, J., I. Hakman, and J. Rydström, The effect of 5OH-1,4-naphthoquinone on Norway spruce seeds during germination. Plant Physiology, 1992. 100 (4): p. 1955-1961.

Example of articles with 4 or more authors

Arasoglu, T., et al., Synthesis, characterization, and antibacterial activity of juglone encapsulated PLGA nanoparticles. Journal of applied microbiology, 2017. 123 (6): p. 1407-1419.

Example for the book;

Kocalishkan, I., Allelopathy. 2006, Ankara, Turkey: Our Office Press-In Turkish.

Example for Book Chapter;

Kaya, Y., F.Z. Huyop, and M.F. Edbeib, Genetic Diversity in Plants, in Advances in Biosciences, F.Z. Huyop and S. Mohammed, Editors. 2019, Penerbit UTM Press. Malaysia: Malaysia. p. 04-24.

Ethical Principles and Publication Policy

Ethical standards for publication exist to ensure high-quality scientific publications, public trust in scientific findings, and that people receive credit for their ideas. In addition, the authors are encouraged to follow the ethic guidelines of the Committee on Publication Ethics (COPE) which can be viewed on the COPE website.

International Journal of Life Sciences and Biotechnology (Int J. Life Sci. Biotechnol.) is an electronic peer-reviewed international journal trying to have the highest standards of publication ethics. For that, we affirm the following principles of the Publication Ethics and Malpractice Statement.

If malpractice is discovered at any time even after the publication, the articles not in accordance with these standards will be removed from the publication. Int J. Life Sci. Biotechnol. is checking all papers in a double-blind peer-review process. We also check for plagiarisms, research fabrication, falsification, and improper use of any organisms in research. We will also report any cases of suspected plagiarism or duplicate publishing. Int J. Life Sci. Biotechnol. reserves the right to use plagiarism detecting software to screen submitted papers at all times.

Author's responsibilities: The author or authors must guarantee that they have written a unique study. Moreover, they must make sure that the article has not been submitted and evaluated elsewhere at the same time. Literature of the other researchers, all contributors and sources (including online sites) should be appropriately credited and referenced. All submitted manuscripts should be edited for language. All references should be cited without been copied or plagiarized. If needed, any financial sources or another conflict of interest should be disclosed. In order to correct the paper, any significant error or inaccuracy in the published works should be notified by the related authors. An author agrees to the license agreement before submitting the article. All articles must be submitted using the online submission procedure. Submitting a paper simultaneously to more than one publication at a time is a violation of publications' ethics.

Editorial responsibilities: Editors along with Editor-in-Chief and Editorial Board have publication decisions. Editors must guarantee a fair double-blind peer-review of the submitted articles for publication. They have to prevent any potential conflict of interests between the author and editors and reviewers. They have to guarantee the confidentiality of submitted articles before publishing. Editor-in-Chief will coordinate the work of the editors.

Peer review/responsibility for the reviewers: They have to review the manuscripts based on content without regard to ethnic origin, gender, sexual orientation, citizenship, religious belief, or political philosophy of the authors. They have to guarantee the confidentiality of submitted articles before publishing. They have to report any plagiarisms, research fabrication, falsification, and improper use of any organisms in research to the editors and/or the Editor-in-Chief. They have to review the papers objectively and state their opinions clearly in the forms and on the paper. A reviewer having inadequate time or feeling unqualified should notify the editors as soon as possible and excuse her/himself from the review process.

Plagiarism

All journals published by IJLSB are committed to publishing only original material, i.e., material that has neither been published elsewhere nor is under review elsewhere. Manuscripts that are found to have been plagiarized from a manuscript by other authors, whether published or unpublished, will incur plagiarism sanctions.

Manuscripts are checked by Ithenticate Plagiarism System.

Duplicate Submission

Manuscripts that are found to have been published elsewhere, or to be under review elsewhere, will incur duplicate submission/publication sanctions. If authors have used their own previously published work or work that is currently under review, as the basis for a submitted manuscript, they are required to cite the previous work and indicate how their submitted manuscript offers novel contributions beyond those of the previous work.

Citation Manipulation

Submitted manuscripts that are found to include citations whose primary purpose is to increase the number of citations to a given author's work or articles published in a particular journal, will incur citation manipulation sanctions.

Data Fabrication and Falsification

Submitted manuscripts that are found to have either fabricated or falsified experimental results, including the manipulation of images, will incur data fabrication and falsification sanctions.

Improper Author Contribution or Attribution

All listed authors must have made a significant scientific contribution to the research in the manuscript and approved all its claims. It is important to list everyone who made a significant scientific contribution, including students and laboratory technicians.

Redundant Publications

Redundant publications involve the inappropriate division of study outcomes into several articles.

Sanctions

In the event that there are documented violations of any of the above-mentioned policies in any journal, regardless of whether or not the violations occurred in a journal published by Int J. Life Sci. Biotechnol., the following sanctions will be applied:

Immediate rejection of the infringing manuscript.

Immediate rejection of every other manuscript submitted to any journal published by Int J. Life Sci. Biotechnol. by any of the authors of the infringing manuscript.

The prohibition against all of the authors for any new submissions to any journal published by IJLSB, either individually or in combination with other authors of the infringing manuscript, as well as in combination with any other authors. This prohibition will be imposed for a minimum of 36 months. Prohibition against all of the authors from serving on the Editorial Board of any journal published by Int J. Life Sci. Biotechnol.

In cases where the violations of the above policies are found to be particularly egregious, the publisher reserves the right to impose additional sanctions beyond those described above.

Publication Charge

"International Journal of Life Sciences and Biotechnology" is an Open Access Journal and does not charge any printing charges from authors, during article delivery, assessment and printing stages.

Aim and Scope

International Journal of Life Sciences and Biotechnology (Int J. Life Sci. Biotechnol.) is an international peer-reviewed journal that publishes original articles from all biology and molecular biology studies, particularly in the fields of life sciences and biotechnology. The language of publication is Turkish and English. Also the main objective of Int J. Life Sci. Biotechnol. is to provide quality publications to scientists, researchers, and engineers from both academia and industry who want to communicate the latest developments and practices in their field.

Int J. Life Sci. Biotechnol. publishes original papers in various fields of Life Sciences and Biotechnology that covers, but is not limited to, the following areas:

- Agricultural Biotechnology

- Animal (livestock and fish production, physiology, breeding and genetics, biotechnology, etc),

- Animal Biotechnology

- Biochemical Genetics,

- Biochemistry

- Biodiversity and biodiscovery

- Bioinformatics and system biology

- Biology and Molecular Biology,

- Bioremediation and biodegradation

- Biotechnology

-Bioethics (Life Sciences and Biotechnology)

- Botany,

- Evolution and Population Genetics,

- Food Biotechnology

- Genetic engineering and cloning

- Lichens

- Genetics,

- Biotechnological product and Halal Food

- Industrial Biotechnology

- Medical Biotechnology

- Molecular Genetics

- Plant (Plant production, physiology, breeding and genetics, biotechnology, agronomy, horticulture, plant protection, etc.),

- Plant Biotechnology

- Soil (soil ecology, physics, and chemistry, etc)

-Polar Science (Life Sciences and Biotechnology)

DECLARATION: This work is part of Gülfidan KUYUMCU's MA thesis. Articles on 27-29 September 2017 held in Bayburt in Turkey was presented as a Oral Presentation I. International Organic Agriculture and Biodiversity Symposium

Genetic Analysis Related To Organized Genetic Changes in Potato And Processed Potatoes

Gulfidan Kuyumcu[1*], Muhammed Majed Abed[2]

Author Addresses: [1] Samsun Ondokuz Mayıs University, Faculty of Agriculture, Department of Agricultural Biotechnology, Samsun / Turkey
[2] Samsun Ondokuz Mayıs University, Faculty of Agriculture, Department of Agricultural Biotechnology, Samsun / Turkey

*Corresponding Autor: Gulfidan Kuyumcu, e-mail: ijlsb@intsa.org

Please write the e-mail addresses and Orcid ID numbers of all authors **(required fields)**

Author 1 mail and Orcid ID:

Author 2 mail and Orcid ID:

Author 3 mail and Orcid ID:

Copyright Transfer Agreement

INTERNATIONAL JOURNAL OF LIFE SCIENCES SCIENCE AND BIOTECHNOLOGY (IJLSB)

Title:

Authors:

This form must be signed by all the authors and sent by you to publish your article at "International Journal of Life Sciences Scıence And Biotechnology (IJLSB)".

By signing this document, the following conditions are considered acceptable:

1. The fact that all publishing rights belong "International Journal of Life Sciences Scıence And Biotechnology,
2. Prepared according to the Writing Rules and Publishing Policies of "International Journal of Life Sciences Scıence And Biotechnology",
3. Article original and not previously published at home or abroad or is not under consideration for publication,
4. It belongs to us by the scientific and ethical responsibility is not reached other authors; All the authors a-re aware of the work and responsibilities of other authors, first author of the article that I have to accept me as I declare;

Authors Name Surname	Date	Signature

Ethics Committee Report

Article If an Ethics Committee Report is required to conduct a research on animals and humans and to conduct this research, it is mandatory that the **Ethics Committee Report be scanned and uploaded as a PDF file**. Otherwise, the article is returned to the author at the preliminary examination and other stages.

1.REVIEWER SUGGESTION

DEGREE:

FIRST NAME:

LAST NAME:

MAIL ADDRESS:

INSTITUTION:

DEPARTMENT:

SUBJECTS:

2.REVIEWER SUGGESTION

DEGREE:

FIRST NAME:

LAST NAME:

MAIL ADDRESS:

INSTITUTION:

DEPARTMENT:

SUBJECTS:

3.REVIEWER SUGGESTION

DEGREE:

FIRST NAME:

LAST NAME:

MAİL ADDRESS:

INSTITUTION:

DEPARTMENT:

SUBJECTS: